İSTANBUL TECHNICAL UNIVERSITY ★ INSTITUTE OF SCIENCE AND TECHNOLOGY

MODELING AND OPTIMAL POWER MANAGEMENT OF A PARALLEL HYBRID ELECTRIC VEHICLE

M.Sc. Thesis by
Volkan SEZER, Eng.
518051020

Date of submission : 24 December 2007
Date of defence examination: 28 January 2008

Supervisor (Chairman): Prof. Dr. Levent GÜVENÇ
Members of the Examining Committee Assoc. Prof.Dr. Emre KÖSE (B.Ü)
Asst.Prof.Dr. Erdinç ALTUĞ (İ.T.Ü)

FEBRUARY 2008

İSTANBUL TEKNİK ÜNİVERSİTESİ ★ FEN BİLİMLERİ ENSTİTÜSÜ

PARALEL HİBRİT ELEKTRİKLİ ARACIN MODELLENMESİ VE OPTİMAL KONTROLÜ

YÜKSEK LİSANS TEZİ
Müh. Volkan SEZER
518051020

Tezin Enstitüye Verildiği Tarih : 24 Aralık 2007
Tezin Savunulduğu Tarih : 28 Ocak 2008

Tez Danışmanı : **Prof.Dr. Levent GÜVENÇ**
Diğer Jüri Üyeleri **Doç.Dr. Emre KÖSE (B.Ü.)**
Yrd.Doç.Dr. Erdinç ALTUĞ (İ.T.Ü.)

ŞUBAT 2008

ACKNOWLEDGEMENT

I would like to express my deep appreciation and thanks to my advisor Prof. Dr. Levent Güvenç for his assists on my thesis. I want to give my appreciates to my wife, y mother and my father too for their patience and love. I also acknowledge the support of Ford Otosan in this thesis.

December 2007 VOLKAN SEZER

TABLE OF CONTENTS

ABBREVIATIONS

BDCM : Brushless Direct Current Machine
BHP : Brake Horse Power
CAN : Controller Area Network
D : Differential
ECMS : Equivalent Consumption Minimization Strategy
ECU : Electronic Control Unit
EM : Electric Motor
EM-G : Electric Motor and Generator
EV : Electric Vehicle
FCM : Fuel Consumption Minimization
HEV : Hybrid Electric Vehicle
ICE : Internal Combustion Engine
IM : Induction Machine
MOES : Maximizing Overall Efficiency Strategy
PMSM : Permanent Magnet Synchronous Machine
P-HEV : Parallel Hybrid Electric Vehicle
SOC : State of Charge
SP-HEV : Series Parallel Hybrid Electric Vehicle
SRM : Switch Reluctance Machine
S-HEV : Series Hybrid Electric Vehicle
T : Transmission
4WD : Four Wheel Drive

LIST OF TABLES

Page No:

LIST OF FIGURES

Page No:

SYMBOL LIST

c.g.	***:***Vehicle Center of Gravity
dr	:Differential ratio
dr_f	:Front differential ratio
dr_r	:Rear differential ratio
$EM1_{reg\_signal}$	:Regenerative braking signal for EM1 (Volt)
$EM2_{reg\_signal}$	:Regenerative braking signal for EM2 (Volt)
$\boldsymbol{FC}_{\boldsymbol{ICE}}$	:Instant amount of consumed fuel of internal combustion engine (gr)
f_{Topt}	:Frequency of optimum torque calculation
$\boldsymbol{F}_{\boldsymbol{xf}}$	: Front wheel lateral force (N)
$\boldsymbol{F}_{\boldsymbol{xr}}$	: Rear wheel lateral force (N)
$\boldsymbol{F}_{\boldsymbol{x}}$	:Projection of wheel longitituonal forces to chassis coordinate axis (N)
$\boldsymbol{F}_{\boldsymbol{y}}$	: Projection of wheel lateral forces to chassis coordinate axis (N)
$\boldsymbol{F}_{\boldsymbol{yf}}$	:Front wheel lateral force (N)
$\boldsymbol{F}_{\boldsymbol{yr}}$	:Rear wheel lateral force (N)
gn	:Gear Number
gr	:Gear ratio
$\boldsymbol{GED}_{\boldsymbol{fuel}}$	:Gravimetric energy density of fuel (Wh/gr)
$\boldsymbol{I}_{\boldsymbol{bat}}$	:Battery current (Ampere)
I_{bat_ch}	:Battery charge current (Ampere)
I_{bat_dch}	:Battery discharge current (Ampere)
$I_{bat\_\min}$	:Minimum battery current (Ampere)
$I_{bat\_\max}$	:Maximum battery current (Ampere)
$\boldsymbol{J}_{\boldsymbol{tire}}$	:Tire inertia (kgm2)
K_{ch}	:Charge efficiency constant
K_{dch}	:Discharge efficiency constant
$\boldsymbol{l}_{\boldsymbol{f}}$	:Distance of front axle-vehicle c.g (m)
$\boldsymbol{l}_{\boldsymbol{r}}$	:Distance of rear axle-vehicle c.g (m)
Md_{front}	:Mass distribution constant for front side of vehicle
Md_{rear}	:Mass distribution constant for rear side of vehicle
$\boldsymbol{M}_{\boldsymbol{cap}\_\mathbf{bat}}$	:Maximum energy capacity of battery. (Wh)
$\boldsymbol{M}_{\boldsymbol{z}}$	:Moment of wheel forces in vertical chassis axis (Nm)

P	:Power
Per_{pch}	:Percentage of parallel charge
P_{fuel_inst}	:Instantaneous power of fuel (W)
P_{fuel_realch}	:Power of fuel in charge condition (W)
$P_{fuel\_realdch}$	:Power of fuel in discharge condition (W)
P_{req}	: Requested power by driver gas pedal input. (Source of the required power is the place where ICE is mounted)(W)
P_{POTE}	:Potential electric power (W)
P_{EM1}	:Power of EM1 (W)
P_{EM2}	:Power of EM2 (W)
P_{EM3}	:Power of EM3 (W)
P_{ICE}	:Power of ICE (W)
P_{POTf}	:Potentiel electric power of fuel (W)
$P_{road\_realdch}$	Power transferred to road in discharge condition (W)
P_{road_realch}	Power transferred to road in charge condition (W)
P_{reg}	:Regenerative braking power (W)
P_{road_real}	:Power transferred to road (W)
$\mathbf{R}$	:Wheel radius (m)
$\boldsymbol{R_c}(\boldsymbol{SOC},\boldsymbol{T})$	:Charge resistance of battery (Ohm)
$\boldsymbol{R_{d(soc,T)}}$	:Discharge resistance of battery (Ohm)
$\boldsymbol{R}_{\text{int}}$	:Internal resistance of battery (Ohm)
$\boldsymbol{R_L}$	:Load resistance (Ohm)
$\boldsymbol{slip_f}$	:Front wheel slip ratio
$\boldsymbol{slip_r}$	:Rear wheel slip ratio
$\boldsymbol{SOC}$	:State of charge
SOC_{hl}	:High limit of state of charge
SOC_{ll}	:Low limit of state of charge
SOC_{sll}	:High security limit of state of charge
SOC_{slh}	:Low security limit of state of charge
T	:Torque
$\boldsymbol{T_{diff\_in}}$	:Input torque of differential (Nm)
$\boldsymbol{T_{diff\_out}}$	:Output torque of differential (Nm)
T_{EM1_min}	:Minimum EM1 torque (Nm)
T_{EM1_max}	:Maximum EM1 torque (Nm)
T_{EM2_min}	:Minimum EM2 torque (Nm)
T_{EM2_max}	:Maximum EM2 torque (Nm)
T_{EM3_min}	:Minimum EM3 torque (Nm)

T_{EM3_max} :Maximum EM3 torque (Nm)

$\boldsymbol{T_{gb\_in}}$:Input torque of gearbox (Nm)

$\boldsymbol{T_{gb\_out}}$:Output torque of gearbox (Nm)

$T_{h\_limICEch}$:The high limit of the ICE charge torque for search algorithm (Nm)

$\boldsymbol{T_{ICE}}$:Internal Combustion Engine Output Torque (Nm)

T_{ice_min} :Minimum ICE torque (Nm)

T_{ice_max} :Maximum ICE torque (Nm)

$\boldsymbol{T_{optEM1dch}}$: Optimum electric motor 1 torque in discharge condition (Nm)

$\boldsymbol{T_{optEM2dch}}$: Optimum electric motor 2 torque in discharge condition (Nm)

$\boldsymbol{T_{optEM3ch}}$: Optimum electric motor 3 torque in charge condition (Nm)

$\boldsymbol{T_{optICEch}}$:Optimum internal combustion engine torque in charge condition (Nm)

$\boldsymbol{T_{optICEdch}}$: Optimum internal combustion engine torque in discharge condition (Nm)

T_{req} :Requested torque by driver gas pedal input. (Source of the required torque is the place where ICE is mounted)(Nm)

$T_{reqroad}$: Required torque from road (Nm)

$\boldsymbol{V_{veh}}$:Vehicle speed (m/sn)

$\boldsymbol{v}$: Vehicle center of gravity speed vector (m/s)

$\boldsymbol{v_f}$: Front wheel speed vector (rad/sec)

$\boldsymbol{v_r}$: Rear wheel speed vector (rad/sec)

$\boldsymbol{v_{xf}}$: Longitituonal speed vector of front wheel (rad/sec)

$\boldsymbol{v_{xr}}$: Longitituonal speed vector of rear wheel (rad/sec)

$\boldsymbol{V_{bat}}$: Battery output voltage (Volt)

$\boldsymbol{V_{oc}}$: Battery open circuit voltage (Volt)

ω :Angular velocity

$\boldsymbol{\omega_{diff\_in}}$: Angular velocity of differential input (rad/sec)

$\boldsymbol{\omega_{diff\_out}}$: Angular velocity of differential output (rad/sec)

$\boldsymbol{\omega_{gb\_in}}$: Angular velocity of gearbox input (rad/sec)

$\boldsymbol{\omega_{gb\_out}}$: Angular velocity of gearbox output (rad/sec)

$\boldsymbol{\omega_{ICE}}$: Internal Combustion Engine Speed (rad/sec)

$\boldsymbol{\omega_f}$: Front wheel angular velocity (rad/sec)

$\boldsymbol{\omega_r}$: Rear wheel angular velocity (rad/sec)

$\boldsymbol{x_0}$-$\boldsymbol{y_0}$: Fixed coordinate plane

$\boldsymbol{x}$ -$\boldsymbol{y}$: Chassis coordinate plane

η_{bat} : Efficiency of battey

η_{EM1} : Efficiency of electric motor 1

η_{EM2} : Efficiency of electric motor 2

η_{EM3} : Efficiency of electric motor 3

η_{ICE} : Efficiency of internal combustion engine

η_{DL1} : Efficiency of driveline 1

η_{DL2} : Efficiency of driveline 2

η_{DL3} : Efficiency of driveline 3

η_{DL4} : Efficiency of driveline 4

η_{belt} : Efficiency of belt mechanism

η_{diff} : Differential efficiency

η_{SYS} : Efficiency of system.

η_{SYSch} :Efficiency of system in charge condition

η_{SYSdch} :Efficiency of system in discharge condition

η_{tr} :Transmission efficiency $\hat{\eta}_{BATdch}$:Average battery efficiency in discharge condition

$\hat{\eta}_{EM_{1,2}dch}$:Average of average efficiencies of EM1 and EM2 in discharge condition including their drivetrain efficiencies to road

$\hat{\eta}_{EM3ch}$ Average EM3 efficiency in charge condition

$\hat{\eta}_{ICEch}$:Average ICE efficiency in charge condition

δ_f :Front wheel orientation angle (Degree)

δ_r :Rear wheel orientation angle (Degree)

α_{clt} :Clutch pedal position

α_{brk} :Brake pedal position

α_{thr} :Throttle pedal position

α_f :Front wheel lateral slip angle (Degree)

α_r :Rear wheel lateral slip angle (Degree)

β :Lateral slip angle (Degree)

β_f :Angle between front wheel speed-vehicle c.g (Degree)

β_r :Angle between rear wheel speed-vehicle c.g (Degree)

ψ :Yaw Angle (Degree)

PARALEL HİBRİT ELEKTRİKLİ ARAÇ MODELLENMESİ VE OPTİMAL GÜÇ YÖNETİMİ

ÖZET

Yakıt tüketimi ve emisyonlar açısından klasik araçlara oranla çok daha başarılı olan hibrit elektrikli araçlar, son yıllarda oldukça popüler olmaya başlamışlardır. Bu tezde, bilgisayar ortamında bir paralel hibrit elektrikli araç matematiksel olarak modellenmiş, yakıt tüketimini azaltma amacıyla bir optimum güç yönetim algoritması geliştirilmiş ve bu algoritma araç modellerine uygulanarak kontolcülü aracın klasik araçla yakıt tüketimi açısından karşılaştırılması simülasyon sonuçlarıyla incelenmiştir.

İlk bölümde, hibrit elektrikli araçlarla ilgili genel bilgiler verilmiş, bu araçların tarihçesine, mimarisine ve ana elemanlarının özelliklerine değinilmiştir.

İkinci bölümde, hibrit elektrikli araçları oluşturan elemanların nasıl modellendiği ve lineer olmayan tek izli hibrit elektrikli araç modelinin nasıl oluşturulduğundan bahsedilmiştir.

Üçüncü bölümde CarMaker adlı simülasyon ve analiz programı kullanılarak bir hibrit elektrikli araç modelinin nasıl oluşturulduğu anlatılmıştır.

Dördüncü bölümde, yakıt tüketiminin azaltılması amacıyla, eşdeğer yakıt tüketimi minimizasyonu tabanlı, toplam verimi maksimize etmeye çalışan yeni bir algoritma anlatılmıştır. Bu algoritmanın tezde işlenen araç konfigürasyonu üzerinde uygulanabilmesi için gereken formüller kısıtlar dahilinde hesaplanmıştır. Bu formüllerin kontrolcü tarafından gerçek zamanlı uygulamalarda nasıl kullanılacağına ilişkin bilgiler de bu bölümde verilmiştir.

Beşinci bölümde araç modeli ECE sürüş çevrimini kullanarak , klasik mod, sadece rejeneratif frenleme modu ve toplam verim maksimizasyonuna dayanan kontrolcülü modda (MOES) koşturulmuştur ve simülasyon sonuçları analiz edilmiştir.

Altıncı ve son bölümde ise çalışmada elde edilen sonuçlar yorumlanmış ve konuyla ilgili gelecekte yapılması öngörülen çalışmalara yer verilmiştir.

MODELING AND OPTIMAL POWER MANAGEMENT OF A PARALLEL HYBRID ELECTRIC VEHICLE

SUMMARY

Hybrid electric vehicles which are more successful than conventional vehicles in terms of fuel consumption and emissions, have become very popular in recent years. In this thesis, a parallel hybrid electric vehicle was modeled mathematically, an optimum power management algorithm was developed for fuel consumption minimization, this algorithm was integrated into the developed vehicle model and the controlled vehicle was compared with conventional vehicle in terms of fuel consumption.

In the first section, general information about hybrid electric vehicles are given and history, architecture and properties of its main components were discussed.

In the second section, modeling the components of hybrid electric vehicle and nonlineer single track hybrid electric vehicle modelling was discussed.

In the third section, hybrid electric vehicle modelling with *CarMaker* vehicle dynamics simulation and analysis software was treated.

In the fourth section, a new approach which maximizes the overall efficiency of the vehicle, based on equivalence fuel consumption minimization strategy was developed for fuel consumption reduction. Formulas were calculated considering the constraints to implement this algorithm for the vehicle architecture that is given in the thesis. In this section informations about using these formulas by the controller in real time applications were also presented.

In the fifth section vehicle models were tested and simulation results were analyzed by using ECE driving cycle in the conventional mode, regenerative braking only mode and the maximizing overall efficiency (MOES) mode.

In the sixth and last section, achieved results were commented upon and possible directions future works were discussed.

1. INTRODUCTION

1.1 Overview of Hybrid Electric Vehicles

Hybrid vehicles are vehicles equipped with at least two different sources of energy. Specifically, in this thesis, these two power sources are an internal combustion engine and electric motor. In a hybrid electric vehicle, the main aim is to decrease the fuel consumption and emissions without any performance loss.

The criteria that a hybrid electric vehicle should meet can be summarized in a brief list [1]:

- Performance – Range, acceleration capability, gradeability and top speed
- Emissions – Compliance with regulatory requirements like Euro 5 emission limits.
- Safety – Crashworthiness, handling/braking capability, protection from hazardous materials, and compliance with regulatory requirements
- Moderate purchasing cost and operating costs
- Convenience of refueling
- Reliability and low cost of repair
- Comfort and convenience – Adequate passenger and storage space, heating and cooling capacity, *etc.*

1.2 History of Hybrid Electric Vehicles

In 1901 Ferdinand Porche designed a series hybrid electric vehicle. This vehicle broke several Austrian speed records and also won the Exelberg Rally in 1901. “This vehicle used a gasoline engine powering a generator which gives power to electric hub motors with a small battery pack. It had a range of 50 km and a top speed of 50km/h.

In 1915, another hybrid electric vehicle was produced by Woods Motor Vehicle company which is an electric car maker. This vehicle had a four cylinder ICE and an electric motor. Electric motor drives the vehicle at speeds below 25 km/h. Between 25 km/h and the top speed of 55 km/h , internal combustion engine drives the vehicle.

A more recent HEV prototype was built by Victor Wouk. Wouk installed a prototype hybrid drivetrain with a 16kW electric motor, into a 1972 Buick Skylark which was provided by GM for the Federal Clean Car Incentive Program, but the program was stopped by the United States Environmental Protection Agency in 1976.

The regenerative braking system, the core design concept of most production HEVs, was developed by David Arthurs in 1978. Arthurs used off-the shelf components from Opel GT along with his voltage controller to link the batteries, electric motor and DC generator.

In 1989, Audi produced an experimental plug-in parallel hybrid electric vehicle based on the Audi 100 Avant Quattro. This car had a 12.6 bhp Siemens electric motor which drove the rear wheels. A nickel-cadmium battery pack supplied the electric motor power. Front wheels of the vehicle are driven with a 2.3 litre five-cylinder engine with an output of 136 bhp. The aim was to produce a vehicle which could operate in ICE only mode in intercity traffic and electric mode in the city. But this vehicle was not efficient enough because of the extra weight of the electric drive.

Two years later, Audi made the second experimental HEV, again based on the Audi 100 Avant Quattro. In this vehicle, 28.6 bhp three-phase machine was driving the rear wheels. But this time, the rear wheels were additionally powered via the torsen differential from the main engine compartment which housed a 2.0 litre four-cylinder engine.

Automotive hybrid electric vehicle technology became successful in the 1990s when the Toyota Prius and Honda Insight commercially became available. These vehicles are parallel HEVs having direct connection from the ICE to the driven wheels, so the engine can directly power the wheels.

The Prius has been in high demand since its first production. Newer designs have more conventional appearance and they are less expensive and reach %40 improvement in fuel economy. Honda Civic Hybrid delivers 4.7 lt/100km. The

Honda Insight stopped production after 2006. Honda has also released a hybrid version of Accord.

Honda and Toyota are the companies which sell the highest quantity of HEV. Toyota sold a 306,862 HEVs between 1997 and November 2004, and Honda sold a total of 81,867 HEVs between 1999 and November 2004 [2].

In 2005, Ford Escape Hybrid which is the first hybrid electric sport utility vehicle was released. The 2007 Camry Hybrid became available in Summer 2006. In 2007, Lexus released a hybrid electric version of their GS sport sedan, Nissan also announced the release of the Altima Hybrid in 2007.

The table given below shows the hybrid car sales in United States between 2004 and 2007.

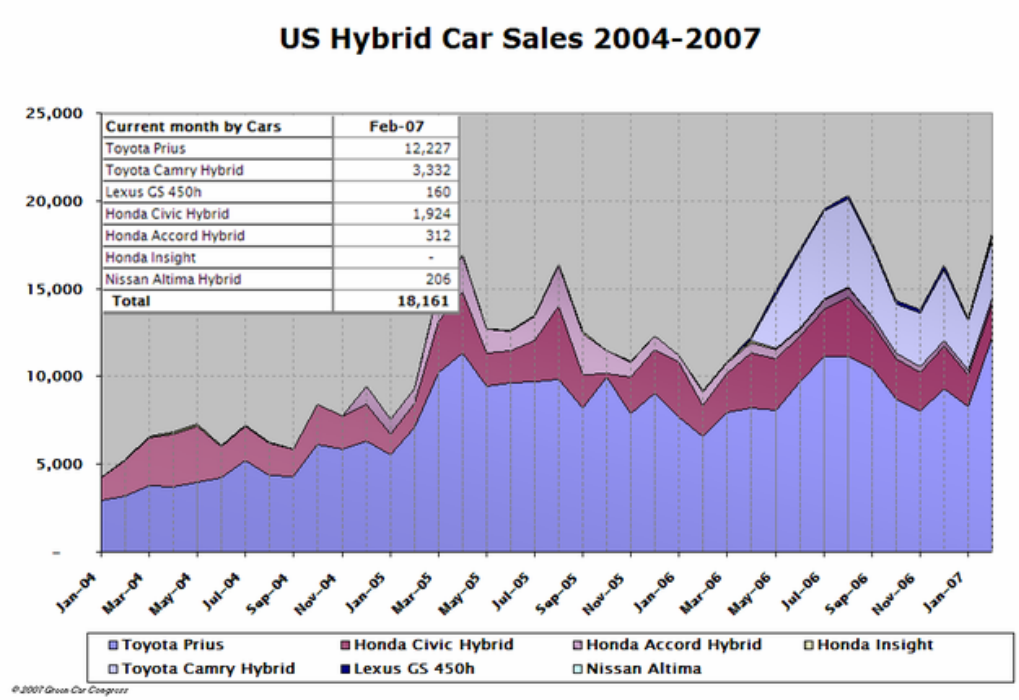

Figure 1.1 : Hybrid Vehicle Sales, as Compiled by Green Car Congress, Feb 2007 [3]

1.3 Hybrid Electric Vehicle Architecture

Hybrid electric vehicles can be divided into three main groups according to their powertrain architectures. These are: series, parallel and series–parallel hybrid electric vehicles [4] .

1.3.1 Series Hybrid Electric Vehicle (S-HEV)

The series HEV is designed for electric driving. In other words, it strongly resembles the configuration of an electric vehicle. The only difference is the use of an ICE which is used to generate electrical power to propel the vehicle at a certain level and to keep the batteries charged. In this configuration there is no mechanical connection between the ICE and the wheels which means that the ICE doesn't contribute to the EM in overcoming the road load. The engine of a series hybrid is uncoupled from the road load and can be run either in a fixed operating point or a restricted range of operating points of the highest efficiency. Series HEV structure is shown in Figure 1.2.

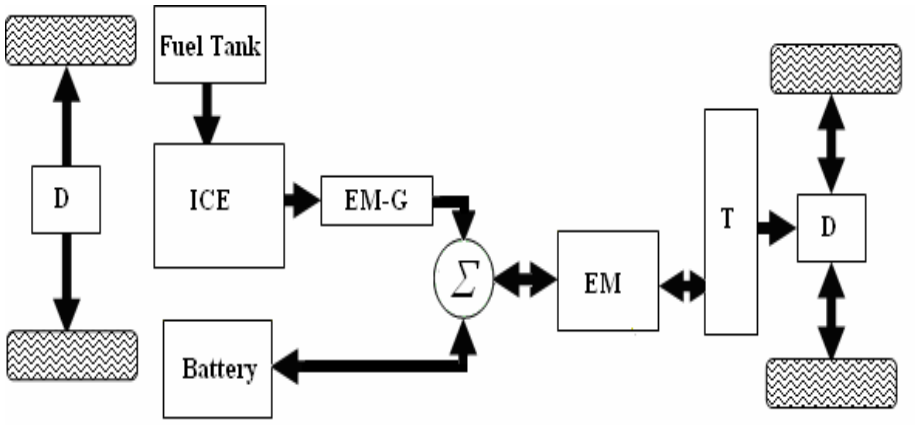

Figure 1.2 : Series HEV Structure[4]

EM must be capable of providing the peak power, which can result in a heavy and expensive electric machine. Furthermore, if an all-purpose vehicle is desired, the sizing of the components must be based on the worst driving case, which can lead to overpowered systems that run at sub-optimal efficiency during average driving. For this reason, the series configuration is often chosen for heavy duty trucks (garbage-collection, distribution, buses) that have less space restrictions and that usually follow standard repeated missions [5].

1.3.2 Parallel Hybrid Electric Vehicle (P-HEV)

The design of a parallel-HEV (P-HEV) differs from S-HEV. Proper combination of EM and ICE let the both power converters drive the vehicle separately or together. Thus, different configurations exist according to the settlement of components. However, there is always a mechanical connection between the wheels and the ICE [5].

A parallel HEV structure is shown in Figure 1.3.

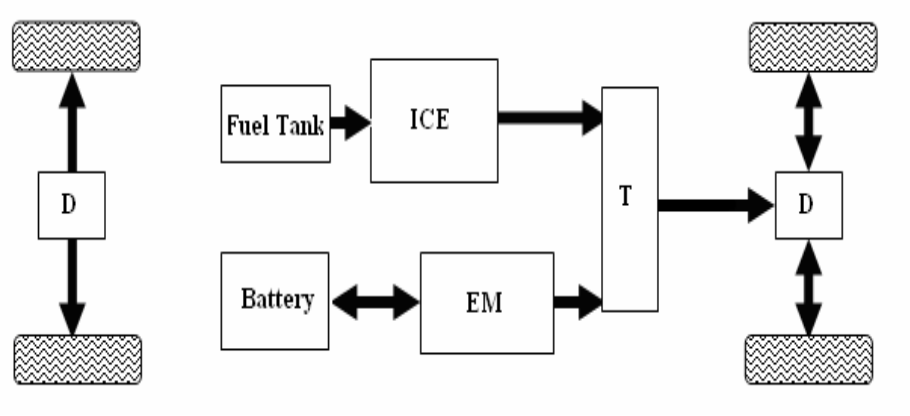

Figure 1.3 : Parallel HEV Structure[4]

A common mode of operation for parallel HEVs has the vehicle functioning like an electric vehicle at low speeds, with only the EM engaged (this is called electric launch); the ICE engages only at higher speeds. This strategy keeps engine operations away from low load operations that generally produce high hydrocarbon (HC) and carbon monoxide (CO) emissions and inefficient fuel use [6].

1.3.3 Series-Parallel Hybrid Electric Vehicle (SP-HEV)

Series-Parallel configuration combines the efficiencies of both series and parallel HEV structure. More flexible power management options are available . So, structure of control is more complicated than others. A series-parallel hybrid structure is shown in Figure 1.4.

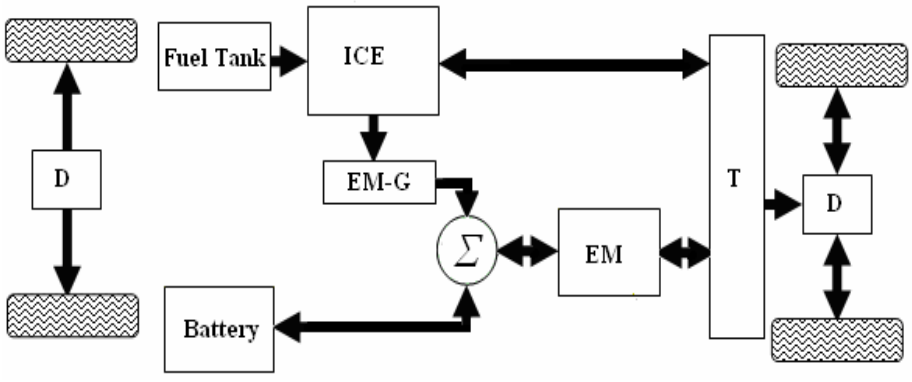

Figure 1.4 : Series -Parallel HEV Structure[4]

1.4 Component Types

1.4.1 Battery Types for HEV

A battery is a collection of one or more electrochemical cells which store chemical energy and converts it into electrical form. To be able to develop a HEV, an electrical energy source should be used with the EM to achieve the required propulsion power or store charge energy. Determining the type of the battery is the first step to develop the electrical power train. There are too many criteria that affect the selection procedure of the battery such as: energy density, cycle life, efficiency, weight, physical dimensions, memory effect, voltage capability, cost *etc*. Table 1.1 gives some general information about battery types that can be used in a HEV.

Table 1.1 : Battery Types by Descending Degree of Popularity [7]

Battery Type	Energy Density [Wh/kg]	Power Density [W/kg]	Cycle Life	Self Discharge Rate [% per month]	Current Cost [$/kWh]	Future Cost ($/kWh]	Vehicles Used_In	Other Notes
Lead-Acid	25 to 35	75 to 130	200 to 400	2 to 3	100 to 125	75	CARTA bus, Solectria E10 (sealed)	
Advanced Lead Acid	35 to 42	240 to 412	500 to 800				Audi Duo, GM EV1 (VLRA), Solectria Force	Potential: 55 Wh/kg, 450 W/kg, and 2000 cycle life
Nickel-Metal Hydride	50 to 80	150 to 250	600 to 1500		525 to 540	115 to 300	Toyota RAV4-EV, Toyota Prius, Chrysler Epic minivan, Honda EV, Chevy S-10	Potential: 120 Wh/kg, and 2200 cycle life
Nickel-Cadmium	35 to 57	50 to 200	1000 to 2000	10 to 20	300 to 600	110	WWU Viking 23	Potential: 2200 cycle life
Lithium-Ion	100 to 150	300	400 to 1200				Nissan Altra EV	Potential: 1000 Wh/kg
Zinc-Bromide	56 to 70	100	500		300			
Lithium Polymer	100 to 155	100 to 315	400 to 600			100		
NaNiCl	90	100		400				
Zinc-Air	110 to 200	100	240 to 450		300	100		
Vanadium Redox	50	110	400		300			

1.4.2 Electric Motor Types for HEV

Electric motor is the machine which converts electrical energy into mechanical energy. It plays a very important role in the electric propulsion unit of a HEV. The choice of the electrical machine depends on a number of factors, including performance, packaging and maintenance. Fig.1.4 shows the classification of EMs.

The first decision to choose an electric motor is whether to use a brush or brushless motor. The brush motor is simple in structure but requires periodic switching of

windings to maintain rotation. DC brush motor consists of a brush-commutator assembly that suffers from brush wear and heat conduction. Brushless motors use electronic commutation instead of mechanical commutation. Thus, no appreciable heat is generated in the rotor and they don't suffer from brush wear. After deciding on the use of brush or brushless type of motor, the next step is to decide the type of EM. Induction machines (IM) are widely accepted for electric propulsion unit of HEVs. This is because of their low cost and high reliability. However the technological developments in the field of permanent magnet technology have recently pushed the permanent magnet (PM) motors into the HEV area. Advantages include lower inertia, higher efficiency, higher power density and smaller size. Therefore, they have become more attractive compared to induction machines. A lot of work has been done to reduce the vibration and noise level of the switch reluctance machines (SRM). They have a very simple structure and low manufacturing cost. Although they are simple, when smooth operation is required a PM or an IM are prefered. Actually, there are similarities between the brushless dc machine (BDCM) and permanent magnet synchronous machine (PMSM). Both of the EM have a PM rotor. Also, they are similar in principle of the drive scheme used. But the distinguishing feature of these two EM types is that PMSM is fed with a sinusoidal current while BDCM requires rectangular currents. This feature leads to the use of different feedback devices and differences in the torque produced [8]. Depending on the power density, efficiency, cost and availability, a choice is made among these alternatives.

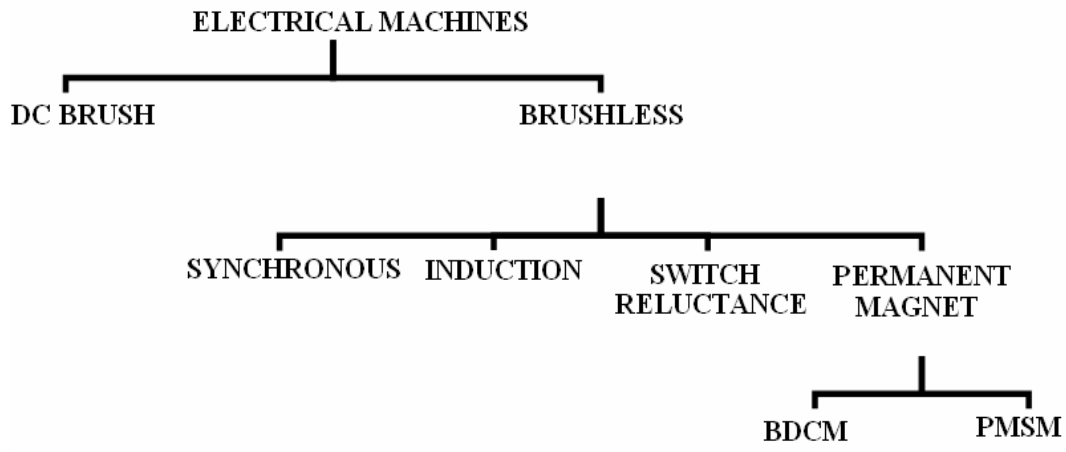

Figure 1.5 : Electric Motor Classification [1]

1.4.3 ICE Types

The internal combustion engine is an engine in which the combustion of fuel and oxidizer (typically air) occurs in a confined space called the combustion chamber. This exothermic reaction creates gases at high temperature and pressure which are permitted to expand. Internal combustion engines can be classified into two categories, as diesel and gasoline engines based on the fuel they use. Both diesel engines and gasoline engines convert fuel into energy through a series of small explosions or combustions. The major difference between diesel and gasoline is the way these explosions happen. In a gasoline engine, fuel is mixed with air, compressed by pistons and ignited by sparks from spark plugs. In a diesel engine, however, the air is compressed first, and then the fuel is injected. Because air heats up when it's compressed, the fuel ignites.

1.5 Thesis Scope and Outline

This thesis concentrates on modelling and control of a parallel hybrid electric vehicle.

The organization of the rest of this thesis is as follows. Modeling a HEV is presented in Chapter 2. Modelling of a HEV using CarMaker is treated in Chapter 3. A new formulation MOES which is based on equivalent consumption minimization strategy is presented in Chapter 4. Vehicle models were tested and simulation results were analyzed by using ECE driving cycle in the conventional mode, regenerative braking only mode and the maximizing overall efficiency mode (MOES) in Chapter 5. The thesis ends with conclusions in Chapter 6.

2. HYBRID ELECTRIC VEHICLE MODEL DEVELOPMENT

In this thesis, an augmented nonlinear single track model is used to capture the longitudinal and lateral dynamics of a hybrid electric vehicle. HEV dynamics are the same as other classical vehicles [9,10,11,12,13]. But there are some additional components like battery and electric motor. These components only bring changes to the torque that is applied to the powertrain. A longitudinal model of the vehicle is usually enough for HEV controller design and performance simulation studies. Use of lateral dynamics allow checking handling dynamics also.

In Fig. 2.1, main blocks of a nonlinear hybrid electric vehicle implemented in Simulink are given. Special components for hybrid electric vehicle (battery pack and electric motors) are inside the gray block. Remaining part of the model is the same as a classical conventional vehicle model.

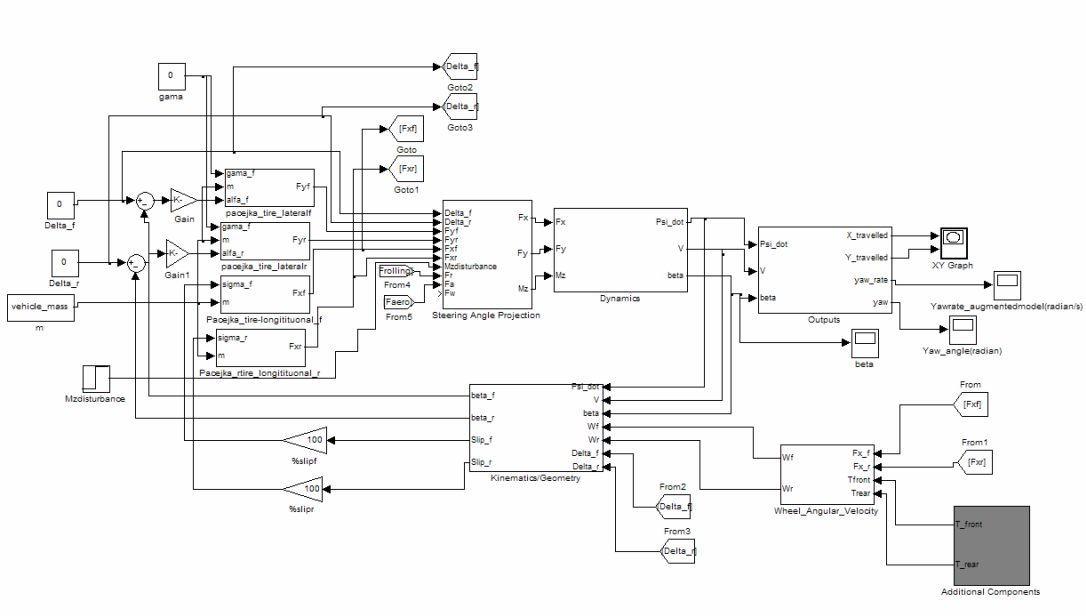

Figure 2.1 : Simulink Blocks of Nonlinear Single Track Hybrid Electric Vehicle Model

Modeling of components that constitute a HEV and equations of motion for the vehicle are given below in the following parts of this chapter.

2.1 Internal Combustion Engine (ICE) Model

The internal combustion engine is an engine in which the combustion of fuel and an oxidizer (typically air) occurs in a confined space called a combustion chamber. The ICE is modeled with two static maps. In a real vehicle,the desired ICE torque is calculated depending on throttle pedal position, gear number and ICE speed. A four dimensional torque map is used for calculating the engine torque as illustrated in Fig. 2.2.

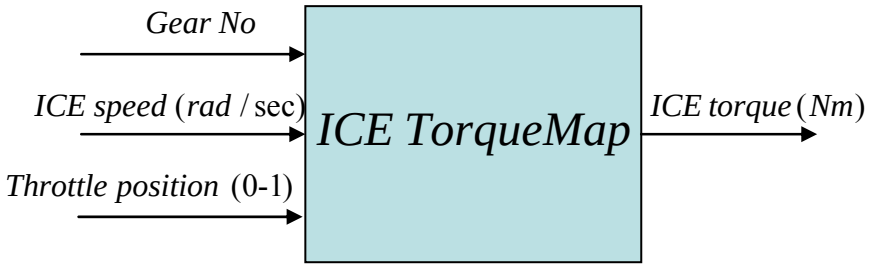

Figure 2.2 : ICE Torque Map Inputs and Output

The ICE fuel consumption map is used for calculating the amount of fuel consumed. This table depends on the ICE speed and torque as illustrated in Fig. 2.3.

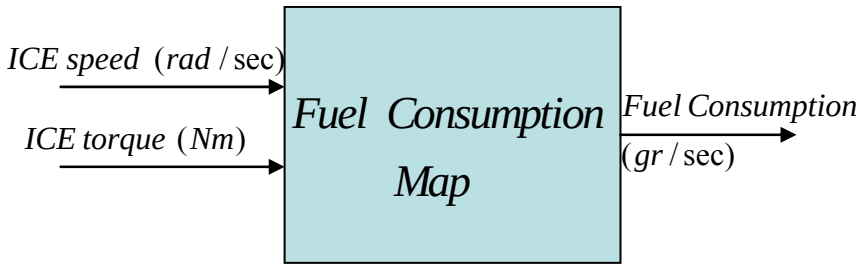

Figure 2.3 : ICE Fuel Consumption Map Inputs and Output

Efficiency of the ICE can be calculated from the fuel consumption map directly. Efficiency is defined as the ratio of output power to the input power of the system. For every speed and torque of the ICE, efficiency can be calculated using:

$$\eta_{ICE} = \frac{T_{ICE}\omega_{ICE}}{FC_{ICE}GED_{fuel}} \qquad \textbf{(2.1)}$$

where, $GED_{fuel}\,(Watt\,\text{sec}/\,gr)$ is the gravimetric energy density of fuel, $FC_{ICE}(gr/\text{sec})$ is the instantaneous amount of fuel consumed, $T_{ICE}\,(Nm)$ is the

output torque of the ICE and ω_{ICE} $(rad/\sec)$ is the speed of the ICE and η_{ICE} is the efficiency internal combustion engine.

A static map of undesired emissions is usually also used to show the amount of emissions reduction that is possible. It should be noted that transient effects are not captured since static maps are used in the engine model.

2.2 Electric Motor (EM) Model

An electric motor converts electrical energy into mechanical energy. The reverse process, of converting mechanical energy into electrical energy can also be accomplished by running the electric motor as a generator.

EM is modeled with two maps. One of them is electric motor torque map. This map depends on the signal sent to the motor driver and the speed of electric motor as illustrated in Fig. 2.4. The signal which is sent to the electric motor driver can be an analog signal or a digital signal if it uses a digital protocol like CAN.

Figure 2.4 : EM Torque Map Inputs and Output

A torque map for an electric motor can be seen in Fig. 2.5. The torque command signal is the input voltage sent to the electric motor driver circuit and scales the maximum electric motor torque.

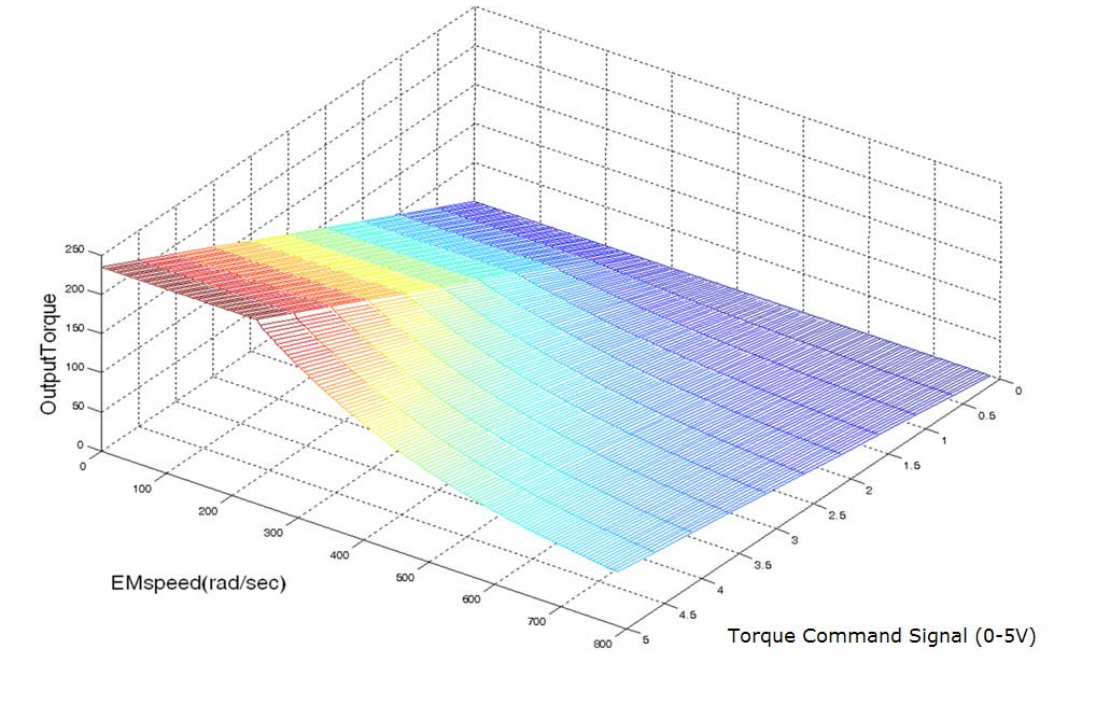

Figure 2.5 : EM Torque Map

The other map used for modeling an electric motor is its efficiency map which is needed for main power split control. Calculations for optimal power split depend on this efficiency value. This table depends on EM speed and EM torque and is illustrated in Fig. 2.6.

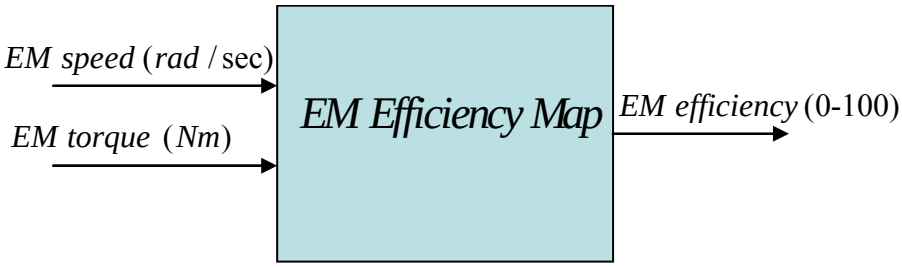

Figure 2.6 : EM Efficiency Map inputs and output

The efficiency map for the electric motor that is used in this thesis can be seen in Fig. 2.7.

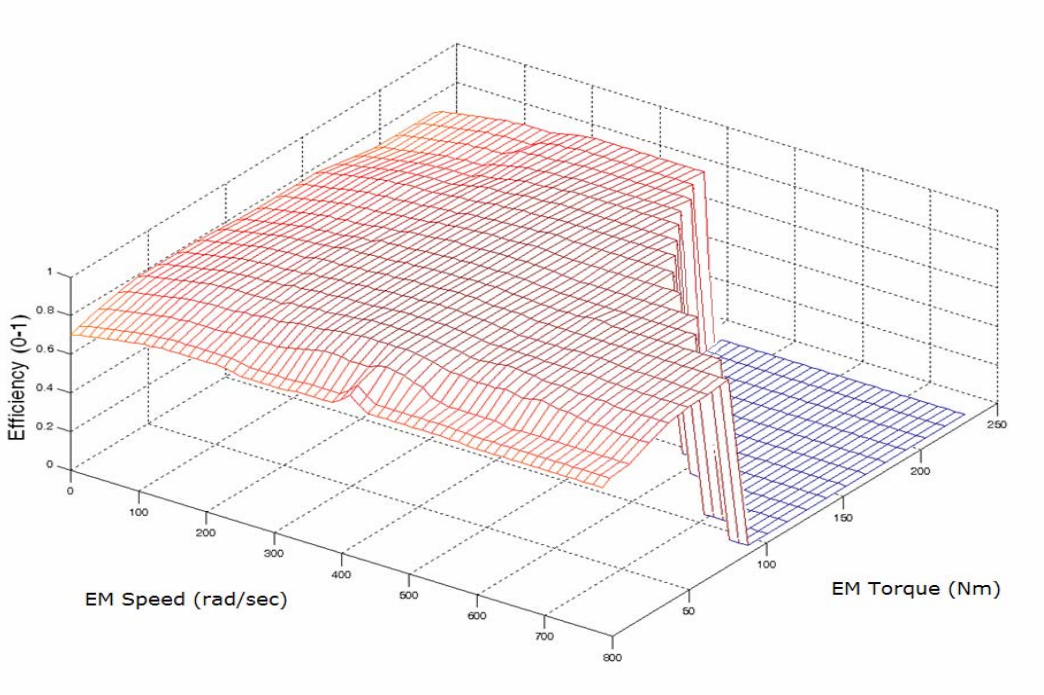

Figure 2.7 : EM Efficiency Map

2.3 Battery Model

The battery system is one of the main parts of a HEV. Battery system is the energy source for electrical motors. It also stores electrical energy converted from mechanical energy by internal combustion engine's direct mechanical power or regenerative braking.

The battery is modeled using its simple electrical equivalent circuit. Electrical drawing of this circuit is shown in Fig. 2.8.

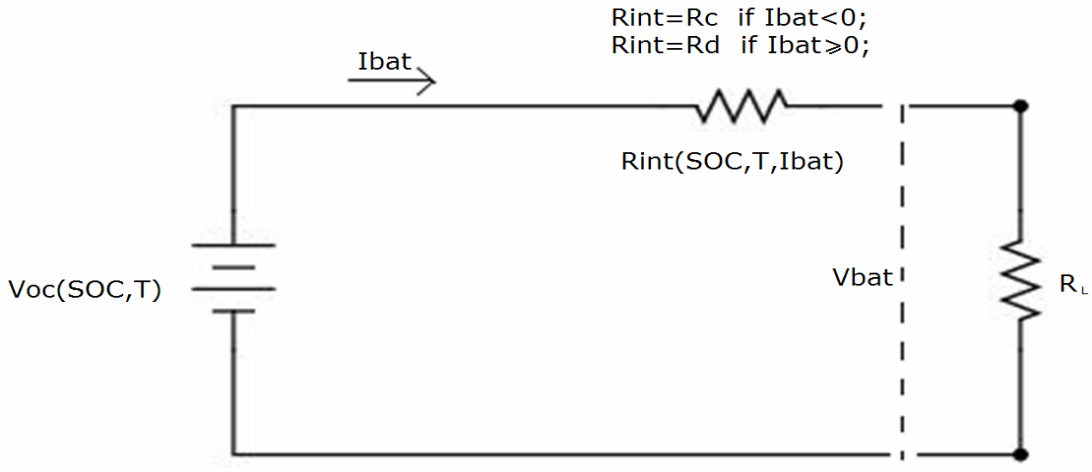

Figure 2.8 : Electrical Equivalent Circuit of Battery

To use the battery model in a HEV model, a power request $\boldsymbol{P_{req}}$ should be the input and state of charge of $\boldsymbol{SOC}$ battery should be the output of model. To be more realistic, a temperature input should be another input to the model. For SOC calculation, battery current $\boldsymbol{I_{bat}}$ should be calculated. The battery model is displayed in Fig. 2.9.

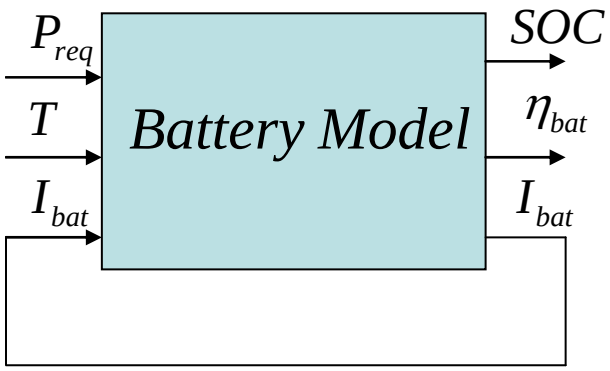

Figure 2.9 : Battery Model Inputs and Outputs

Equations are given below to solve the circuit and calculate the SOC.

$$R_{\text{int}} = \begin{Bmatrix} R_c(SOC,T) \ \ if \ I_{bat} < 0 \\ R_d(SOC,T) \ \ if \ I_{bat} >= 0 \end{Bmatrix} \quad \textbf{(2.2)}$$

$$V_{bat} = V_{oc}(SOC,T) + I_{bat} R_{\text{int}} \quad \textbf{(2.3)}$$

$$I_{bat} = \frac{P_{req}}{V_{bat}} \quad \textbf{(2.4)}$$

$$\Delta SOC = \frac{\int_{t_0}^{t} V_{bat} I_{bat} dt}{M_{cap\_\text{bat}} 3600} \quad \textbf{(2.5)}$$

$$SOC = SOC_i + \Delta SOC \quad \textbf{(2.6)}$$

With equations (2.2) , (2.3) and (2.4) the current which passes through the battery is calculated. With equations (2.5) and (2.6) , ratio of integrated power which is taken from battery or given to battery and maximum capacity of battery is calculated. Change of state of charge (ΔSOC) is integrated again and overall state of charge change is calculated. State of charge (SOC) at that instant is calculated by summing

initial charge condition and all state of charge changes. The state of charge value is written into the initial state of charge SOC_i variable, when integration starts at time t_0.

The battery internal resistance characteristic, for constant temperature, can be seen in Fig. 2.10.

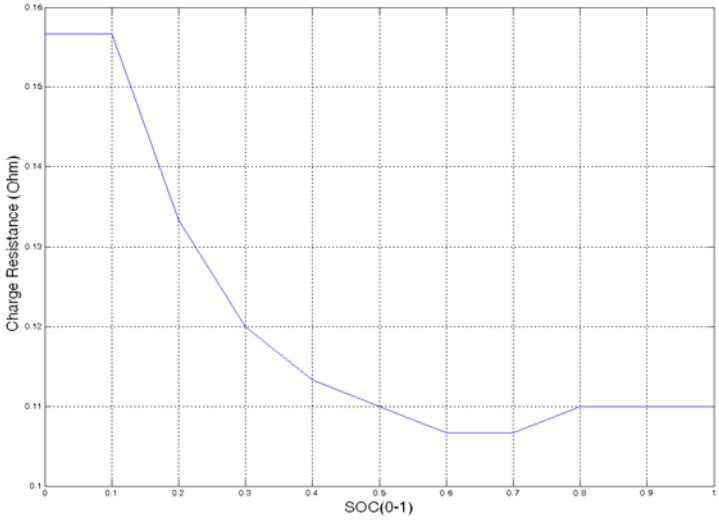

Figure 2.10 : SOC Versus Battery Internal Resistance for Charging(T=35C)

It is seen from Fig. 2.10 that SOC values between 0.6 and 0.7 (60 to 70 %) are ideal for charging the battery as they result in the smallest values of battery internal resistance. A similar characteristic is seen in Fig. 2.11 for discharging the battery. A SOC value of 0.6 (60%) is seen to be ideal for discharging the battery , i.e. moving the HEV using EM power.

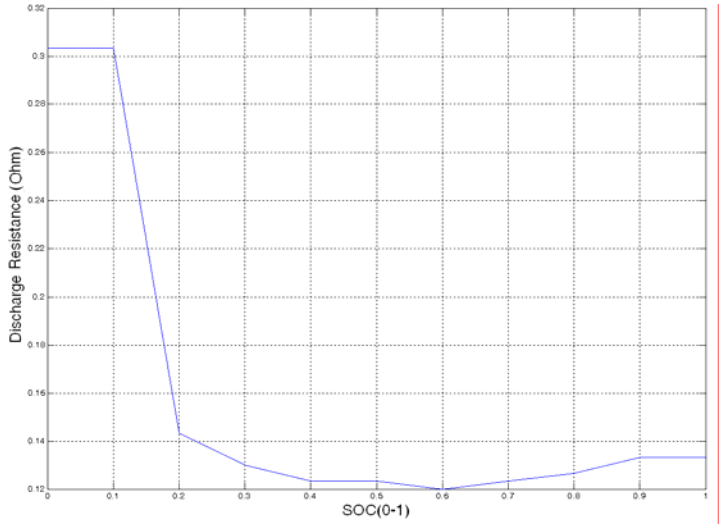

Figure 2.11 : SOC-Discharge Resistance (T=35C)

In the HEV model, it is important to analyse the battery efficiency at its operating points. Battery efficiency is formulated with the equation given below:

$$\eta_{bat} = \begin{cases} \dfrac{V_{oc} * I_{bat}}{V_{oc} * I_{bat} - I_{bat}^{2} * R_{\text{int}}} & if\ I_{bat} < 0 \\ \dfrac{V_{oc} * I}{V_{oc} * I_{bat} + I_{bat}^{2} * R_{\text{int}}} & if\ I_{bat} >= 0 \end{cases} \qquad \textbf{(2.7)}$$

In this equation, ratio of net power which enters to or is taken from the battery and sum of this with power loss in internal resistance is calculated and battery efficiency is obtained.

2.4 Driveline Components

The torque produced by the car's engine is not applied to the road directly; it passes through the driveline as shown in Fig. 2.12. The transmission, gearbox and differential are modeled as efficiencies here, i.e static power transmission devices with no transient dynamics.

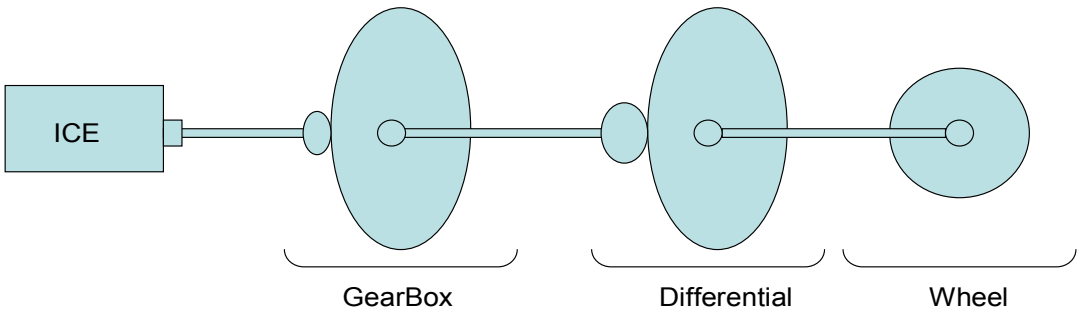

Figure 2.12 : Powertrain Components

2.4.1 Transmission Gearbox

The transmission gearbox is modeled with a constant efficiency η_{tr} value and different conversion ratio g_r values for different gear choices as shown in Fig. 2.13.

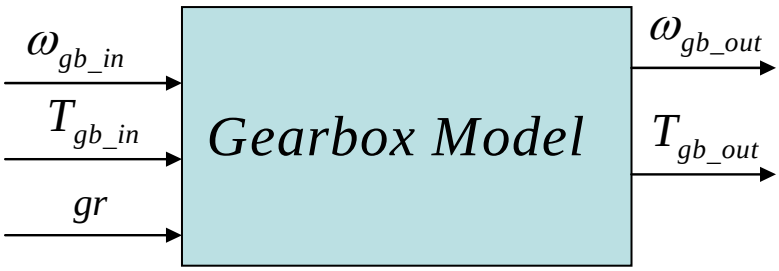

Figure 2.13 : Gearbox Model Inputs and Outputs

In the transmission gearbox model, gear number gn to gear ratio gr table is used for calculations as shown in Fig. 2.14. The gear number is the shift position between 1 and 6.

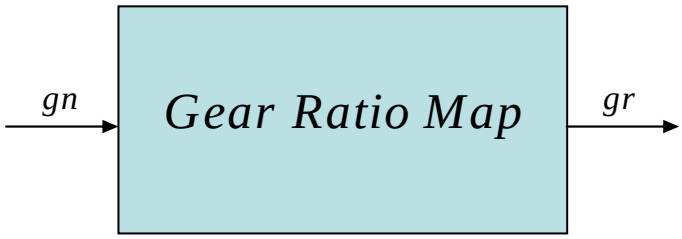

Figure 2.14 : Gear Number to Gear Ratio Map

Equations for gearbox are:

$$\omega_{gb\_out} = \frac{\omega_{gb\_in}}{gr} \tag{2.8}$$

$$T_{gb\_out} = T_{gb\_in} gr \eta_{tr} \tag{2.9}$$

2.4.2 Differential

The differential is modeled with a constant efficiency η_{diff} and a conversion ratio d_r and is illustrated in Fig. 2.15.

Figure 2.15 : Differential Model Inputs and Outputs

The model equations for the differential are:

$$\omega_{diff\_out} = \frac{\omega_{diff\_in}}{dr} \qquad \textbf{(2.10)}$$

$$T_{diff\_out} = T_{diff\_in} dr\, \eta_{diff} \qquad \textbf{(2.11)}$$

2.5 Augmented Nonlinear Single Track Vehicle Modeling Equations

The single track vehicle model augmented with longitudinal dynamics is illustrated in Fig. 2.16.

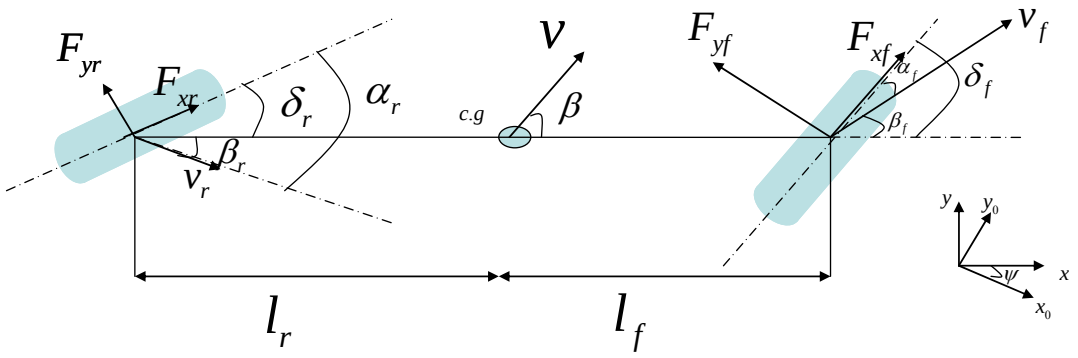

Figure 2.16 : Single Track Vehicle Model

The augmented single track model consists of tire, steering angle projection, lateral and longitudinal vehicle dynamics, kinematics and geometry and wheel velocity calculation subsystems[9].

2.5.1 Tire Model

Tires enable vehicle motion by providing for traction, braking, steering, and load support. Tires are inflated with air, which provides a flexible cushion between the vehicle and the road that smoothes out shock and provides for a comfortable ride.

Pacejka tire model is used for modeling tire of HEV. This model is based on the Pacejka Magic Formula which is obtained by empirical results. Outputs of model which are tire lateral and longitudinal forces and self aligning moment are given below.

2.5.1.1 Pacejka Longitudinal Force

$$F_{x(f,r)} = D\sin[C\arctan(Bs + Sh) - E(Bs + Sh) - \arctan(B(s + Sh)))] + S_v \qquad \textbf{(2.12)}$$

where ,

$$C = b_0 \tag{2.13}$$

$$D = \mu_p F_z \tag{2.14}$$

$$BCD = (b_3 F_z^2 + b_4 F_z) e^{-b_5 F_z} \tag{2.15}$$

$$E = b_6 F_z^2 + b_7 F_z + b_8 \tag{2.16}$$

$$S_h = b_9 F_z + b_{10} \tag{2.17}$$

$$S_V = 0 \tag{2.18}$$

Simulink implementation of this model is given in Fig. 2.17

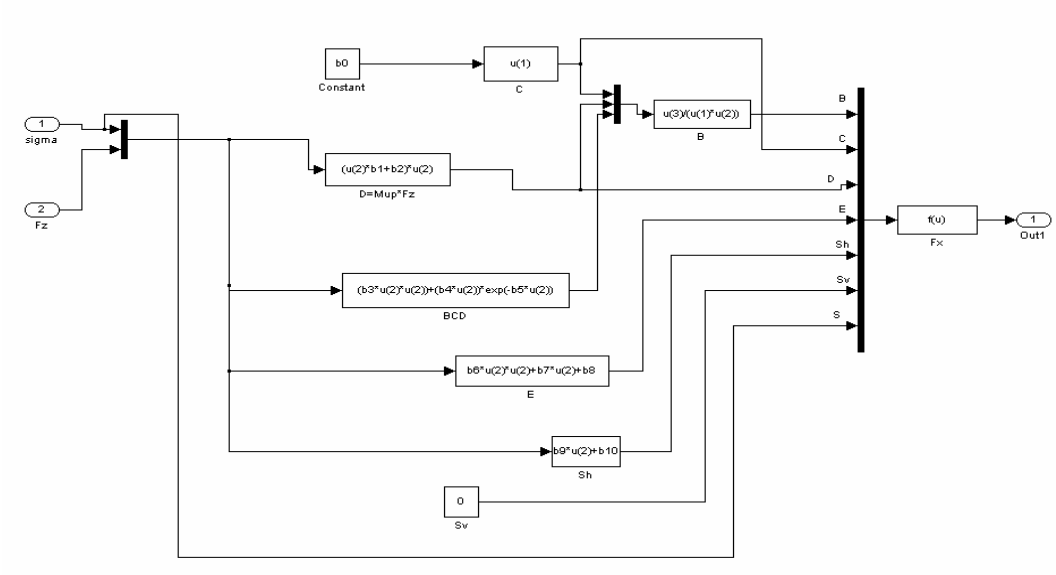

Figure 2.17 : Pacejka_Fx Subsystem

2.5.1.2 Pacejka Lateral Force

$$F_{y(f,r)} = Dsin[Carctan(B(a + Sh) - E(Ba - arctan(B(a + Sh))))] \tag{2.19}$$

Where;

$$C = a_0 \tag{2.20}$$

$$D = \mu_{yp} F_z \tag{2.21}$$

$$\mu_{yp} = a_1 F_z + a_2 \tag{2.22}$$

$$E = a_6 F_z + a_7 \tag{2.23}$$

$$a_{11} = a_{111} F_z + a_{112} \tag{2.24}$$

$$BCD = a_3 \sin[2\arctan(\frac{F_z}{a_4})](1\text{-}a_5 |\gamma|) \tag{2.25}$$

$$S_h = a_8 \gamma + a_9 F_z + a_{10} \tag{2.26}$$

$$S_v = a_{11_z} \gamma F_z + a_{12} F_z + a_{13} \tag{2.27}$$

Simulink implementation of this model is given in Fig. 2.18:

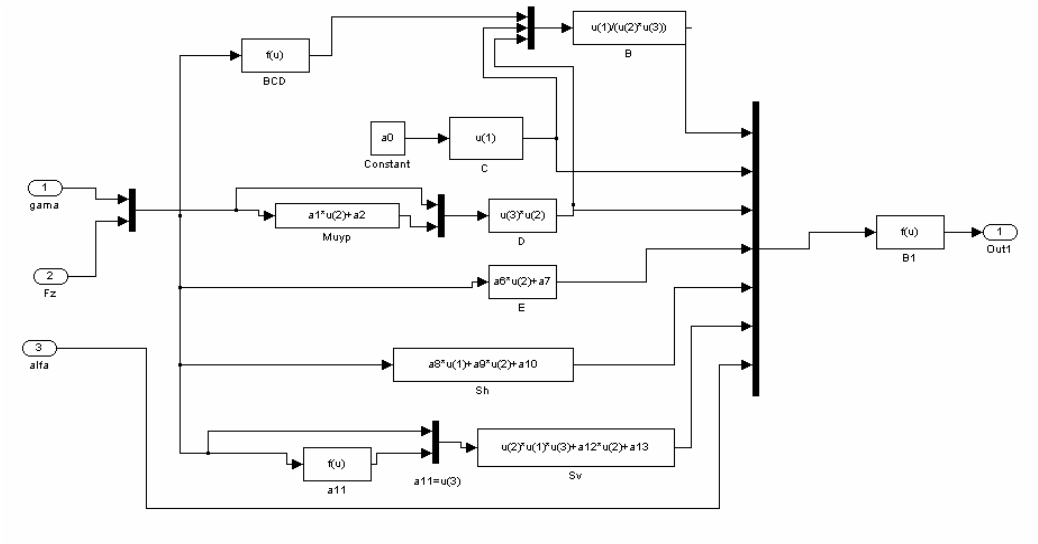

Figure 2.18 : Pacejka_Fy Subsystem

2.5.1.3 Self Aligning Moment

$$M_{z(f,r)} = D\sin(C\arctan\{B(1-E)(a+Sh)+E\arctan[B(a+Sh)]\})+Sv \tag{2.28}$$

Where;

$$C = c_0 \tag{2.29}$$

$$D = (c_1 F_z^{\,2} + c_2 F_z) \tag{2.30}$$

$$E = (c_7 F_z^{\,2} + c_8 F_z + c_9)(1\text{-}c_{10}\,|\gamma|) \tag{2.31}$$

$$BCD = (c_3 F_z^{\,2} + c_4 F_z)(1\text{-}c_6\,|\gamma|)e^{-c_5 F_z} \tag{2.32}$$

$$S_h = c_{11}\gamma + c_{12} F_z + c_{13} \tag{2.33}$$

$$S_v = (c_{14} F_z^{\,2} + c_{15} F_z)\gamma + c_{16} F_z + c_{17} \tag{2.34}$$

Simulink implementation of this model is given in Fig. 2.19.

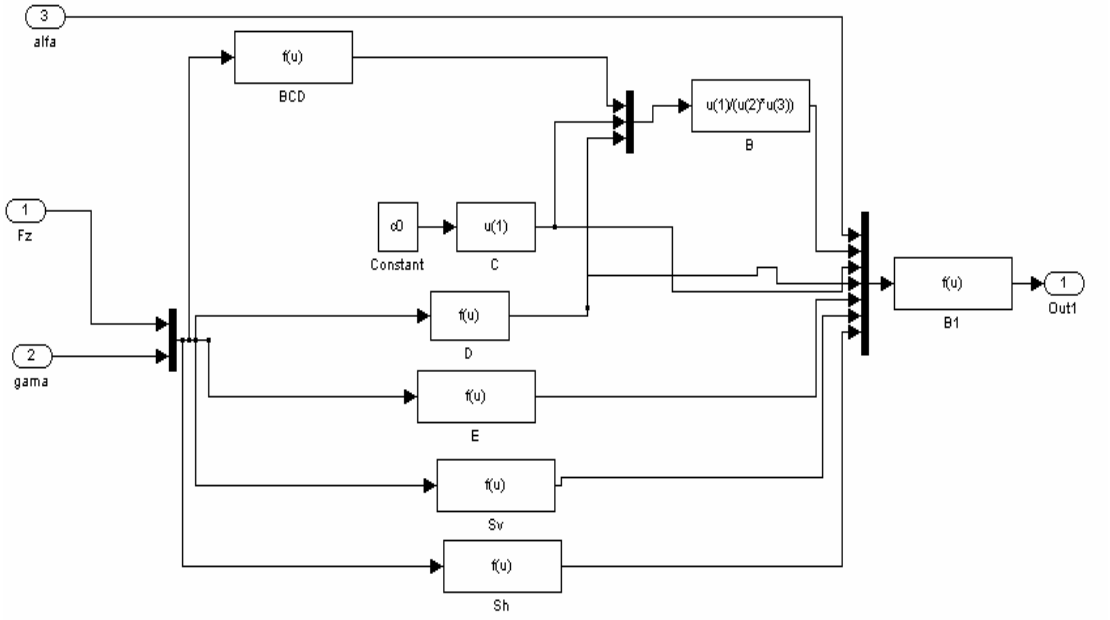

Figure 2.19 : Pacejka_Msa Subsystem

2 5.2 Steering Angle Projection

Steering angle projection block takes front wheel longitudinal force F_{xf}, front wheel lateral force F_{yf}, rear wheel longitudinal force F_{xr}, rear wheel lateral force F_{yr} and steering angles for rear and front wheels δ_f, δ_r to calculate the corresponding forces at the vehicle center of gravity F_x, F_y and M_Z. Here, wheel longitudinal and lateral

forces are projected on chassis coordinate axes. Forces and moment that affect vehicle chassis are calculated below in terms of wheel forces and steering angles .

$$F_x = -\sin(\delta_f)F_{yf} - \sin(\delta_r)F_{yr} + \cos(\delta_f)F_{xf} + \cos(\delta_r)F_{xr} \quad \textbf{(2.35)}$$

$$F_y = \cos(\delta_f)F_{yf} + \cos(\delta_r)F_{yr} + \sin(\delta_f)F_{xf} + \sin(\delta_r)F_{xr} \quad \textbf{(2.36)}$$

$$M_z = l_f \cos(\delta_f)F_{yf} - l_r \cos(\delta_r)F_{yr} + l_f \sin(\delta_f)F_{xf} - l_r \sin(\delta_r)F_{xr} \quad \textbf{(2.37)}$$

Simulink implementation of these calculations are given in Fig. 2.20.

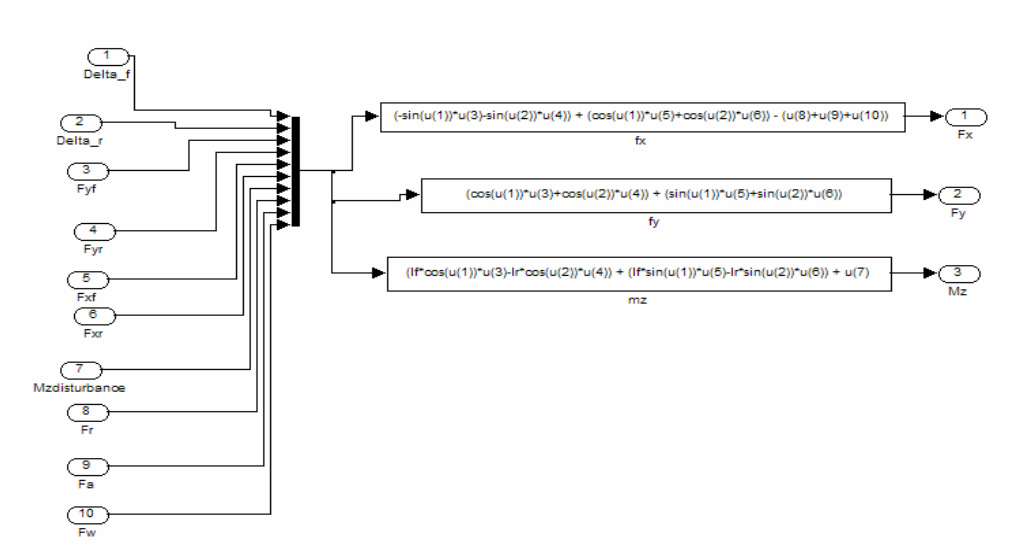

Figure 2.20: Steering Angle Projection Subsystem

2.5.3 Vehicle Dynamics

In this block vehicle side slip angle β vehicle speed v and yaw rate $\dot{\psi}$ are calculated using chassis forces F_x, F_y and yaw moment M_z. Formulation is given below.

$$\dot{\psi} = \int_{t_0}^{t} \frac{M_z}{J} dt \quad \textbf{(2.38)}$$

$$v = \int_{t_0}^{t} \frac{\cos(\beta)F_x + \sin(\beta)F_y}{m} dt \quad \textbf{(2.39)}$$

$$\beta = \int_{t_0}^{t} (\frac{-\sin(\beta)\mathrm{F_x} + \cos(\beta)F_y}{mv} - \psi)dt \qquad \textbf{(2.40)}$$

Simulink implementation of these calculations are given in Fig. 2.21.

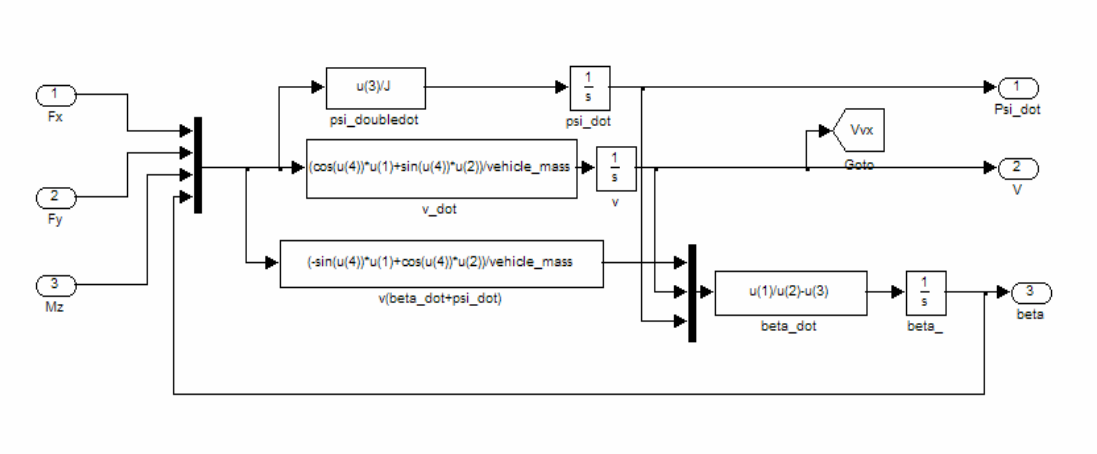

Figure 2.21: Vehicle Dynamics Subsystem

2.5.4 Kinematics and Geometry

This block calculates the angle between wheel speed and chassis for front and rear wheel β_f, β_r and slip ratios for front and rear wheels $slip_f, slip_r$ by using $F_x, F_y, M_z, \delta_f, \delta_r$ and wheel angular velocity values ω_f and ω_r. Formulation is given below.

$$\beta_f = \mathrm{atan}(\tan(\beta) + \frac{l_f\dot{\psi}}{v\cos(\beta)}) \qquad \textbf{(2.41)}$$

$$\beta_r = \mathrm{atan}(\tan(\beta) - \frac{l_r\dot{\psi}}{v\cos(\beta)}) \qquad \textbf{(2.42)}$$

$$v_{xf} = \sqrt{(v\cos(\beta))^2 + (v\sin(\beta) + \dot{\psi}l_f)^2}\,\cos(\delta_f - \beta_f) \qquad \textbf{(2.43)}$$

$$v_{xr} = \sqrt{(v\cos(\beta))^2 + (v\sin(\beta) - \dot{\psi}l_r)^2}\,\cos(\delta_r - \beta_r) \qquad \textbf{(2.44)}$$

$$slip_f = \frac{\omega_f \mathrm{R} - v_{xf}}{v_{xf}} \; slip_r = \frac{\omega_r \mathrm{R} - v_{xr}}{v_{xr}} \Leftrightarrow \omega_{f,r}\mathrm{R} < v_{xr}\,(Braking) \qquad \textbf{(2.45)}$$

$$slip_f = \frac{\omega_f R - v_{xf}}{\omega_f R} \; slip_r = \frac{\omega_r R - v_{xr}}{\omega_r R} \Leftrightarrow \omega_{f,r} R > v_{xr} \; (Accelerating) \qquad \textbf{(2.46)}$$

Simulink implementation of these calculations are given in Fig. 2.22.

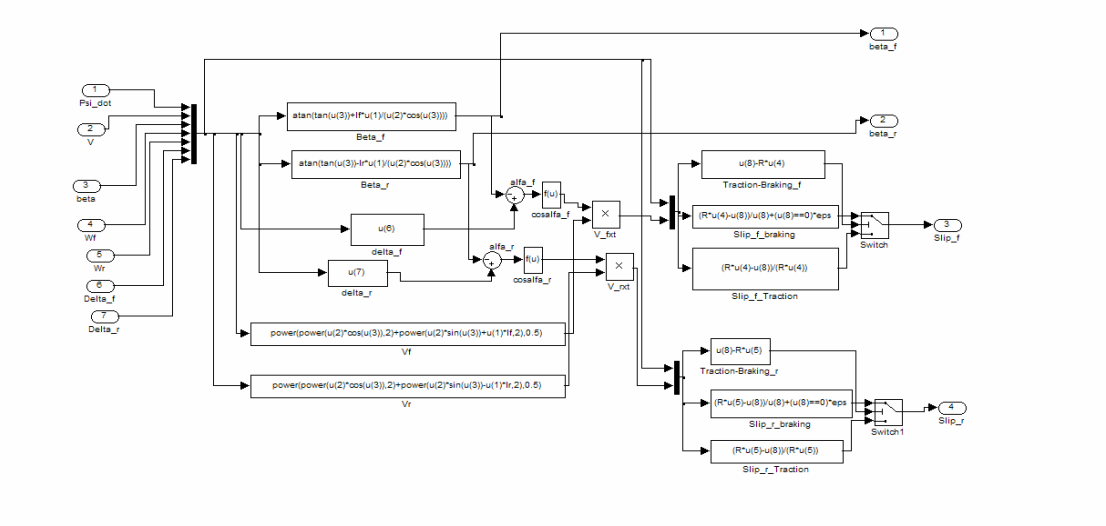

Figure 2.22 : Kinematics and Geometry Subsystem

2.5.5 Wheel Velocity Calculation

This block calculates the wheel angular velocity values ω_f , ω_r. by using wheel longitudinal forces F_{xf} , F_{xr}, torques that act on wheel axes T_f , T_r and tire inertia J_{tire}. Formulation is given below.

$$\omega_f = \int_{t_0}^{t} \frac{T_f - F_{xf} R}{J_{tire}} dt \qquad \textbf{(2.47)}$$

$$\omega_r = \int_{t_0}^{t} \frac{T_r - F_{xr} R}{J_{tire}} \qquad \textbf{(2.48)}$$

Simulink implementation of these calculations are given in Fig. 2.23.

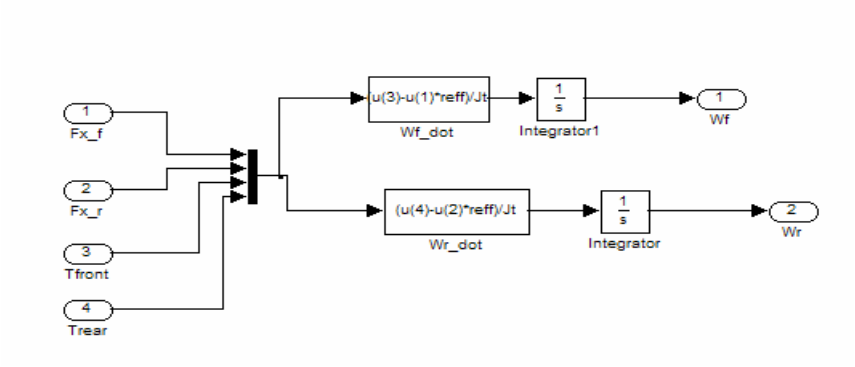

Figure 2.23: Wheel Angular Velocity Calculation Subsystem

3. HYBRID ELECTRIC VEHICLE MODELING USING CARMAKER

3.1 About Carmaker

CarMaker is a simulation and analysis software program which includes reliable vehicle model. A graphical user interface screenshot is given in Fig. 3.1. This model includes the powertrain, chassis, suspension, tire, brake and all other vehicle subsystems. But special components like battery and electric motors are not modeled in this software for a hybrid electric vehicle.

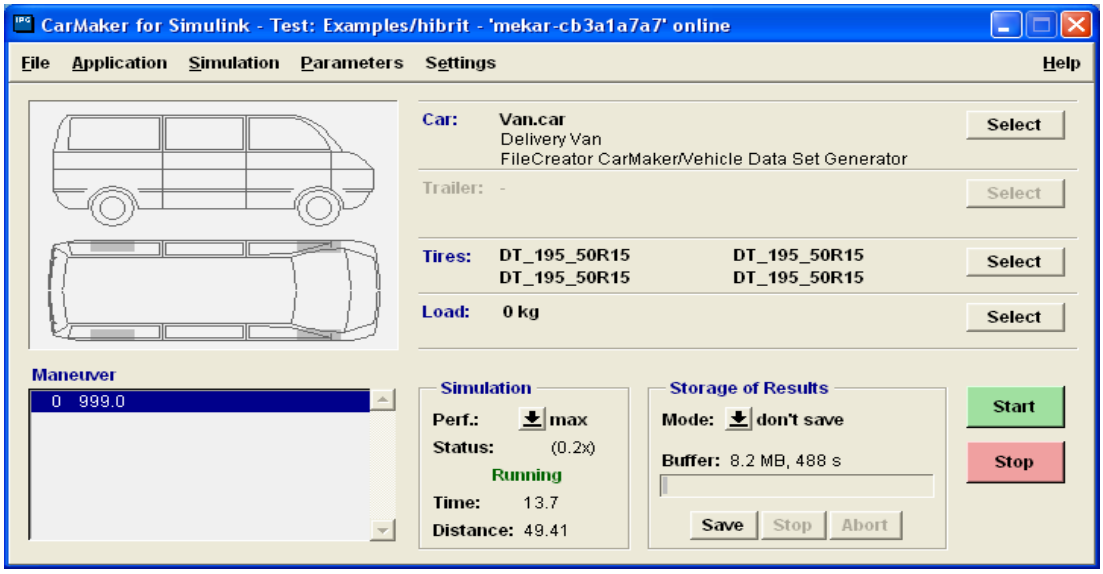

Figure 3.1 : CarMaker General Graphical User Interface

Detailed vehicle parameters can be integrated into vehicle models. Interface for parameter settings is shown in Fig. 3.2.

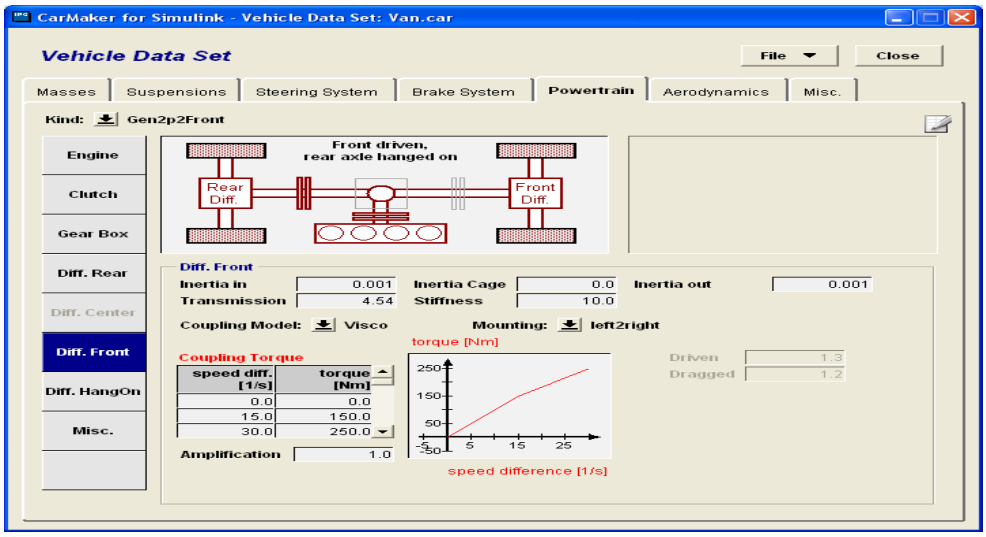

Figure 3.2 : Parameter Setting Interface Page of CarMaker

Vehicle movements can be observed with its visual interface, “IPG Movie” software. Longitudinal, lateral and vertical wheel forces can also be observed with this visuality. A screenshot from IPG Movie is shown in Fig. 3.3.

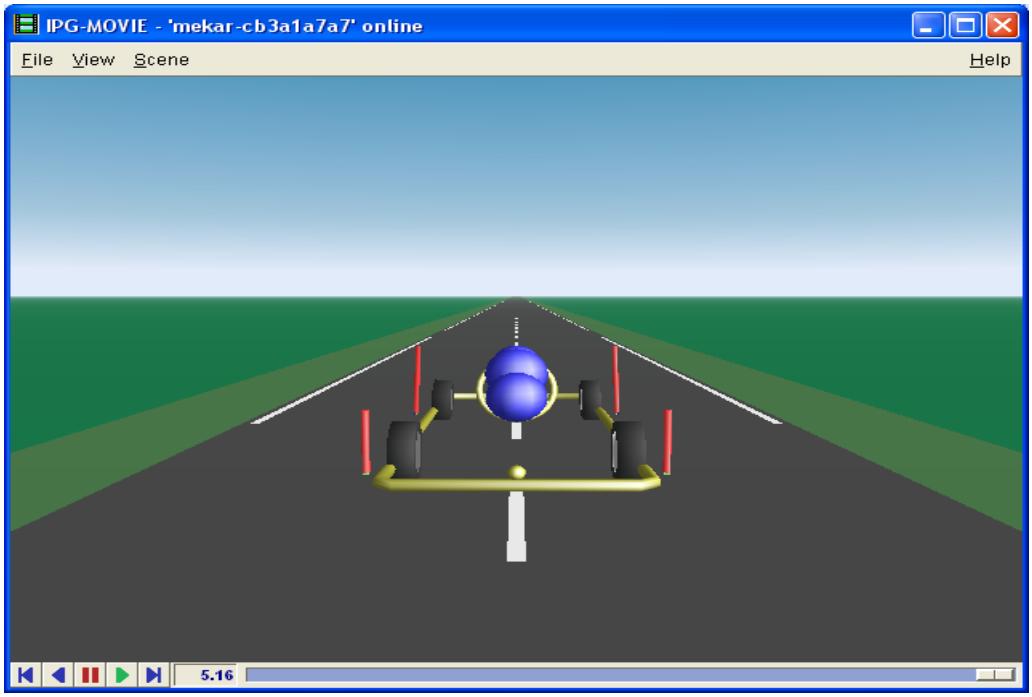

Figure 3.3 : CarMaker Animation, “IPG Movie”

3.2 CarMaker Adaptation for Modeling Hybrid Electric Vehicle

First of all, there is no hybrid powertrain in CarMaker powertrain library. The desired powertrain is hown in Fig. 3.4.

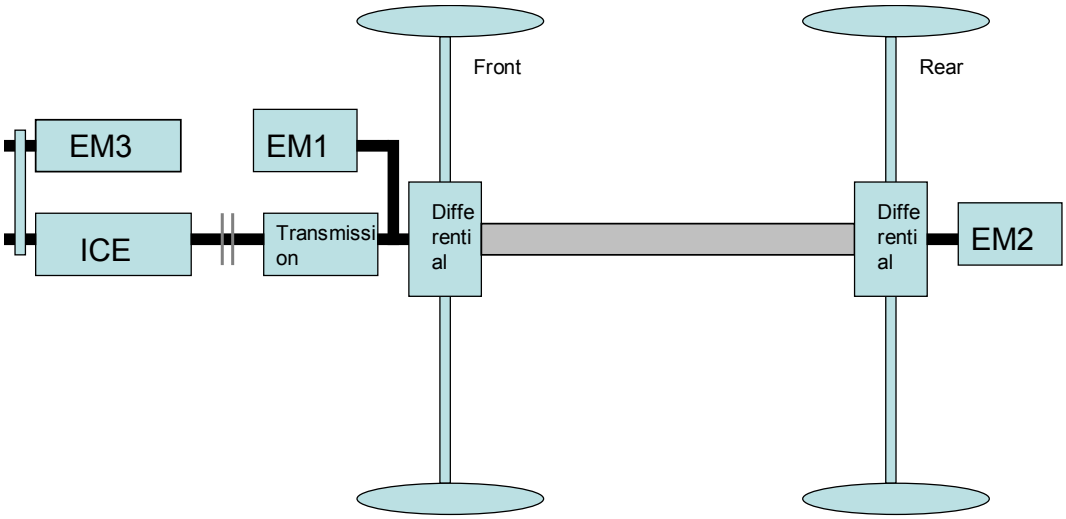

Figure 3.4 : Desired Powertrain of HEV

To model this hybrid powertrain, first a 4WD (Front driven rear axle hand on) powertrain is selected from library. This powertrain can be seen in Fig. 3.5.

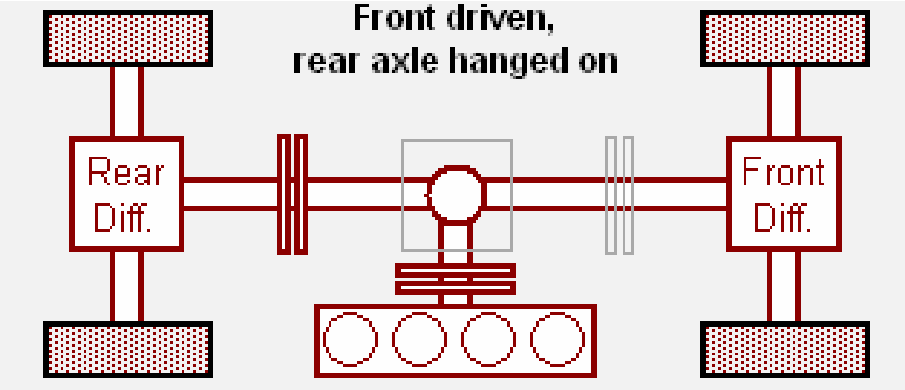

Figure 3.5 : Front Driven Rear Axle Hanged on Powertrain

Rear clutch is opened and torque transmission from engine to rear axle is cancelled. So, rear electric motor torque can be written into "PT.Gen.DL.HangOn.Trq_Cpl2B" and front electric motor torque is written into "PT.GearBox.Trq_ext2GBout" variables directly (See Fig. 3.6).

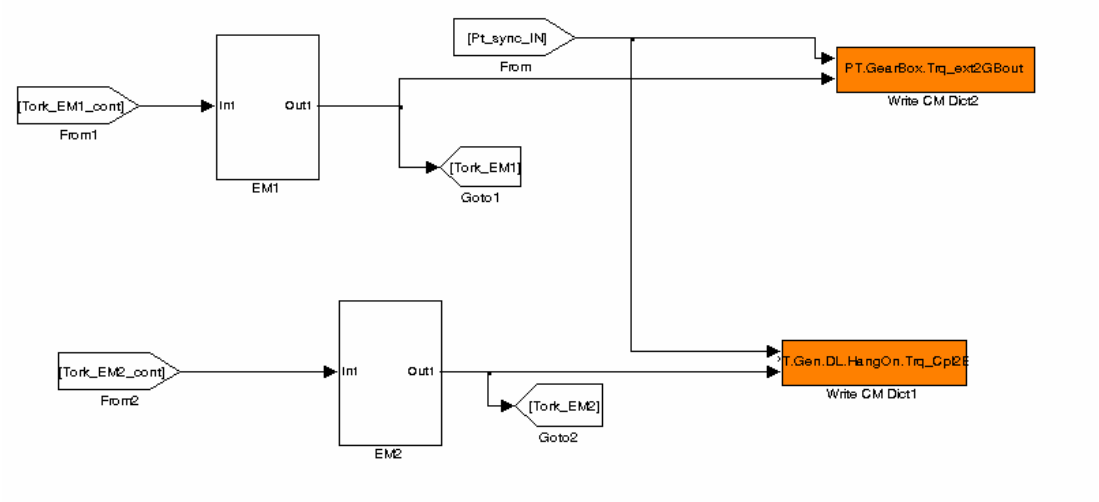

Figure 3.6 : Additional Torques for EM1 and EM2

Other electric motor EM3 is directly connected to ICE. So, this motor torque is superimposed on ICE torque in the Simulink. Block diagram is shown in Fig. 3.7.

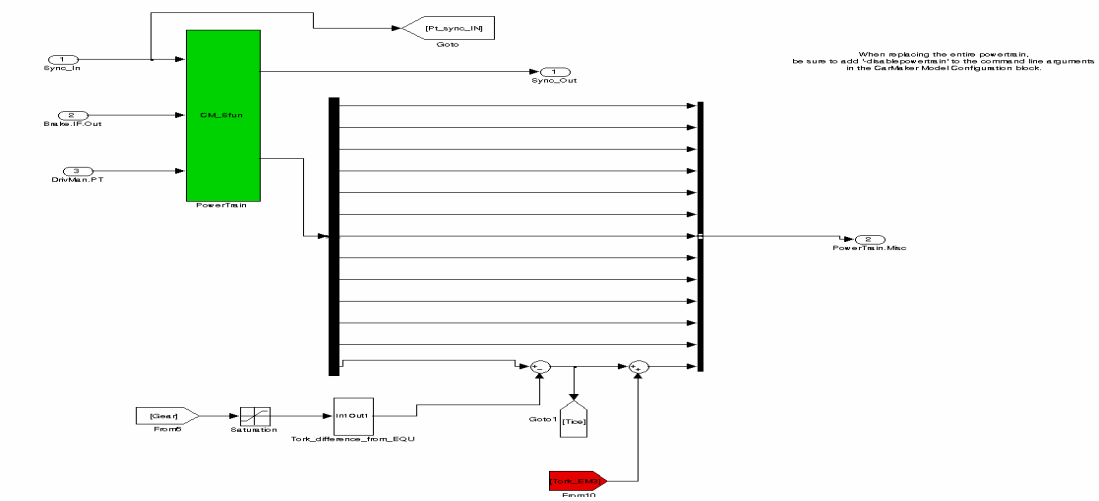

Figure 3.7 : Addition of EM3 Torque

Another adaptation is for ICE parameters. Desired parameters of ICE shown in Fig. 3.8 are changed by using ICE parameter setting page. Pedal position, ICE speed, ICE torque map are changed into desired values. Also idle speed value, speed range and engine inertia values are changed.

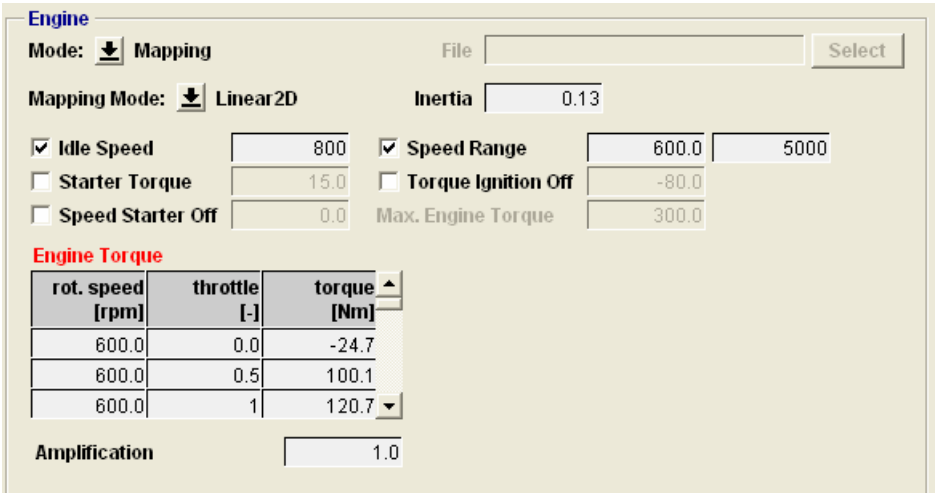

Figure 3.8 : ICE Parameter Setting Page

In a real vehicle, the electronic control unit (ECU) uses different torque maps for each gear number. But Carmaker has a constant pedal position, ICE speed -ICE torque map. For this reason additional blocks which calculate the difference of constant map and real maps are constructed. This difference is then subtracted from engine torque in Simulink. This is illustrated in Fİg. 3.9.

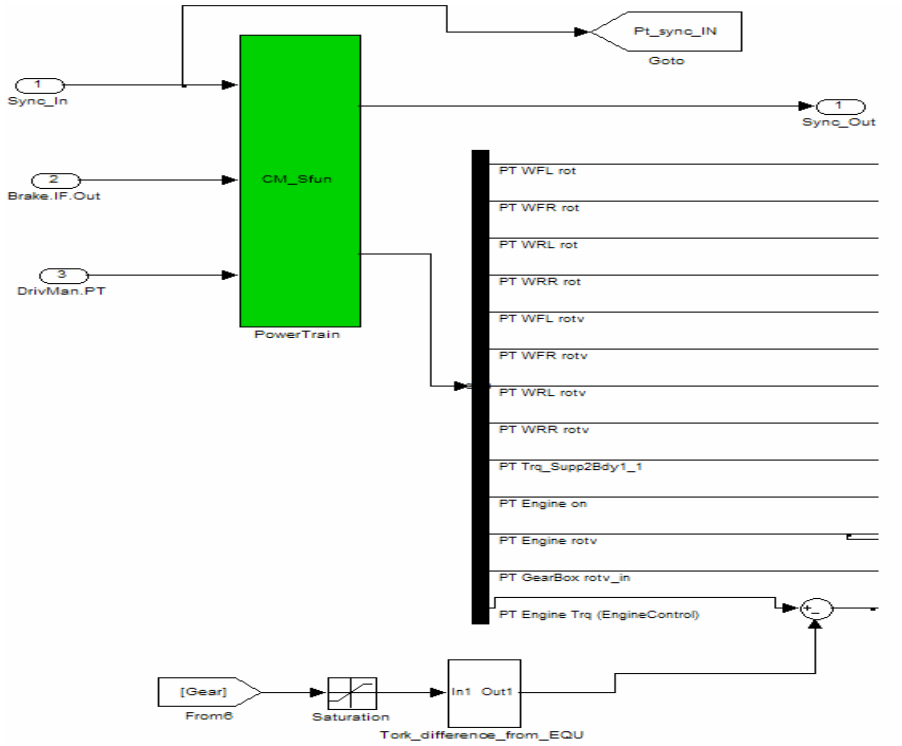

Figure 3.9 : Torque Map Adjusting for Each Gear Number

As mentioned before, CarMaker doesn't include electric motor and battery models. These should be modeled separately. Modeling of these components were explained

in sections 2.2 and 2.3. CarMaker vehicle model and additional blocks for HEV modeling are shown in figure below.

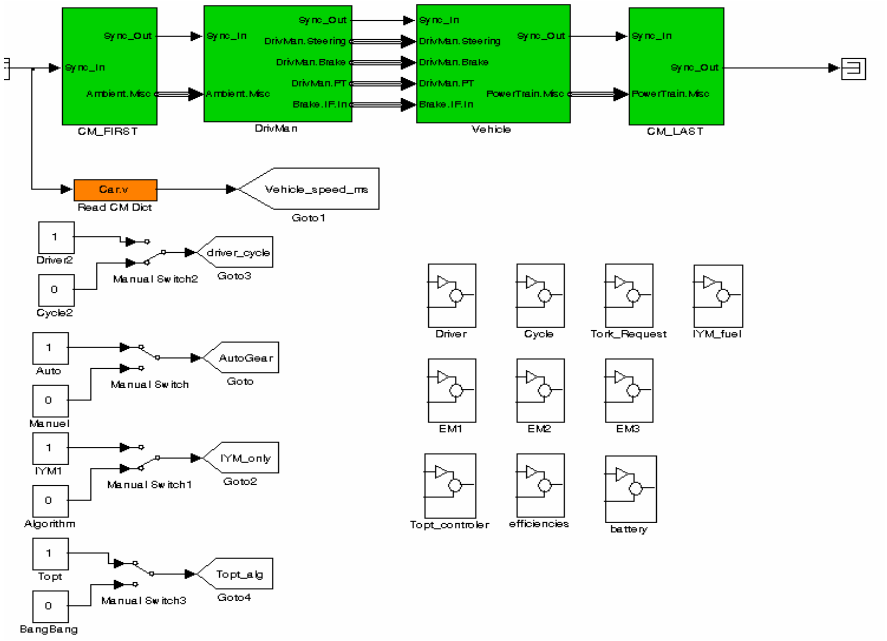

Figure 3.10 CarMaker Vehicle Model and Additional Blocks for HEV Modeling

4. MAXIMIZING OVERALL EFFICIENCY STRATEGY (MOES) FOR HYBRID ELECTRIC VEHICLE

4.1 Objective

Main idea of the hybrid electric vehicle power split strategy is to operate all power sources at their most efficient operating points. But this is not as easy as it is seen because all sources are depend on each other. One must also consider the efficiency of the drivelines. Dynamic programming can be used to solve this problem [14, 15]. Most efficient combinations of power split can be calculated using dynamic programming but there are two main problems with this technique. One of them is that the driver request in the future can not be known a priori and exactly. Even if the driver request could be properly estimated, the other problem is the necessity of very high computational power, depending on the estimation horizon. This makes dynamic programming a hard to apply solution for real time control.

For real time applications, Maximizing Overall Efficiency Strategy (MOES) which maximizes overall efficiency of vehicle by making some efficiency assumptions from previous operating points of power sources is more applicable than dynamic programming. This approach has some similarities with equivalent fuel consumption minimization strategy (ECMS) [5, 6, 16, 17]. The main difference of MOES is its formulation. Overall efficiency term states the efficiency value from fuel tank to wheels. This efficiency value is calculated by using instantaneous and average efficiencies of the components which are internal combustion engine, electric motors, battery and mechanical efficiencies of the vehicle. With MOES, vehicle is thought as a system and overall efficiency of the vehicle which is changing between 0 and 1 is more meaningful to analyze the vehicle. Another difference of MOES comes from the percentage of parallel charge to regenerative braking Per_{pch} value. This is a new definition. This value is a factor for electric motors to consume the electric power easy or hard. In this algorithm, vehicle states are divided into two main parts, charging and discharging. For the stability of the automatic clutch which

connects the ICE to the drivetrain, SOC is oscillated between the desired limits. This oscillation has an hysteresis effect on the automatic clutch system and avoids the chattering.

In this strategy, the vehicle is considered a system whose input is power of consumed fuel P_{fuel_real} and output is power which is transferred to the road P_{road_real} as illustrated in Fig.4.1. Content of P_{fuel_real} and P_{road_real} vary according to charge and discharge conditions.

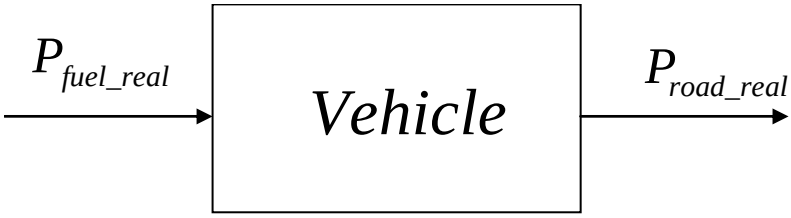

Figure 4.1 : System Input and Output.

Optimal operating points of components are found by maximizing the net overall efficiency of system η_{SYS}. η_{SYS} is calculated as:

$$\eta_{SYS} = \frac{P_{road\_real}}{P_{fuel\_real}} \qquad \textbf{(4.1)}$$

If power of the controller's processor is not enough for MOES calculations in real time, these calculations can be carried out offline. Then the results can be used in tables for real time applications as explained at the end of this chapter.

4.2 Operation of the MOES Algorithm

The algorithm has 3 main modes: Battery charging, battery discharging and regenerative braking. The algorithm flowchart is shown in Fig. 4.2.;

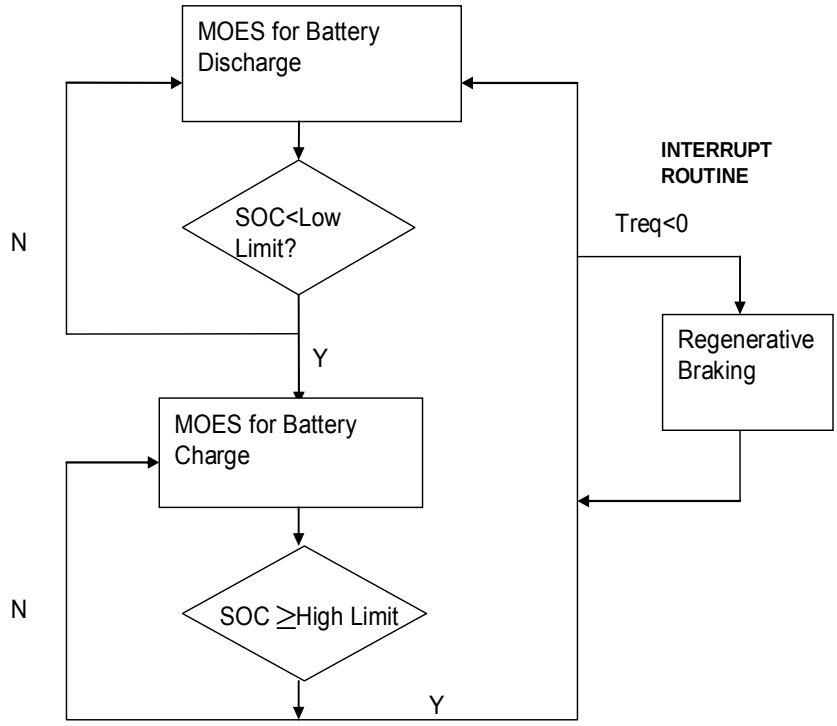

Figure 4.2 : Flowchart of Algorithm

Depending on the SOC value, one of the two modes of MOES charge or MOES discharge is activated. If required torque from driver is negative, regenerative braking mode is activated regardless of other conditions. This means that regenerative braking acts as an interrupt for the algorithm.

With this algorithm the SOC value oscillates between its high limit SOC_{hl} and low limit SOC_{ll} depending on when regenerative braking is activated. Fig. 4.3 shows that SOC passes over the high limit for a short time period.

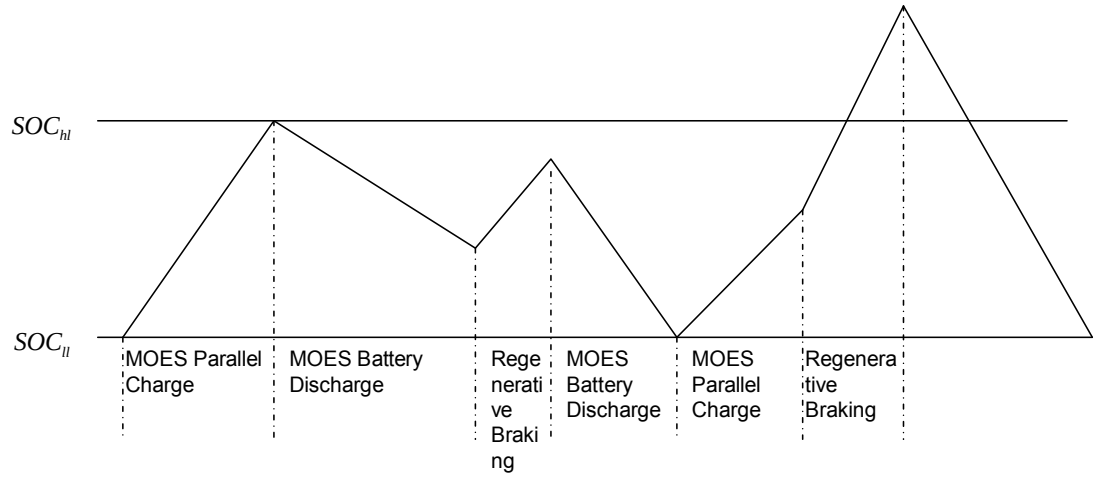

Figure 4.3 : SOC Oscillating in MOES Algorithm

Even if braking continuously for long time is a very low possibility for a vehicle, it may happen. Coasting down a very high hill can be an example of this situation. To avoid batteries from overcharging in such an extraordinary condition, a high security limit SOC_{slh} is added to the algorithm. When SOC exceeds this value, regenerative power is consumed on a resistor to avoid further SOC increases. Fig. 4.4. shows this condition.

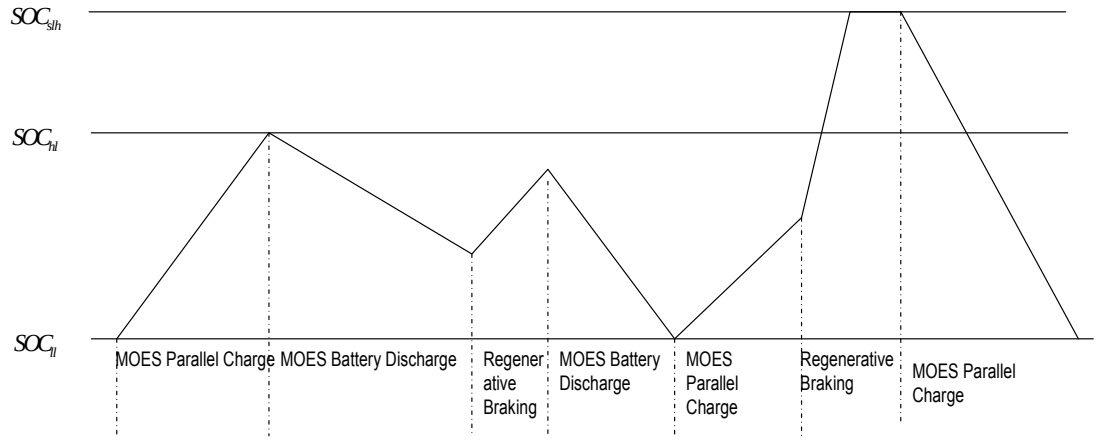

Figure 4.4 : SOC Oscillating in MOES Algorithm with Security Limit

4.3 Vehicle Architecture

In this thesis, the MOES algorithm is used in the vehicle configuration which is given in Fig. 4.5.

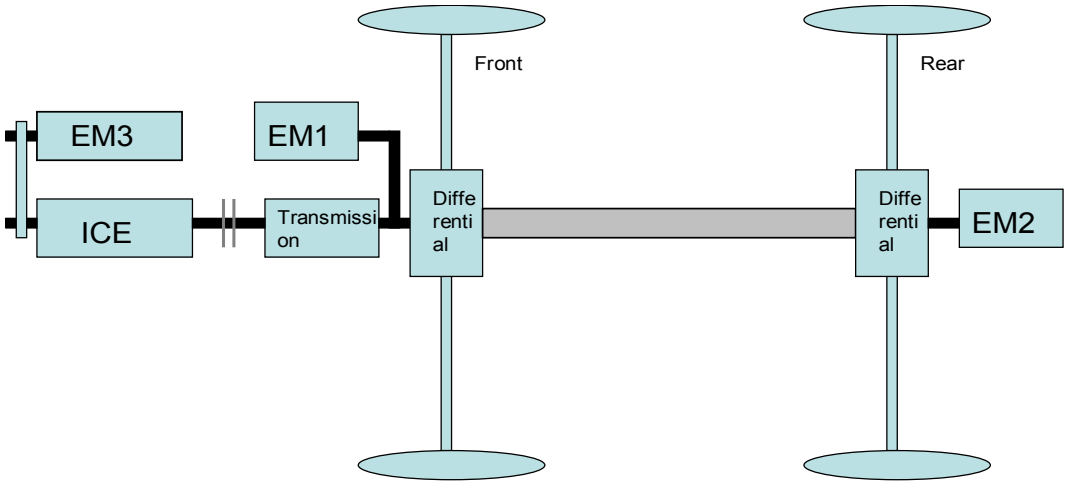

Figure 4.5 : Vehicle Architecture

EM3 is used for parallel charge. EM1 and EM2 is used for battery discharging and regenerative braking.

4.4 Driveline and Component Efficiencies

Nine efficiency values are defined for calculations in this architecture. These efficiencies are illustrated in Figure 4.6. Mechanical efficiencies of transmission η_{tr} and differential η_{diff} are assumed to be constant.

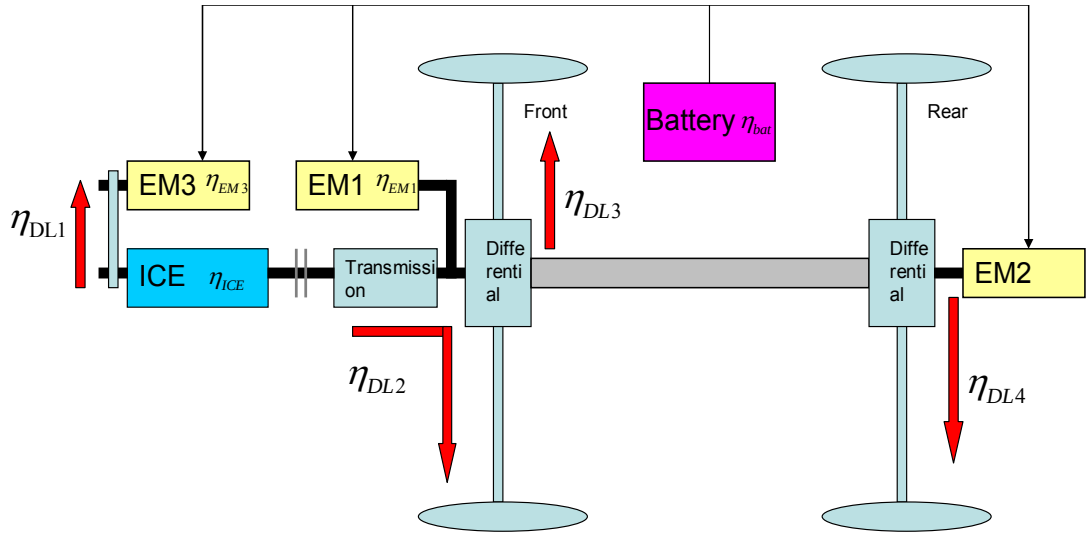

Figure 4.6 : Driveline and Component Efficiencies

η_{DL1} is the mechanical connection efficiency value between ICE and EM3. In this vehicle, a belt mechanism is planned between EM3 and the ICE. So, the efficiency of this belt mechanism is η_{DL1}.

$$\eta_{DL1} = \eta_{belt} \qquad \textbf{(4.2)}$$

η_{DL2} is the efficiency of the mechanical systems between the ICE and the front wheels. So, η_{DL2} is related to transmission and front differential efficiencies.

$$\eta_{DL2} = \eta_{trans}\eta_{diff_f} \qquad \textbf{(4.3)}$$

η_{DL3} is the efficiency of the mechanical system between EM1 and the front wheels. So, η_{DL3} is related with only front differential efficiency.

$$\eta_{DL3} = \eta_{diff_f} \qquad \textbf{(4.4)}$$

η_{DL4} is the efficiency of the mechanical system between EM2 and wheels. So, η_{DL4} is related with only rear differential efficiency.

$$\eta_{DL4} = \eta_{diff_r} \quad \textbf{(4.5)}$$

There are also component efficiencies that are:

η_{BAT} : Efficiency of battery.

η_{EM1} : Efficiency of electric motor 1

η_{EM2} : Efficiency of electric motor 2

η_{EM3} : Efficiency of electric motor 3

η_{ICE} : Efficiency of internal combustion engine

4.5 Constraints

There are some constraints for optimizing the torque distribution. These constraints come from the physical limits of the components. These limits are given in Table 4.1.

Table 4.1 Constraints of the Components

COMPONENT	LIMIT	CONSTRAINT
ICE	Torque	$T_{ice\_min} < T_{ice} < T_{ice\_max}$
EM1	Torque	$T_{EM1\_min} < T_{EM1} < T_{EM1\_max}$
EM2	Torque	$T_{EM2\_min} < T_{EM2} < T_{EM2\_max}$
EM3	Torque	$T_{EM3\_min} < T_{EM3} < T_{EM3\_max}$
BATTERY	Current	$I_{bat\_min} < I_{bat} < I_{bat\_max}$
BATTERY	State of Charge	$SOC_{sll} < SOC < SOC_{slh}$

In this thesis charge and discharge mean charging and discharging of the battery, respectively. The charging and discharging algorithms in MOES are different and are explained in the following two subsections.

4.6 Charge Condition in MOES

The power flow for charging is illustrated in the flowchart of Fig.4.7.

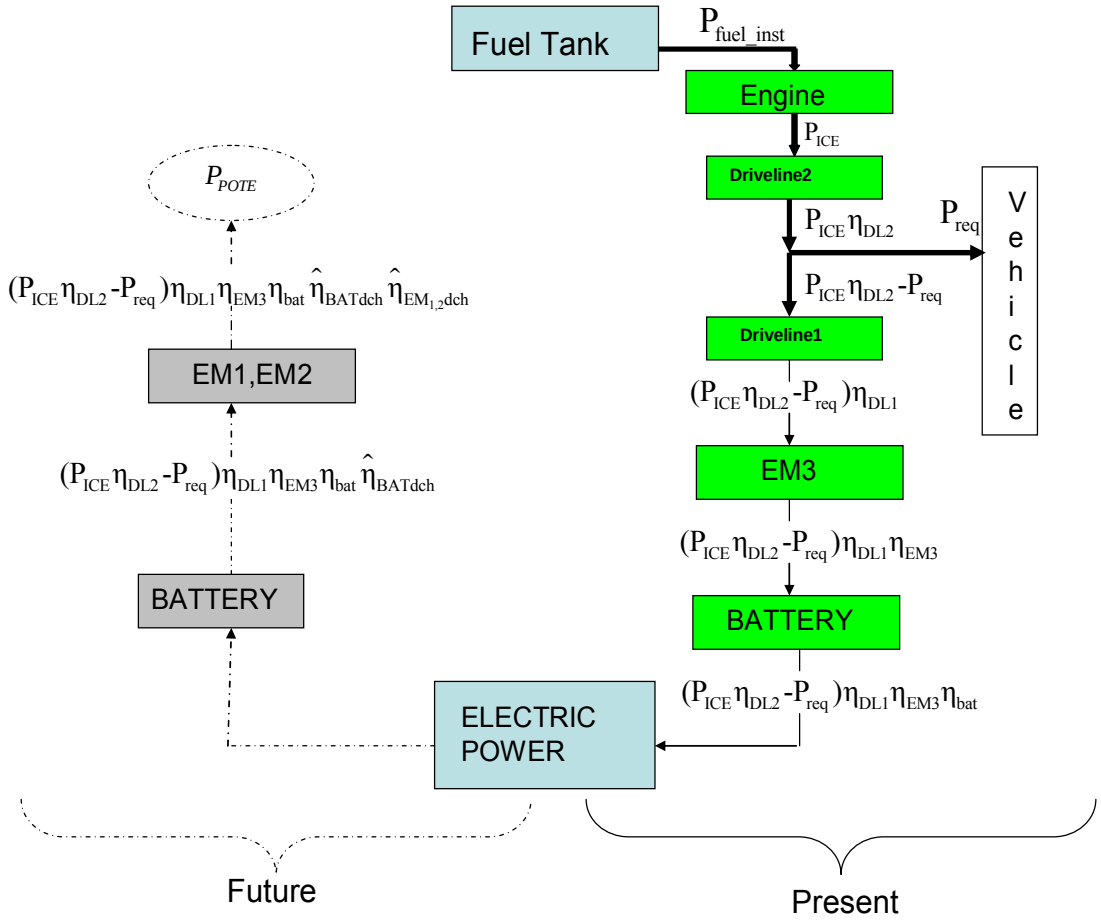

Figure 4.7 : Power Flow with Efficiencies for Parallel Charge

Here the system input is defined as the instantaneous power of fuel P_{fuel_inst}. The system output is defined as the sum of the requested power from the ICE (which is equal to tractive power part of ICE) P_{req}, and the potential mechanical power of stored electric power from parallel charging which will be used at a later instant of time P_{POTE}.

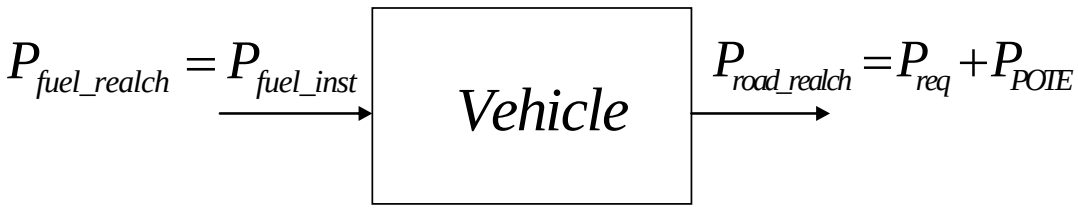

Figure 4.8 : System Input and Output for Parallel Charging

Overall charge efficiency can be found by:

$$\eta_{SYSch} = \frac{P_{road\_realch}}{P_{fuel\_realch}} \quad \textbf{(4.6)}$$

System output P_{road_realch} is defined as the sum of P_{req} and P_{POTE} because charged electric power is power capacity that can be used in the future. So the mechanical power which is given to the wheels must be thought of as this potential power:

$$P_{road\_realch} = P_{req} + P_{POTE} \quad \textbf{(4.7)}$$

As illustrated in Fig. 4.8, system input P_{fuel_realch} is defined as instantaneous fuel power of system and results in the power P_{ICE} at the output of the engine as:

$$P_{fuel\_inst} = \frac{P_{ICE}}{\eta_{ICE}(T_{ICE}, \omega_{ICE})} \quad \textbf{(4.8)}$$

$$P_{fuel\_realch} = P_{fuel\_inst} = \frac{P_{ICE}}{\eta_{ICE}(T_{ICE}, \omega_{ICE})} \quad \textbf{(4.9)}$$

Potential electric power is calculated below, with the efficiencies shown in fig.4.7 :

$$P_{POTE} = (P_{ICE}\eta_{\mathrm{DL2}} - P_{req})\eta_{DL1}\eta_{EM3}(T_{EM3}, \omega_{EM3})\eta_{BAT}(I_{bat}, SOC)\hat{\eta}_{BATdch}\hat{\eta}_{EM_{1,2}dch} \quad \textbf{(4.10)}$$

$\hat{\eta}_{BATdch}$ and $\hat{\eta}_{EM_{1,2}dch}$ values are the average battery discharge efficiency and average electric motors discharge efficiency respectively. These values are calculated during the discharge mode of vehicle and they are updated along the whole drive cycle. Instant electric power that is being stored into batteries is assumed to be discharged with these average efficiencies in the future.

From here, $\hat{\eta}_{BATdch}\hat{\eta}_{EMdch}$ value is performed with "K_{dch}" for simplicity.

$$K_{dch} = \hat{\eta}_{BATdch}\hat{\eta}_{EM_{1,2}dch} \quad \textbf{(4.11)}$$

In order to find the P_{road_realch} in equation 4.6, substitute the equations 4.10 and 4.11

into equation 4.7 for P_{POTE} to obtain:

$$P_{road\_realch} = P_{req} + (P_{ICE}\eta_{DL2} - P_{req})\eta_{DL1}\eta_{EM3}(T_{EM3}, \omega_{EM3})\eta_{BAT}(I_{bat}, SOC)K_{dch} \quad \textbf{(4.12)}$$

Substitute from (4.8) and (4.12) into (4.6) to obtain:

$$\eta_{SYSch} = \frac{P_{req} + (P_{ICE}\eta_{DL2} - P_{req})\eta_{DL1}\eta_{EM3}(T_{EM3}, \omega_{EM3})\eta_{BAT}(I_{bat}, SOC)K_{dch}}{\frac{P_{ICE}}{\eta_{ICE}(T_{ICE}, \omega_{ICE})}} \quad \textbf{(4.13)}$$

Here, speed of ICE is constant so power values can be thought as torques:

$$\eta_{SYSch} = \frac{T_{req} + (T_{ICE}\eta_{DL2} - T_{req})\eta_{DL1}\eta_{EM3}(T_{EM3}, \omega_{EM3})\eta_{BAT}(I_{bat}, SOC)K_{dch}}{\frac{T_{ICE}}{\eta_{ICE}(T_{ICE}, \omega_{ICE})}} \quad \textbf{(4.14)}$$

This is the overall charge efficiency of vehicle. Aim is to find the optimum torque of the ICE. When (4.14) is maximized, optimum EM torque will automatically be found because T_{req} is constant.

$$T_{optICEch} = \arg\max_{(T_{ICE})} \left| (\eta_{SYSch}) \right. \quad \textbf{(4.15)}$$

$$T_{optEM3ch} = (T_{req} - T_{optICEch}\eta_{DL2})\eta_{DL1} \quad \textbf{(4.16)}$$

But there are three constraints, one of them comes from ICE torque $T_{ICEmax}(W_{ICE})$, other one comes from EM3 torque $T_{EM3\min}(\omega_{EM3})$ and last one comes from battery current $I_{bat\_\min}$. Torque combinations don't pass over battery current limits because batteries have capability of taking maximum power from the electric motor . Then determinative limit is calculated by:

$$T_{limICEch} = min(T_{ICEmax}(\omega_{ICE}), T_{req} + T_{EM3max}(\omega_{EM3})) \quad \textbf{(4.17)}$$

η_{SYSch} value is calculated by changing T_{ICE} value between T_{req} and $T_{limICEch}$. Lower limit of T_{ICE} is T_{req} because ICE can not charge the batteries below the required torque value. $T_{ICE\max}(\omega_{ICE})$ is the maximum torque value that can be provided by

ICE at an instant speed. $T_{EM3\max}(\omega_{EM3})$ is maximum electric motor torque that can be taken at instant speed. The optimum ICE torque search algorithm for charging is illustrated in Fig. 4.9.

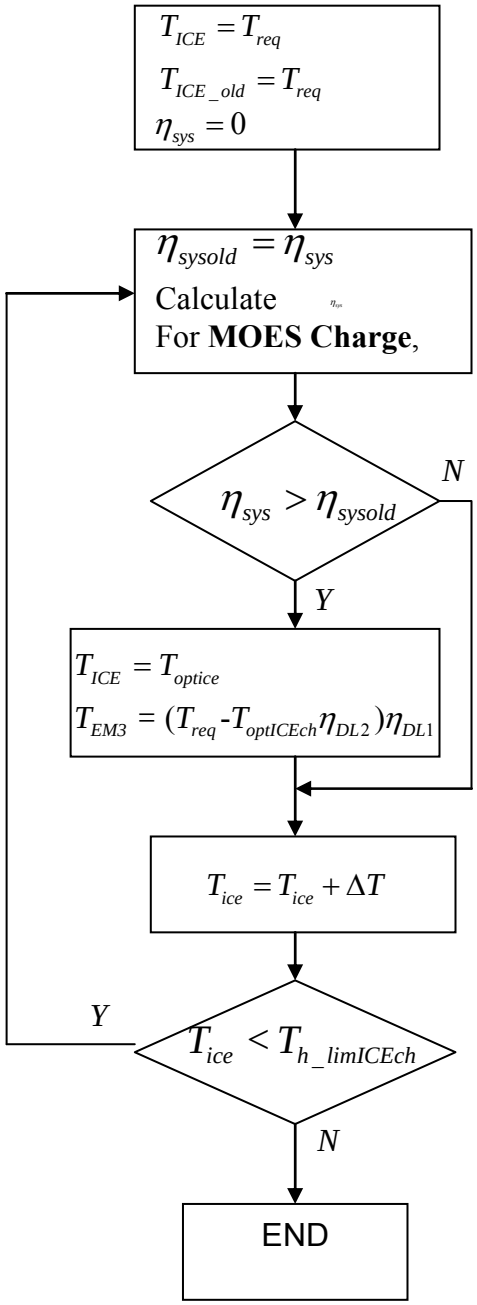

Figure 4.9 : Flowchart of MOES Charge

$T_{h\_limICEch}$ is the high limit of the ICE torque for search algorithm. This limit comes from ICE's maximum available torque $T_{ICE\max}(\omega_{ICE})$ or maximum EM3 charge torque as:

$$T_{h\_limICEch} = \min(T_{ICE\max}(\omega_{ICE}), T_{req} + T_{EM3\max}(\omega_{EM3})) \quad \textbf{(4.18)}$$

The searching process for MOES charge is shown in Fig. 4.10.

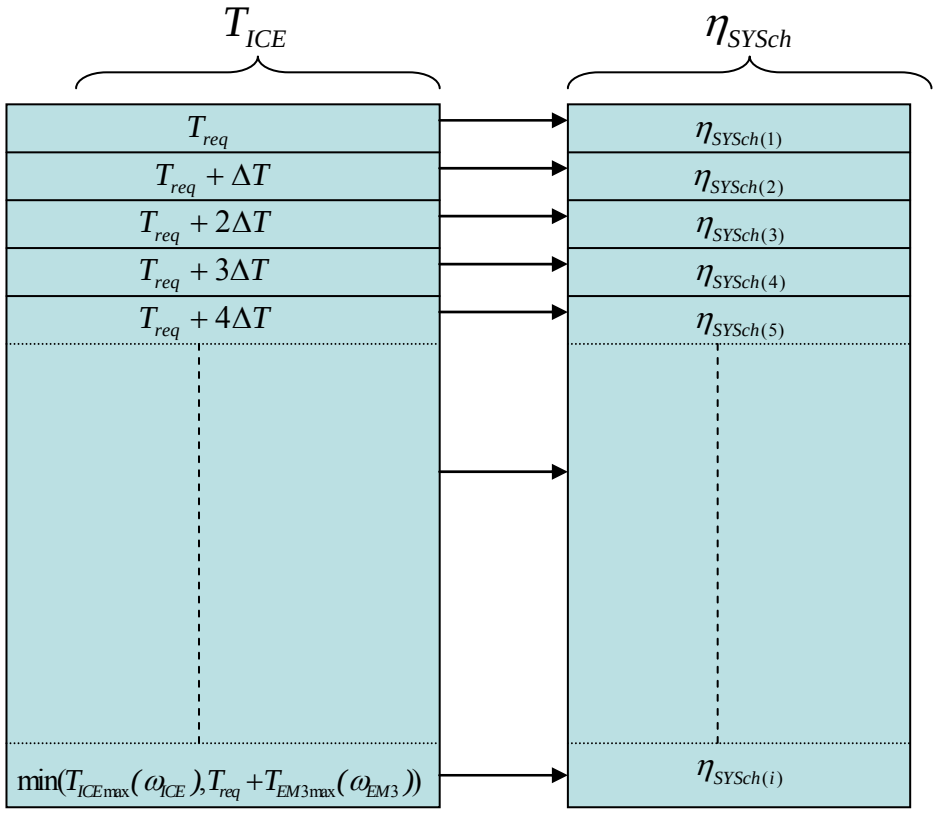

Figure 4.10 : Optimum ICE Torque Search for Charging

Amount of increase value ΔT for T_{ICE} and updating frequency (f_{Topt}) of $T_{optICEch}$ depend on computational power capacity of the controller. These values can be defined statically or dynamically.

If these are defined statically, worst case scenario should be taken into account. But at this time, whole computational power can't be used for all scenarios. Here, worst case scenario means the maximum searching area for optimum charge torque $T_{optICEch}$.

Depending on the searching area if ΔT and f_{Topt} are defined dynamically, maximum computational power can be utilized at any scenario. This means more accurate results than static one.

In equation 4.14, all parameters can be measured or calculated .

Table 4.2 Measurements, Calculations and Constants for MOES Charge Efficiency Variables

Parameter	Measured/Calculated From
T_{req}	Can be measured from gas pedal.
W_{EM3}	Can be measured from EM3 directly or calculated from wheel speed sensors.
W_{ICE}	Can be measured from ECU directly or calculated from wheel speed sensors.
SOC	Can be measured from battery controller
η_{BAT}	Can be taken from efficiency map
η_{EM3}	Can be taken from its efficiency map
η_{ICE}	Can be taken from its efficiency map
K_{dch}	Can be calculated from previous drivings
η_{DL1}	Constant
I_{bat}	$I_{bat\_ch} = \frac{P_{bat}}{V_{bat}} = \frac{T_{EM3} * W_{EM3}}{\eta_{EM3} * V_{bat}}$ **(4.19)**
V_{bat}	Can be measured from battery controller.

4.7 Discharge Condition in MOES

The power flow for discharging is illustrated in the flowchart of Fig.4.7.

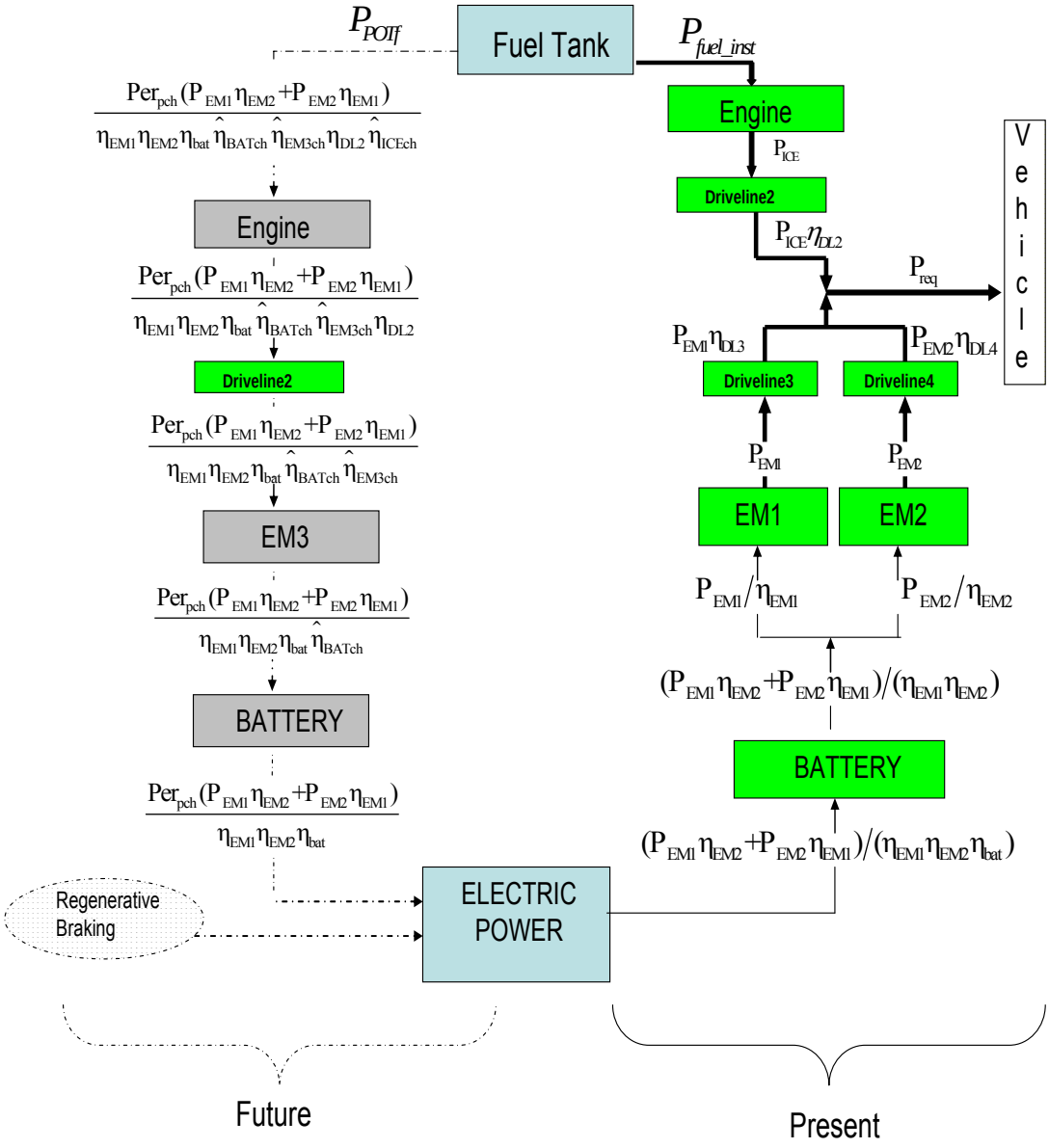

Figure 4.11 : Power Flow with Efficiencies for Discharge Algorithm

This mode is for discharging of batteries until SOC comes to the pre-selected set value. EM1, EM2 and ICE are used in this mode. Here, system input is defined as sum of instant power of fuel P_{fuel_inst} and power of potential fuel P_{POTf} which will be converted into electric power in the future. System output is defined as the sum of power requested from the driver which is equal to the tractive power requirement from the ICE P_{req} input by the driver through the gas pedal.

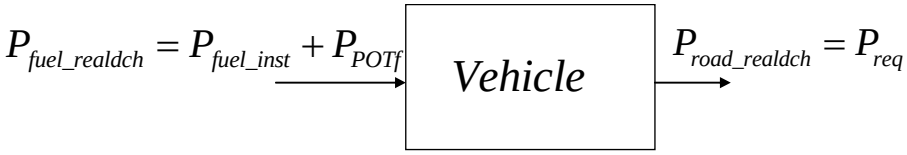

Figure 4.12 : System Input and Output for Battery Discharging

Overall charge efficiency can be found by:

$$\eta_{SYSdch} = \frac{P_{road\_realdch}}{P_{fuel\_realdch}} \tag{4.20}$$

System input $P_{fuel\_realdch}$ is defined as the sum of P_{fuel_inst} and P_{POTf} because the electric power consumed during discharging has to be charged again in the future. This can be done by parallel charging or regenerative braking. This corresponds to the left coloumn in Fig. 4.11. So, there will be a fuel consumption for parallel charging part of this gain. Then, this potential fuel power P_{POTf} is added to intantaneous fuel power P_{fuel_inst} to obtain:

$$P_{fuel\_realdch} = P_{fuel\_inst} + P_{POTf} \tag{4.21}$$

where

$$P_{fuel\_inst} = \frac{P_{ICE}}{\eta_{ICE(T_{ICE}, W_{ICE})}} \tag{4.22}$$

Potential fuel power is calculated below, with the efficiencies shown in Fig .4.11.

$$P_{POTf} = \frac{Per_{pch}(P_{EM1}\eta_{EM2}(T_{EM2}, \omega_{EM2}) + P_{EM2}\eta_{EM1}(T_{EM1}, \omega_{EM1}))}{\eta_{EM1}(T_{EM1}, \omega_{EM1})\eta_{EM2}(T_{EM2}, \omega_{EM2})\eta_{bat}(I_{bat}, SOC)\hat{\eta}_{BATch}\hat{\eta}_{EM3ch}\eta_{DL2}\hat{\eta}_{ICEch}} \tag{4.23}$$

While the vehicle is in operation, the percentage of replaced electric power Per_{pch} that comes from parallel charging, must be calculated and updated continuously. Per_{pch} is given by:

$$Per_{pch} = \frac{\int_{t_0}^{t} P_{pc}(t)dt}{\int_{t_0}^{t} P_{pc}(t)dt + \int_{t_0}^{t} P_{reg}(t)dt} \quad \textbf{(4.24)}$$

Per_{pch} value is very important in MOES and is a new variable is a new definition. This value can be thought as an encouragement factor for using electric energy. Regenerative braking power is free energy gained. But the vehicle has to consume fuel for parallel charging. If a vehicle has a high regenerative braking capability, Per_{pch} decreaes.

$\hat{\eta}_{BATch}$, $\hat{\eta}_{EM3ch}$ and $\hat{\eta}_{ICEch}$ values are the average battery parallel charge efficiency, average electric motor parallel charge efficiency and average internal combustion engine parallel charge efficiency respectively. These values are calculated during the parallel charge mode of the vehicle and they are updated along the whole drive cycle. Instantaneous electric power that is being used by the electric motor is assumed to be recharged with these average efficiency values in the future.

From here, $\hat{\eta}_{BATch} * \hat{\eta}_{EMch} * \hat{\eta}_{ICEch}$ value is performed with "K_{ch}" for simplicity.

$$K_{ch} = \hat{\eta}_{BATch} * \hat{\eta}_{EM3ch} * \hat{\eta}_{ICEch} \quad \textbf{(4.25)}$$

In order to find the main formula's denumerator $P_{fuel\_realdch}$ in (4.20), the equations (4.21), (4.22), (4.23) and (4.25) is substituted into (4.21) as

$$P_{fuel\_realdch} = \frac{P_{ICE}}{\eta_{ICE}(T_{ICE}, \omega_{ICE})} + \frac{Per_{pch}(P_{EM1}\eta_{EM2}(T_{EM2}, \omega_{EM2}) + P_{EM2}\eta_{EM1}(T_{EM1}, \omega_{EM1}))}{\eta_{EM1}(T_{EM1}, \omega_{EM1})\eta_{EM2}(T_{EM2}, \omega_{EM2})\eta_{bat}(I_{bat}, SOC)\eta_{DL2}K_{ch}} \quad \textbf{(4.26)}$$

The system output $P_{road\_realdch}$ is defined as the power requested by the driver and is given by:

$$P_{road\_realdch} = P_{req} \quad \textbf{(4.27)}$$

Substitute from (4.26) and (4.27) into (4.20) to obtain:

$$\eta_{SYSdch} = \frac{P_{req}}{\frac{P_{ICE}}{\eta_{ICE(T_{ICE},W_{ICE})}} + \frac{Per_{pch}(P_{EM1}\eta_{EM2}(T_{EM2},\omega_{EM2}) + P_{EM2}\eta_{EM1}(T_{EM1},\omega_{EM1}))}{\eta_{EM1}(T_{EM1},\omega_{EM1})\eta_{EM2}(T_{EM2},\omega_{EM2})\eta_{bat}(I_{bat},SOC)\eta_{DL2}K_{ch}}} \quad \textbf{(4.28)}$$

There is a relationship between the ICE, EM1 and EM2 torques. To find this relation, requested torque by driver from ICE (T_{req}) is converted to the torque request from the road $T_{reqroad}$ as:

$$T_{reqroad} = T_{req}\eta_{DL2}dr_f\,gr \quad \textbf{(4.29)}$$

If all torques are written as road level torques by us,ng the appropriate efficiency and transmission coefficients:

$$T_{reqroad} = T_{EM1}\eta_{DL3}dr_f + T_{EM2}\eta_{DL4}dr_r + T_{ICE}\eta_{DL2}dr_f\,gr \quad \textbf{(4.30)}$$

is obtained. In the two electric motor mode, the optimal operating point for maximum overall efficiency is not found by only changing the ICE torque because there are three optimum output values. At least two of the outputs should be found by searching and the third one can be found with equations (4.30) and (4.29). Hence, T_{ICE} is written in terms of T_{EM1}, T_{EM2} and $T_{reqroad}$ as:

$$T_{ICE} = \frac{(T_{req}\eta_{DL2}dr_f\,gr - T_{EM1}\eta_{DL3}dr_f - T_{EM2}\eta_{DL4}dr_r)}{\eta_{DL2}dr_f\,gr} \quad \textbf{(4.31)}$$

Power values do not correspond torque values in equation (4.28) in the same manner because all components speeds are not the same. Power P is the product of torque T and angular velocity ω given by:

$$P = T * \omega \quad \textbf{(4.32)}$$

If (4.28) is written again using (4.32) as;

$$\eta_{SYSdch} = \frac{P_{req}}{\frac{T_{ICE}\omega_{ICE}}{\eta_{ICE(T_{ICE},W_{ICE})}} + \frac{Per_{pch}(T_{EM1}\omega_{EM1}\eta_{EM2}(T_{EM2},\omega_{EM2}) + T_{EM2}\omega_{EM2}\eta_{EM1}(T_{EM1},\omega_{EM1}))}{\eta_{EM1}(T_{EM1},\omega_{EM1})\eta_{EM2}(T_{EM2},\omega_{EM2})\eta_{bat}(I_{bat},SOC)\eta_{DL2}K_{ch}}} \quad \textbf{(4.33)}$$

When equation(4.31) is substituted into equation (4.33);

$$\eta_{SYSdch} = \frac{P_{req}}{\frac{(T_{req}\eta_{DL2}dr_f\,gr - T_{EM1}\eta_{DL3}dr_f - T_{EM2}\eta_{DL4}dr_r)\omega_{ICE}}{\eta_{DL2}dr_f\,gr\,\eta(T_{ICE},W_{ICE})} + \frac{Per_{pch}(T_{EM1}\omega_{EM1}\eta_{EM2}(T_{EM2},\omega_{EM2}) + T_{EM2}\omega_{EM2}\eta_{EM1}(T_{EM1},\omega_{EM1}))}{\eta_{EM1}(T_{EM1},\omega_{EM1})\eta_{EM2}(T_{EM2},\omega_{EM2})\eta_{bat}(I_{bat},SOC)\eta_{DL2}K_{ch}}} \quad \textbf{(4.34)}$$

is obtained.

Searching in the two dimension plane of T_{EM1}, T_{EM2} combinations will give us the optimum torque values for EM1($T_{optEM1ch}$) and EM2 ($T_{optEM2ch}$)

$$T_{optEM1dch}, T_{optEM2dch} = \underset{(T_{EM1},T_{EM2})}{\arg\max}\left|(\eta_{SYSdch})\right. \quad \textbf{(4.35)}$$

. Finally, optimum ICE torque can be calculated by using equation (4.31) as:

$$T_{optICEdch} = \frac{(T_{req}\eta_{DL2}dr_f\,gr - T_{optEM1dch}\eta_{DL3}dr_f - T_{optEM2dch}\eta_{DL4}dr_r)}{\eta_{DL2}dr_f\,gr} \quad \textbf{(4.36)}$$

But there are three torque constraints, one of them is $T_{EM1\max}(\omega_{EM1})$ other one is $T_{EM2\max}(\omega_{EM2})$, which are the maximum torques that electric motors can give at their instant speeds and the last one is battery current limit $I_{bat\_\max}$. $T_{ICE\max}(\omega_{ICE})$ is not an actual constraint because, maximum T_{req} torque which occurs when gas pedal is pushed maximum must be equal to or smaller than sum of all available maximum torques from EM1, EM2 and ICE. So if EM1 and EM2 give their maximum torques at any speed, ICE torque will be enough for satisfying the driver's request.

Searching procedure is given in Fig.4.11. By changing T_{EM1} and T_{EM2}, T_{ICE} can be calculated automatically using equation (4.31). After that, T_{EM1}, T_{EM2} and T_{ICE} values which maximize η_{SYSdch} are chosen as the optimum operating points.

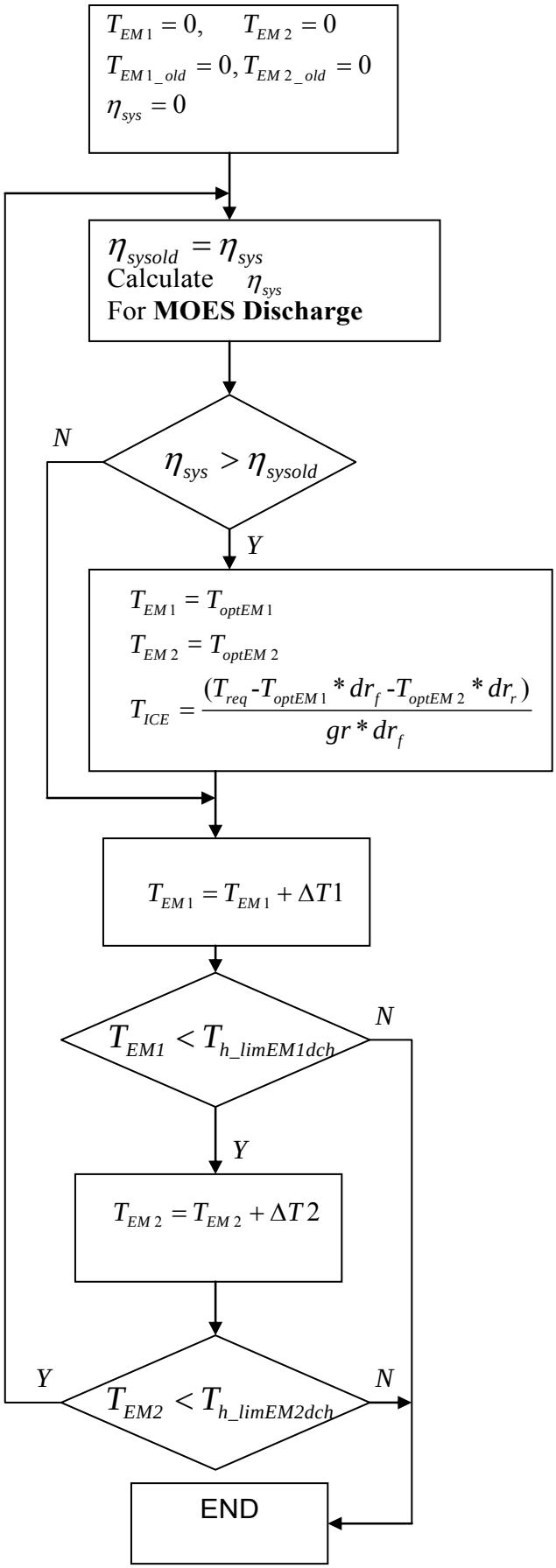

Figure 4.13 : Flowchart of MOES Discharge

$T_{h\_limEM1dch}$ and $T_{h\_limEM2dch}$ are the high limits of the EM1 and EM2 torques for search algorithm. This limits come from requested torque by driver T_{req} and maximum available torques of EM1 $T_{EM1max}(W_{EM1})$ and EM2 $T_{EM2max}(W_{EM2})$. Torque combinations don't pass over battery current limits because batteries have capability of giving maximum power to the electric motors. T_{req} was converted to road torque $T_{reqroad}$ in equation (4.29). Using this, determinative torque limits are calculated as:

$$T_{h\_limEM1dch} = min(\frac{T_{reqroad}}{dr_f \eta_{DL3}}, T_{EM1max}(W_{EM1})) \quad \textbf{(4.37)}$$

$$T_{h\_limEM2dch} = min(\frac{T_{reqroad} - T_{EM1}\eta_{DL3} dr_f}{\eta_{DL4} dr_r}, T_{EM2max}(W_{EM1})) \quad \textbf{(4.38)}$$

The searching process for MOES charge is shown in Fig. 4.10.

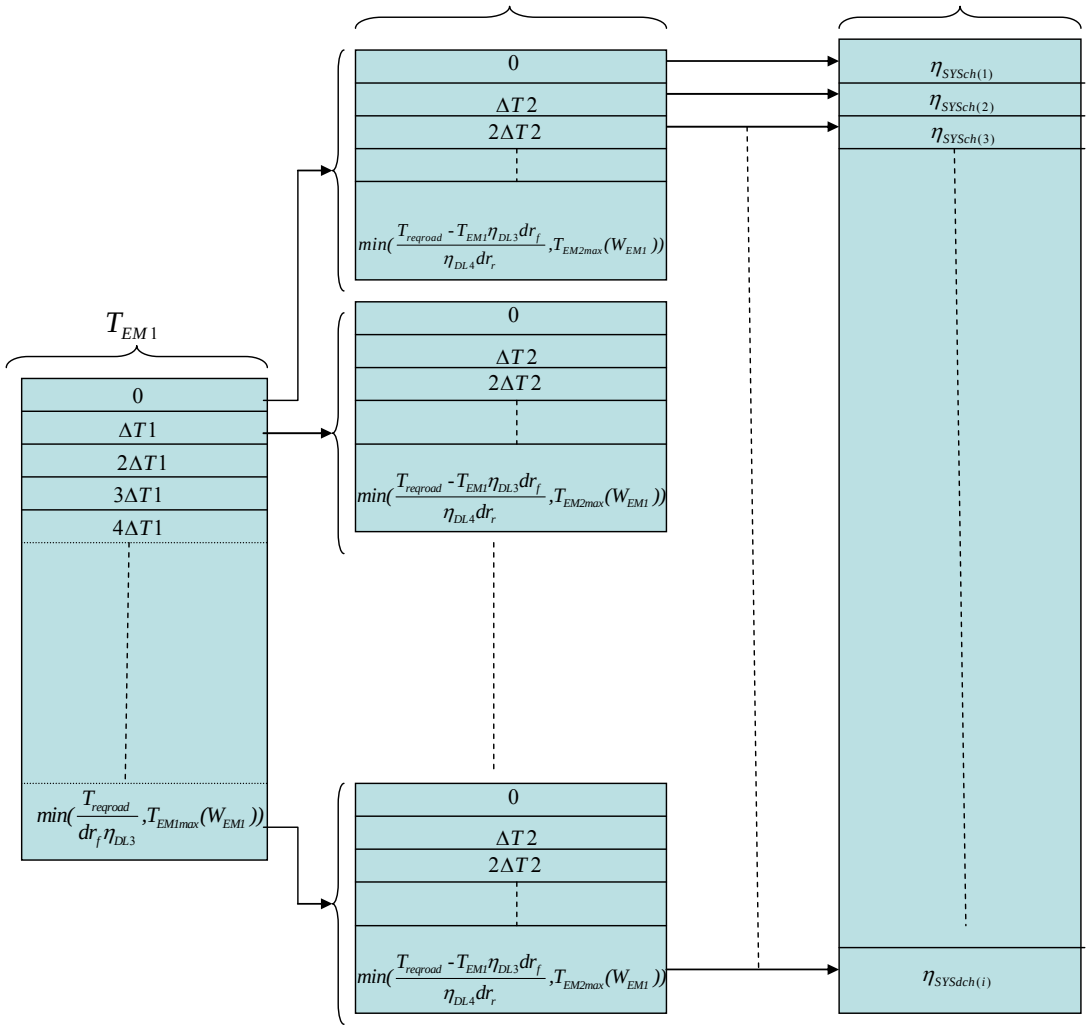

Figure 4.14 : Optimum EM1 and EM2 Torque Search for Discharging

Amount of increase in the values of $\Delta T1$ and $\Delta T2$ for T_{EM1} and T_{EM2} and the updating frequency f_{Topt} of optimum torque calculation depend on computational power capacity of the controller. These values can be defined statically or dynamically.

If these are defined statically, worst case scenario should be taken into account. But at this time, whole computational power can't be used for all scenarios.

Depending on the searching area if $\Delta T1$, $\Delta T2$ and f_{Topt} are defined dynamically, maximum computational power can be utilized at any scenario. This means more accurate results are obtained as compared to the static one.

All parameters in (4.34), can be measured or calculated as illustrated in Table 4.3.

Table 4.3 Measurements, Calculations and Constants for MOES Discharge Efficiency Variables

Parameter	**Measured/Calculated From**
T_{req}	Can be measured from gas pedal.
W_{EM1}	Can be measured from EM1 directly or calculated from wheel speed sensors.
W_{EM2}	Can be measured from EM2 directly or calculated from wheel speed sensors.
W_{ICE}	Can be measured from ECU directly or calculated from wheel speed sensors.
SOC	Can be measured from battery controller
η_{BAT}	Can be taken from its efficiency map
η_{EM1}	Can be taken from its efficiency map
η_{EM2}	Can be taken from its efficiency map

η_{ICE}	Can be taken from its efficiency map
η_{DL2} , η_{DL3} , η_{DL4}	Constant
K_{ch}	Can be calculated from previous drivings.
I_{bat}	Can be measured from battery driver or calculated as: $I_{bat_{dch}} = \frac{P_{bat}}{V_{bat}} = \frac{T_{EM1} * W_{EM1}}{\eta_{EM1*} V_{bat}} + \frac{T_{EM2} * W_{EM2}}{\eta_{EM2*} V_{bat}}$ **(4.39)**
V_{bat}	Can be measured from battery controller.

4.8 Regenerative Braking

Regenerative braking is converting the mechanical brake power into electric power [18]. In regenerative braking, negative torques for electric motors are given in proportional to the mass distribution of the vehicle with respect to the front and rear axles. Regenerative braking signal is between 0-5 Volts. So the control signal for regenerative braking is calculated as:

$$EM1_{reg\_signal} = Per_{brake\_pedal} * 5 * Md_{front} \quad \textbf{(4.40)}$$

$$EM2_{reg\_signal} = Per_{brake\_pedal} * 5 * Md_{rear} \quad \textbf{(4.41)}$$

In equations (4.40) and (4.41), the constant term "5" represents the maximum regenerative brake signal of the electric motors. When the regenerative brake signal is given to the electric motors, the controlled clutch seperates the ICE and drivetrain to avoid the engine brake torque from being transmitted to the wheels.

4.9 Offline Calculations for Tables

Calculations for MOES need a process power for calculations, depending on the sensitivity of searching algorithm. If controllers power capability is not enough for

providing this power demand, tables can be used for optimum solutions. These tables contain all electric motor and internal combustion engine torques for optimum operating point, which is calculated from offline simulations.

Dimensions of the tables depend on the parameters which effect efficiency of components (speeds and torques of electric motors and ICE), average electrical efficiencies of charge and discharge conditions(K_{ch} , K_{dch}) and percentage of parallel charge Per_{pch}. Gear number $\boldsymbol{g}_{\boldsymbol{n}}$ effects the MOES discharge table because discharge torque is the sum of EM1 EM2 and ICE torques. So according to the gear number, these components torque percentage for the torque which is given to the road change.

ICE and EM efficiencies depend on their output torques and speeds. ICE speed and EM3 speed are same. If gear number is known, EM1 and EM2 speeds can be calculated. In charge mode, EM1 and EM2 don't have a role so gear number is not an input for MOES charge table. But, ICE speed and gear number are both inputs of MOES discharge tables. Table outputs are component torque values so all parameters that effect EMs and ICE efficiencies are used in table.

Battery efficiency depends on SOC and battery current. Battery current can be calculated for all combinations of torque distribution. So battery current is not an input for the tables.

SOC can be thought as a constant value because algorithm will keep SOC of battery around a constant value. According as the table storage capability of the controller, SOC can be an input for the tables or can be assumed as a constant..

Average electrical efficiencies (K_{ch} , K_{dch}) and percentage of parallel charge values can also be thought as the inputs for the tables or assumed as constant depending on the storage capability of controller.

Inputs and outputs of tables for MOES charge and discharge are given below.

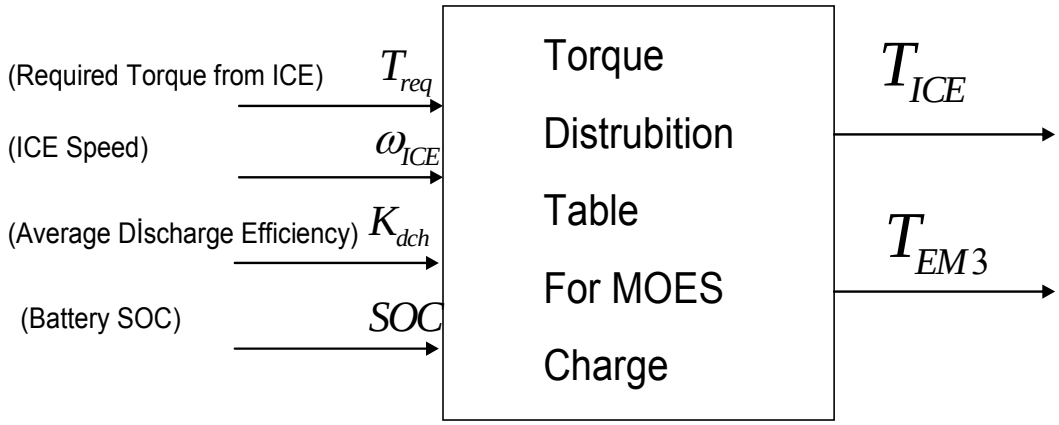

Figure 4.15 : Torque Distribution Table Inputs-Outputs for MOES Charge

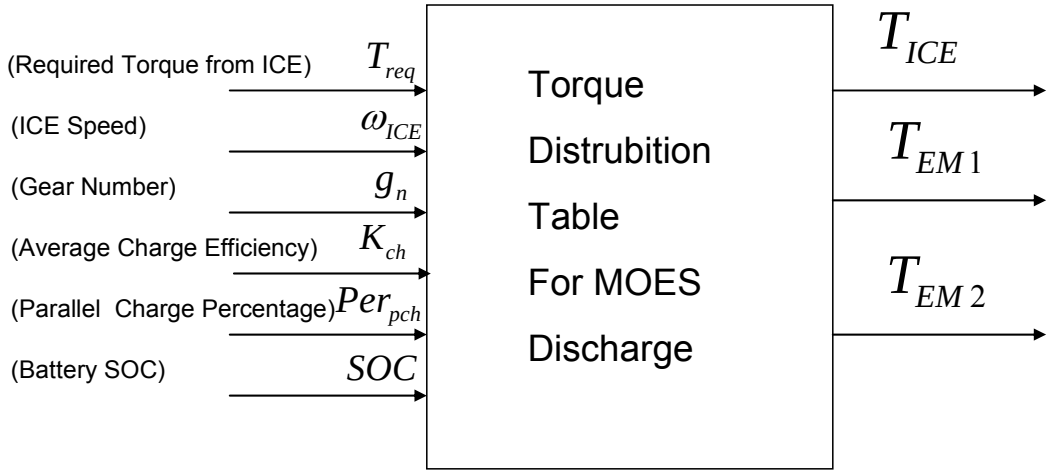

Figure 4.16 : Torque Distribution Table Inputs-Outputs for MOES Discharge

4.9.1 MOES Charge Table

Average discharge efficiency (K_{dch}), and SOC of batteries are taken as constant in charge table for visibility. Values of these constants are given below.

Table 4.4 Constants of MOES Charge Table

K_{dch}	SOC
0.8	0.65

According to the availability of controller storage, dimension of the table can be increased. Every parameter will add one dimension to the table. So element number

of table will increase extremely for every added parameter of the charge efficiency (η_{SYSch}) given in formula(4.15).

Charge tables are constructed as the function of the desired torque from ICE $\boldsymbol{T_{req}}$ and speed of ICE $\boldsymbol{\omega_{ICE}}$. This speed value can also be the speed of vehicle because of direct relation between ICE speed and vehicle speed. Other parameters that are shown in fig. 4.15 are taken as constants and given in table 4.2.

Optimum torques of EM1, EM2, EM3, ICE for all combinations of torque request from ICE $\boldsymbol{T_{req}}$ and ICE speed $\boldsymbol{\omega_{ICE}}$ are given below.

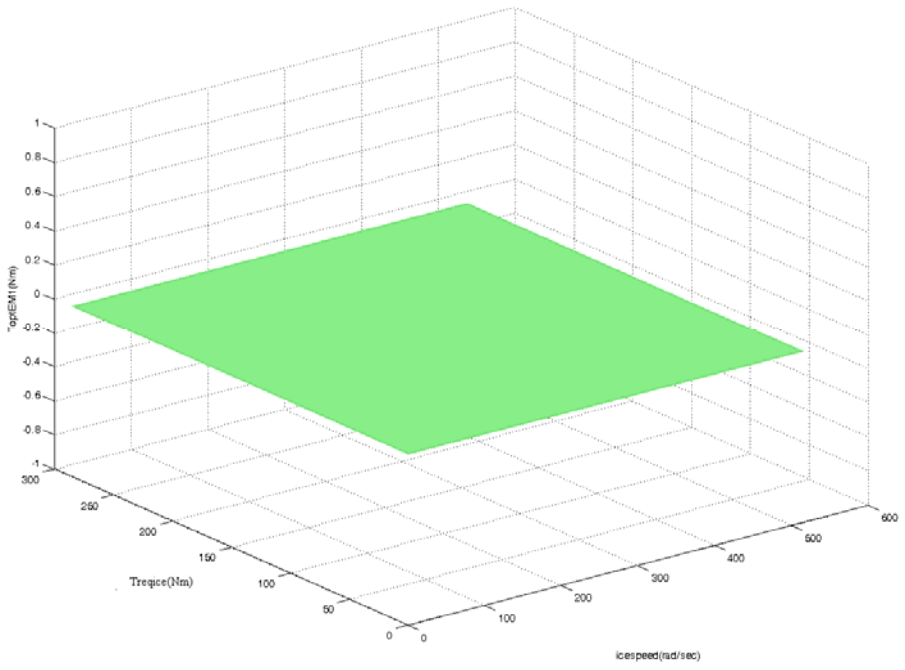

Figure 4.17: Optimum Torque of EM1 for MOES Charge

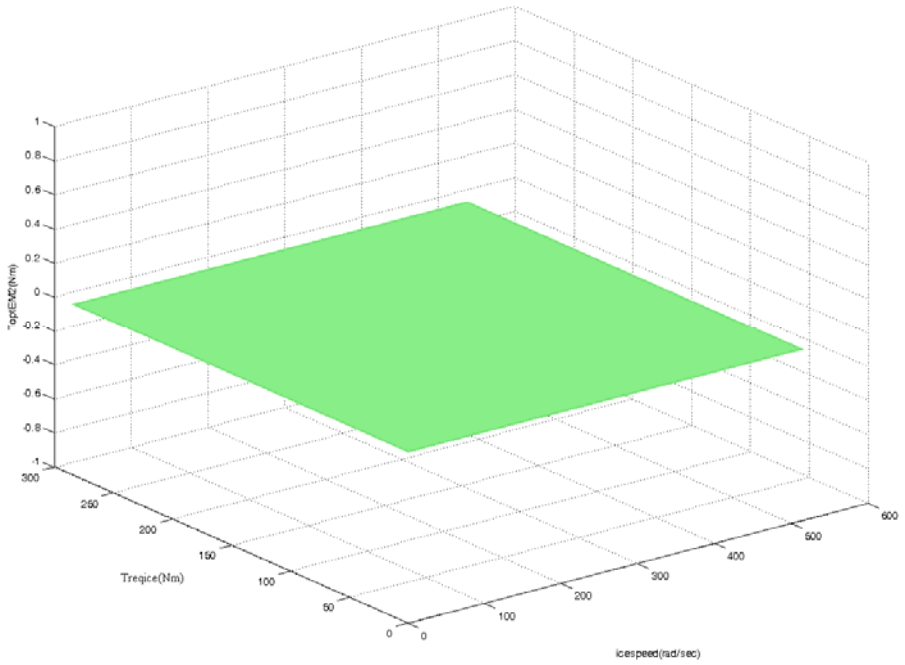

Figure 4.18: Optimum Torque of EM2 for MOES Charge

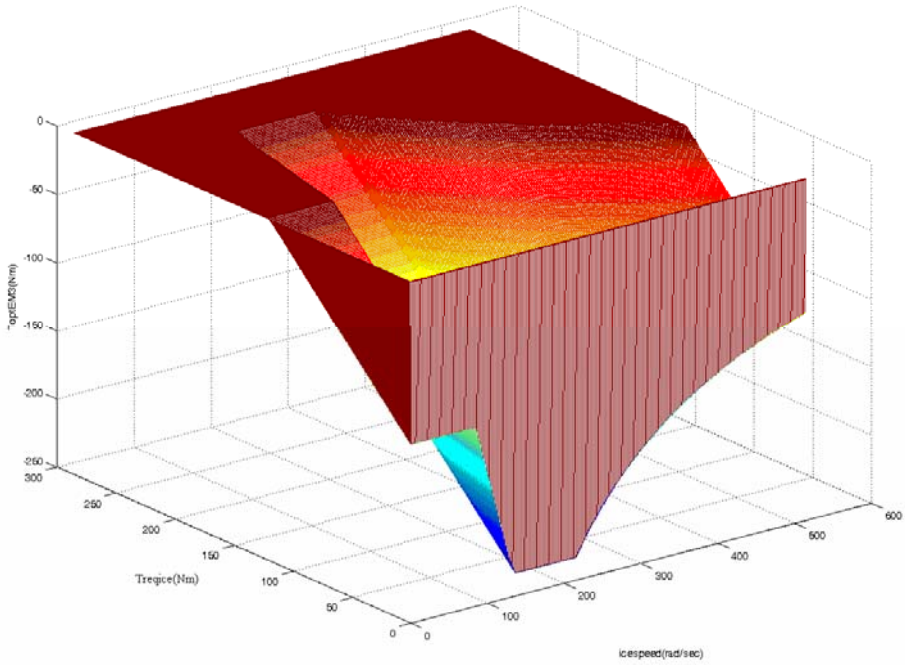

Figure 4.19: Optimum Torque of EM3 for MOES Charge

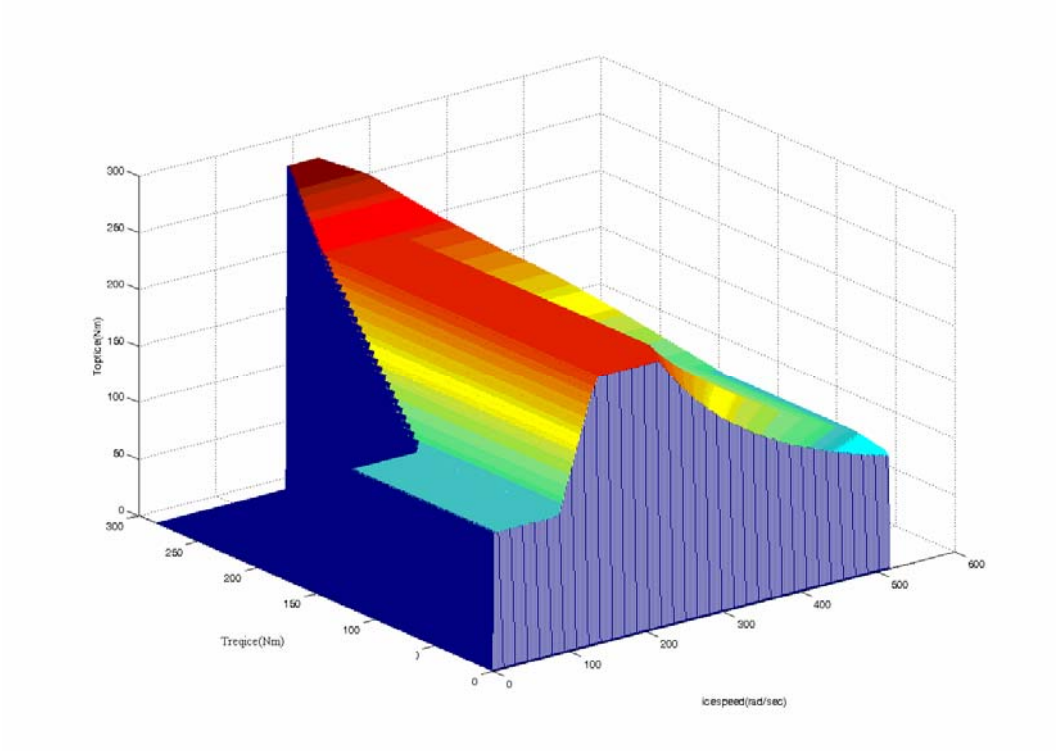

Figure 4.20: Optimum Torque of ICE for MOES Charge

4.9.2 MOES Discharge Table

Average charge efficiency (K_{ch}), percentage of parallel charge (Per_{pch}) and SOC of batteries are taken as constant in charge table for visibility. Values of these constants are given below.

Table 4.5 Constants of MOES Discharge Table

K_{ch}	Per_{pch}	SOC
0.25	0.5	0.65

According to the availability of controller storage, dimension of the table can be increased. Every parameter will add one dimension to the table. So element number of table will increase extremely for every added parameter of the discharge efficiency (η_{SYSdch}) given in formula (4.34).

Discharge tables are constructed as the function of the desired torque from ICE (T_{req}), gear number (g_n) and speed of ICE (W_{ICE}). This speed value can also be the speed of vehicle because of direct relation between ICE speed and vehicle speed. Other parameters shown in fig. 4.16 are taken as constants and given in table 4.3.

Optimum torques of EM1, EM2, EM3, ICE for all combinations of torque request from ICE (T_{req}) and ICE speed(W_{ICE}) are given below. These results are for first gear number. Results for other gear numbers are given in Appendix A.

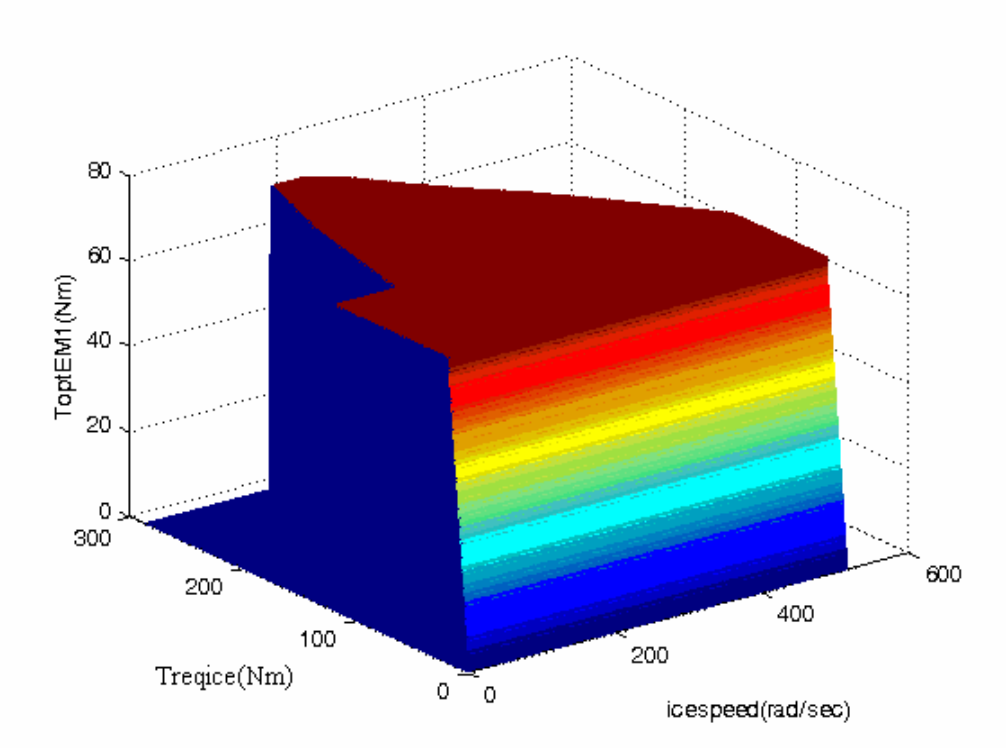

Figure 4.21: Optimum Torque of EM1 for MOES Discharge for 1. Gear Number

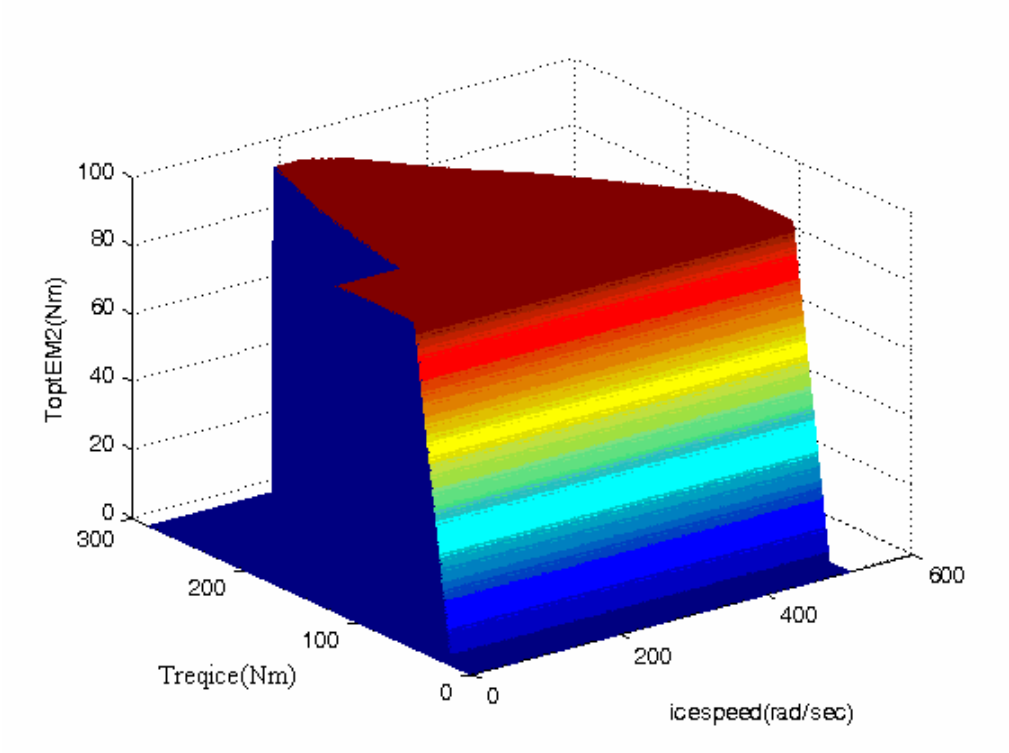

Figure 4.22: Optimum Torque of EM2 for MOES Discharge for 1. Gear Number

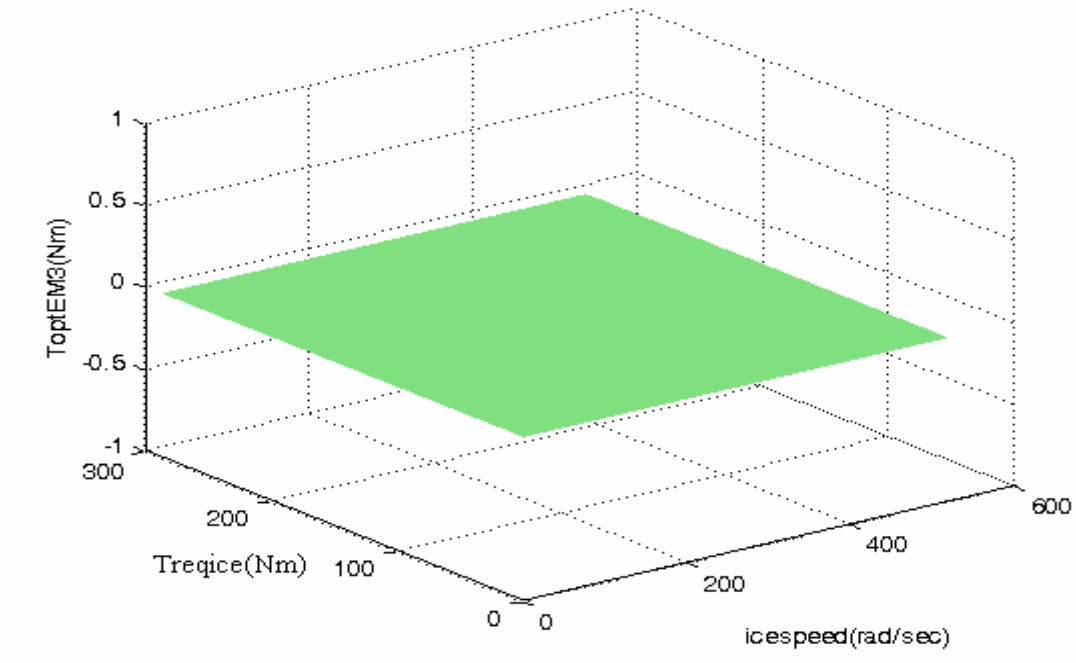

Figure 4.23: Optimum Torque of EM3 for MOES Discharge for 1. Gear Number

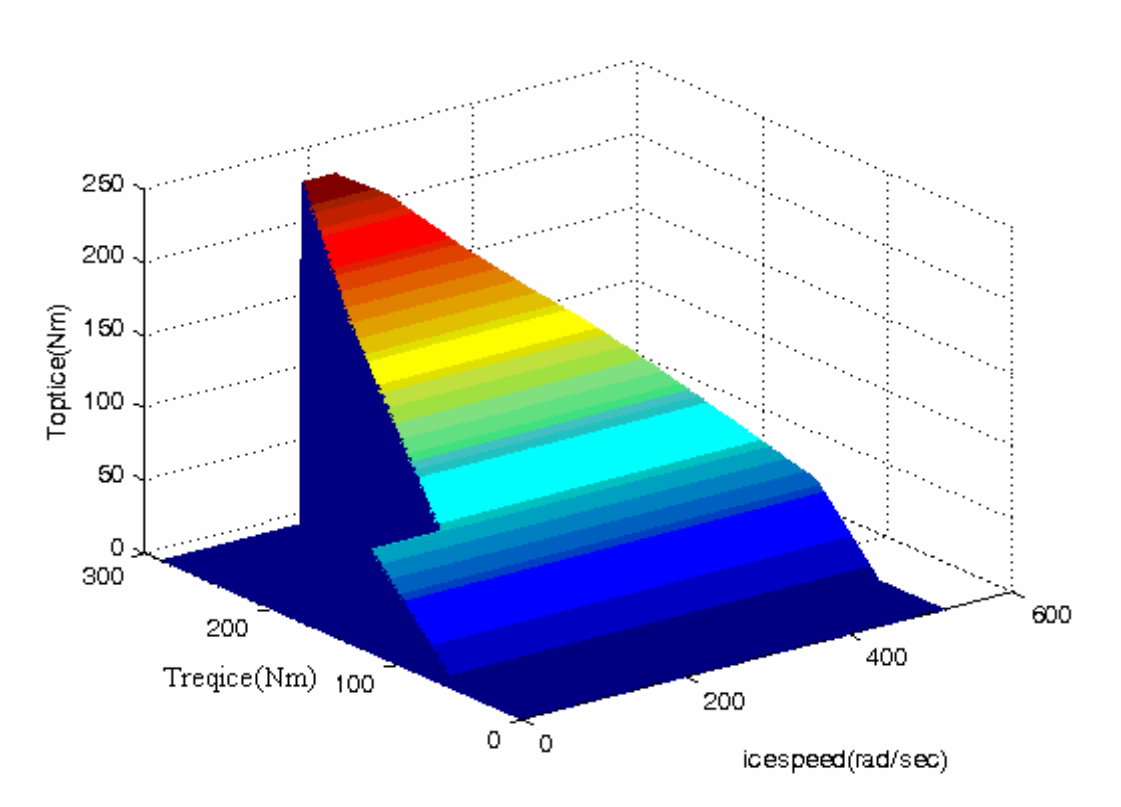

Figure 4.24: Optimum Torque of EM3 for MOES Discharge for 1. Gear Number

5. SIMULATIONS

CarMaker models were used for simulations. The drive cycle used in the simulations the ECE cycle's inner city part. The drive cycle determines the speed versus time profile of the vehicle.

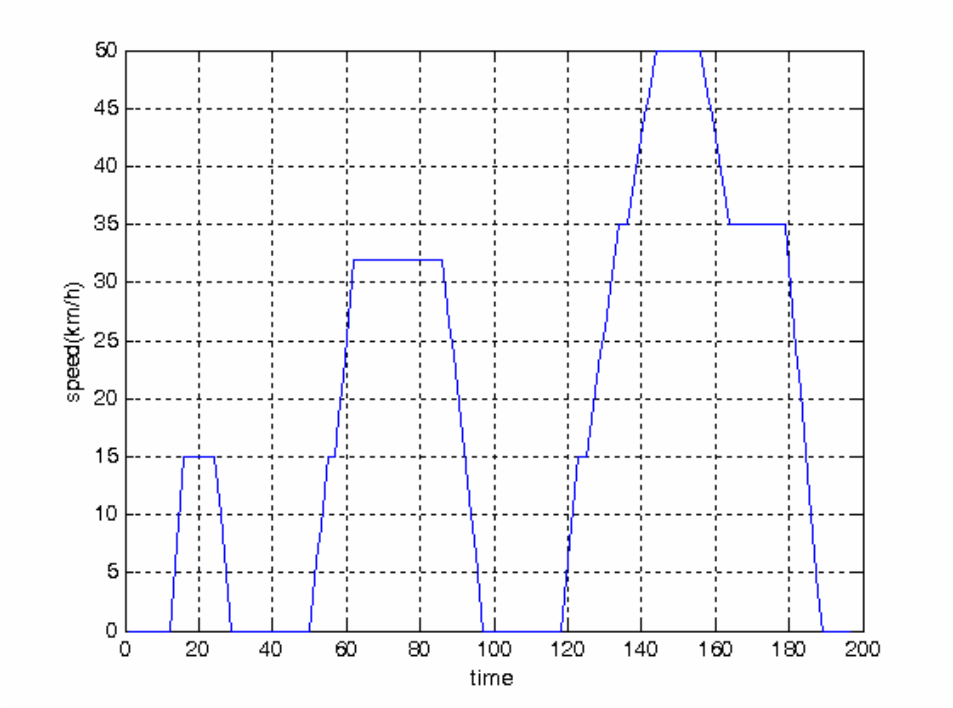

Figure 5.1 : ECE Cycle

General block scheme of simulations is illustrated in Fig. 5.2.

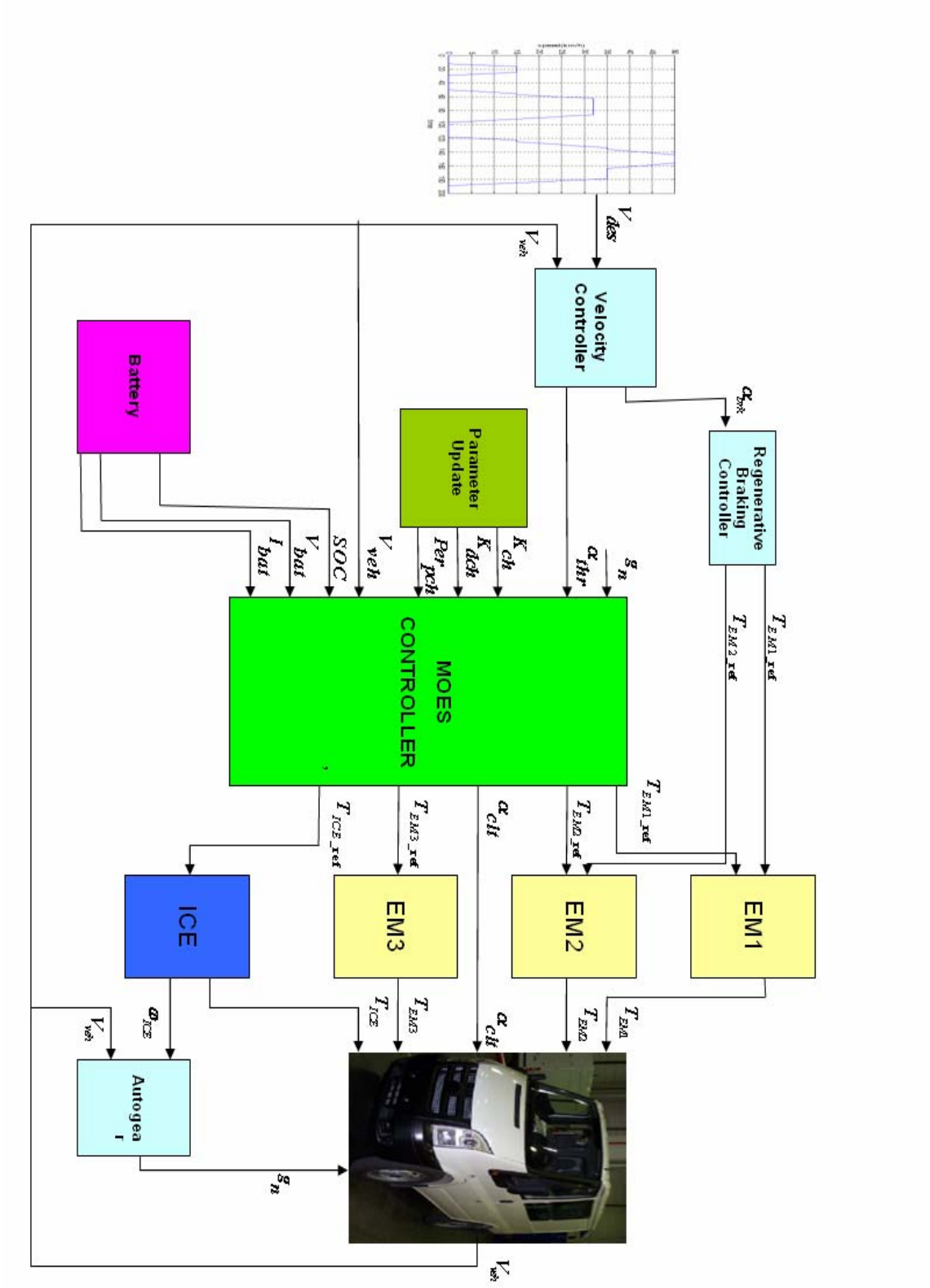

Figure 5.2 : Block Scheme of Simulation Model

A PI longitudinal speed controller was designed and used as the driver model. An automatic gear shift algorithm was also designed as part of the driver. Parameter

update block calculates the average efficiencies for charging K_{ch} , discharging K_{dch} and percentage of parallel charge Per_{pch} values. Torque and speed values for ICE, EM1, EM2, EM3, voltage, current and SOC of battery; efficiency values for all components; vehicle speed; and consumed fuel values are analyzed in these simulations.

Simulations were performed in three different control modes to analyze the optimization results better.

5.1 Only ICE (Conventional) Mode

First part of the simulations is only ICE mode. This is the conventional operation of the vehicle. There is no optimization and any other HEV feature. All required torque is taken from internal combustion engine and mechanical brakes are used for negative torque request.

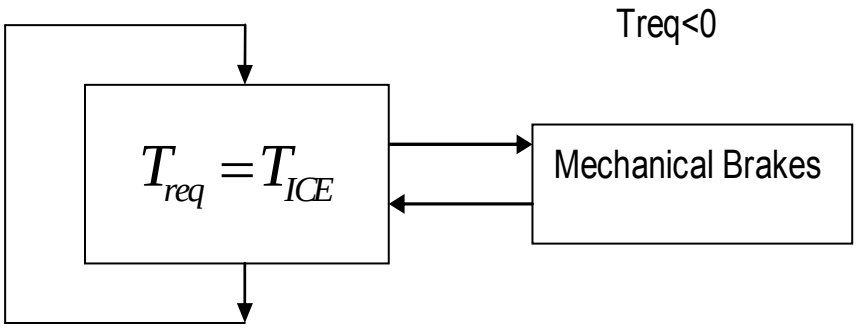

Figure 5.3 : Flowchart of Only ICE Mode

5.2 Only Regenerative Braking Mode

Second part of simulations is only regenerative braking mode. Aim of this mode is to calculate the fuel consumption minimization (FCM) which comes from regenerative braking. Regenerative braking is one of the main sources of FCM. So for analyzing the success of optimization, FCM which is obtained from regenerative braking should be calculated first. After optimization algorithm results, percentage of FCM from regenerative braking and optimization can be calculated.

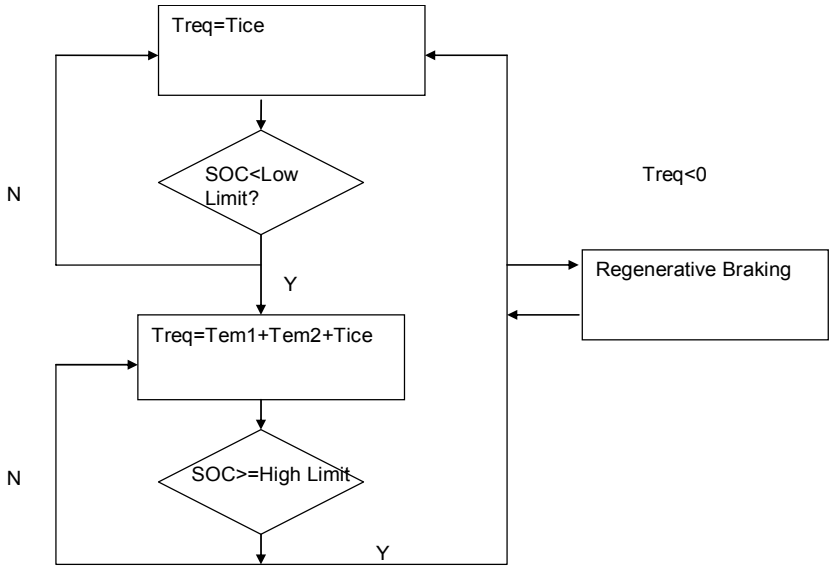

Figure 5.4 : Flowchart of Only Regenerative Braking Mode

5.3 Maximizing Overall Efficiency Strategy (MOES) Mode

This strategy is the main subject of this thesis and it was explained in fourth section. Aim of this strategy is to maximize the overall efficiency of vehicle. Inside of MOES for charge and MOES for discharge flowcharts can be seen in Fig.4.10 and Fig.4.14.

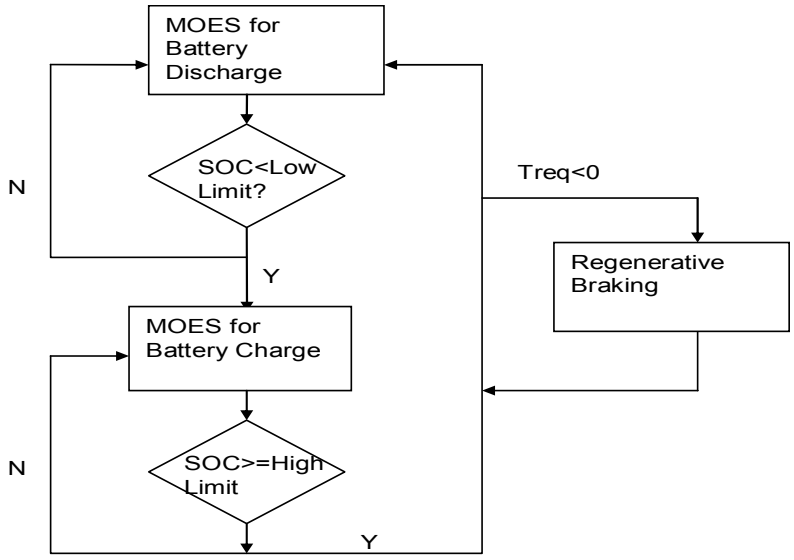

Figure 5.5 : Flowchart of MOES Mode

5.4 Simulation Results

Simulation results for only ICE mode, only regenerative braking mode and MOES mode are given in Appendix B, Appendix C and Appendix D respectively.

5.4.1 Simulation Results for Only ICE (Conventional) Mode

In only ICE mode, it can be seen that whole required torque is provided from only internal combustion engine. Other components torques are always zero (Fig. B.2). Hence battery SOC does not have any change (Fig. B.4).

As it can be seen on Fig. B.6, ICE operating points are scattered in the efficiency map without optimization. Some operating points are in efficient areas and some of them are in inefficient areas. In Fig. B.5, this inefficiency can be seen in time domain.

Fuel consumption is 82.95gr (Fig. B.3) and final SOC is same as its initial value (Fig. B.4) in this mode.

5.4.2 Simulation Results for Only Regenerative Braking Mode

In this mode, battery charging is provided by only regenerative braking. So, EM1 and EM2 is used with ICE and SOC changes during the cycle (Fig. C. 2, Fig.C.4).

There are still not any optimization here. Aim is only to see the effect of regenerative braking to fuel consumption. Component efficiencies are given in fig. C.5, Fig.C.6, Fig.C.7, Fig.C.8 and C.9 in time domain. In Fig. C.10, it can be seen that ICE operating points are scattered in the efficiency map like only ICE mode.

Fuel consumption is 74.19gr (Fig. C.3) and final SOC is %65.46 (fig. C.4) in this mode.

5.4.3 Simulation Results for MOES Mode

In this mode all the components are used during the cycle with optimization. EM3 is used for parallel charging, EM1 and EM2 are used for regenerative braking and electric driving (Fig. D.2).

Component efficiencies are given in Fig. D.5, Fig.D.6, Fig.D.7, Fig.D.8 and D.9 in time domain. These component efficiencies are their optimum efficiency values for maximum overall efficiency. In fig. D.10, it can be seen that ICE operating points are not scattered in efficiency map like only ICE mode or only regenerative braking mode. ICE is forced to operate its efficient areas in this mode. It can be asked that why ICE doesn't operate at its most efficient points for every speed. Answer is maximizing overall efficiency or in other words combined efficiency. Aim of strategy is not operate ICE at its most efficient points, aim is to maximize overall efficiency of the vehicle.

According to the simulation results, fuel consumption is 58.77gr (Fig. D.3) and final SOC is %65.36 (Fig. D.4) in this mode.

5.5 Charge Sustaining Fuel Consumption Calculation

To compare the results correctly for fuel consumption minimization, SOC of vehicles should be brought to its beginning value. To make this possible, charge sustaining fuel consumption(fc_{cs}) should be calculated.

First, the difference between the final battery energy and initial battery energy is calculated.

If this value is positive, it means vehicle gained some electrical energy, if it is negative vehicle lost some electrical energy. Amount of fuel which gives the same power to road with this gained or lost electric energy is calculated. Difference of real fuel consumption fc_r and this calculated fuel amount gives the charge sustaining fuel consumption. Formulation is given below:

$$fc_{cs} = fc_r - \frac{(E_{bat} * \Delta SOC) * K_{dch}}{\eta_{ICE_t} * GED_{fuel}} \qquad (5.1)$$

GED_{fuel} is the gravimetric energy density of fuel (Wh/gr), K_{dch} is average discharge efficiency, η_{ICE_t} is average ICE efficiency for traction, E_{bat} (Wh) is energy of battery

, fc_r (gr) is real fuel consumption , ΔSOC is the difference of final SOC and initial SOC.

Results for three modes of vehicle are given below.

For only ICE mode:

$$fc_{cs} = 82.95 - \frac{(8800 * (0.65 - 0.65)) * 0.8}{0.25 * 12.7} = 82.95 \quad (5.2)$$

For only regenerative braking mode:

$$fc_{cs} = 74.19 - \frac{(8800 * (0.6546 - 0.65)) * 0.8}{0.25 * 12.7} = 64gr \quad (5.3)$$

For MOES mode:

$$fc_{cs} = 58.77 - \frac{(8800 * (0.6536 - 0.65)) * 0.8}{0.25 * 12.7} = 50.8gr \quad (5.4)$$

5.6 Comparison of Results

Results of only ICE mode, only regenerative braking mode and MOES mode are given in the table below.

Table 5.1 Fuel Economy Results of Three Modes

	Fuel Consumption(gr)	Initial SOC (%)	Finale SOC (%)	Charge Sustaining Fuel Consumption(gr)	%Fuel economy
Conventional (Only-ICE)	82.95	65	65	82.95	-
Only Regenerative Braking (Bang-Bang)	74.19	65	65.46	64	22.85
Optimization (MOES)	58.77	65	65.36	50.8	38.76

6. CONCLUSIONS

Modeling and optimal power management for a hybrid electric vehicle were discussed in this thesis. The developed power management algorithm depends on maximizing overall efficiency strategy (MOES) which brings a new formulation for a hybrid electric vehicle power split control. Algorithm was compared with the conventional operation of the vehicle. Only regenerative braking mode algorithm was simulated to see the effect of the MOES in fuel consumption minimization. With these results, it was seen that % 22.85 of %38.76 total minimization was obtained from regenerative braking and the remaining part % 15.91 was obtained from optimization.

Two methods were given for real time implementation of the controller; one of them was solving the efficiency equations and searching the optimum torques, the other one was working with tables which were calculated by offline simulations.

Driver model was a simple PI controller longitudinal speed in simulations. This model can be improved and more realistic driver actions can be obtained for simulations in next step.

In this work, emissions were not taken into account by the controller. It is clear that emissions are reduced because of regenerative braking, electric drive and less usage of internal combustion engine in this study but better results can be achieved in terms of emissions. However, taking into account the emissions will increase the fuel consumption.

Other types of hybrid electric vehicle power management controller performance can be applied to the vehicle model and these results can be compared with MOES in the future.

Main work that should be done in the future is implementing this controller on a real hybrid electric vehicle and comparing the results with simulations to analyze the, reliability of models and the performance of the MOES algorithm.

REFERENCES

[1] **Plotkin, S., Santini, D., Vyas, A., Anderson, J., Wang, M., He, J., Bharathan, D.**, 2001 ,Hybrid Electric Vehicle Technology Assessment: Methodology, Analytical Issues, and Interim Results, Argonne National Laboratory, USA.

[2] http://www.fuelcellsworks.com/Supppage1855.html

[3] http://www.greencarcongress.com/2007/03/us_sales_of_hyb.html

[4] **Sezer,V., Uygan, C.M.İ, Hartavi E.A., Acarman, T. and Güvenç, L.** ,2007, Propulsion System Design of a Hybrid Electric Vehicle, Workshop on Hybrid Electric Vehicle Modeling and Control, İstanbul, Turkey.

[5] **Musardo, C., Staccia, B.**, 2003, Energy Management Strategies For Hybrid Electric Vehicle, *M.S. Thesis*, Politecnico Di Milano, Milano

[6] **Paganelli, G., Delptrat S., Guerra, T.M., Rimaux, J. and Santin, J.J**., 2002, Equivalent Consumption Minimization Strategy for Parallel Hybrid Powertrains, *"Vehicular Technology Conference*" ,4, 2076-2081.

[7]http//www.dolcera.com/wiki/index.php?title=Hybrid_Electric_Vehicle_Battery_System

[8] **J. R. Hendershot., T. Milller,** 2003, The Design of Brushless Permanent Magnet Motors, Oxford Univ Press , England.

[9] **Yiğit, T.,** 2004, "Araç Dinamiği Modelleri Geliştirilmesi ve Savrulma Devrilme Engelleyici Kontrolde Kullanımları, *M.S. Thesis***,** İ.T.Ü. Fen Bilimleri Enstitüsü, İstanbul.

[10] **Güvenç, L**., Lecture Notes on Vehicle Dynamics and Control

[11] **Güvenç, B, A.,** MAK 450 course notes

[12] **Kural, E., Güvenç, B, A.,** June 2006, Adaptive cruise control simulator: a low-cost, multiple-driver-in-the-loop simulator, *"IEEE Transactions On Control Systems Technology",* 42-55.

[13] **Rajamani R.,** 2006 , Vehicle Dynamics and Control, Mechanical Engineering Series, Springer

[14] **Koot, M., Kessels, J.T.B.A. de Jager, B., Heemels, W.P.M.H. van den Bosch, P.P.J. , Steinbuch, M.**, 2005, Energy Management Strategies For Vehicular Electric Power Systems, *"IEEE Transactions on Vehicular Technology"* , 54, 771-782.

[15] **Lin, C.C., Kang, M.J.,. Grizzle, J.W., Peng, H**., 2001, Energy Management Strategy for a Parallel Hybrid Electric Truck, "*Proceedings of the American Control Conference",* 2878-2873

[16] **Sciarretta, A., Back, M., Guzzella, L.**, 2004, Optimal Control of Parallel Hybrid Electric Vehicles, *"IEEE Transactions On Control Systems Technology"*,12, 352-363.

[17] **Paganelli, G., Tateno, M., Brahma, A., Rizzoni, G. and Guezennec, Y.,**2001, Control Development For a Hybrid-Electric Sport-Utility

Vehicle: Strategy, "*Proceedings of the American Control Conference"*, 5064-5069.

[18] **Hartavi E.A., Uygan, C.M.İ, Sezer,V., Acarman, T. and Güvenç, L.** ,2007, Development of Hybrid Braking Algorithm for Electric/Hybrid Electric Vehicles, Workshop on Hybrid Electric Vehicle Modeling and Control, İstanbul, Turkey.

APPENDICES

APPENDIX A : More Offline Simulation Results for MOES Optimization Tables

APPENDIX A

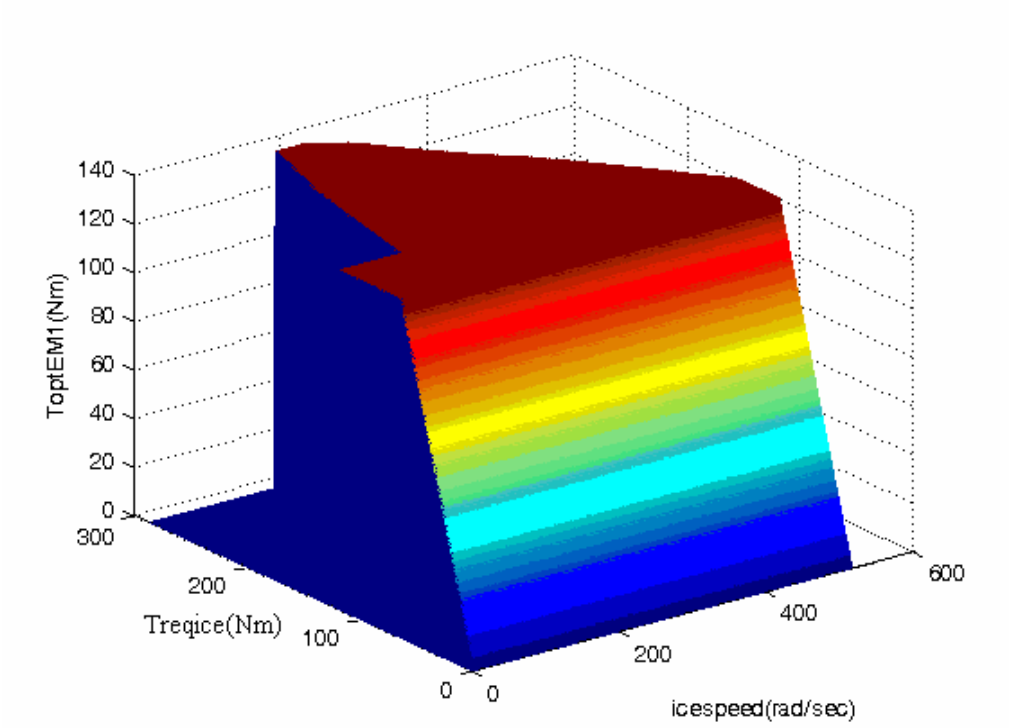

Figure A.1 : Optimum Torque of EM1 for MOES Discharge for 2. Gear Number

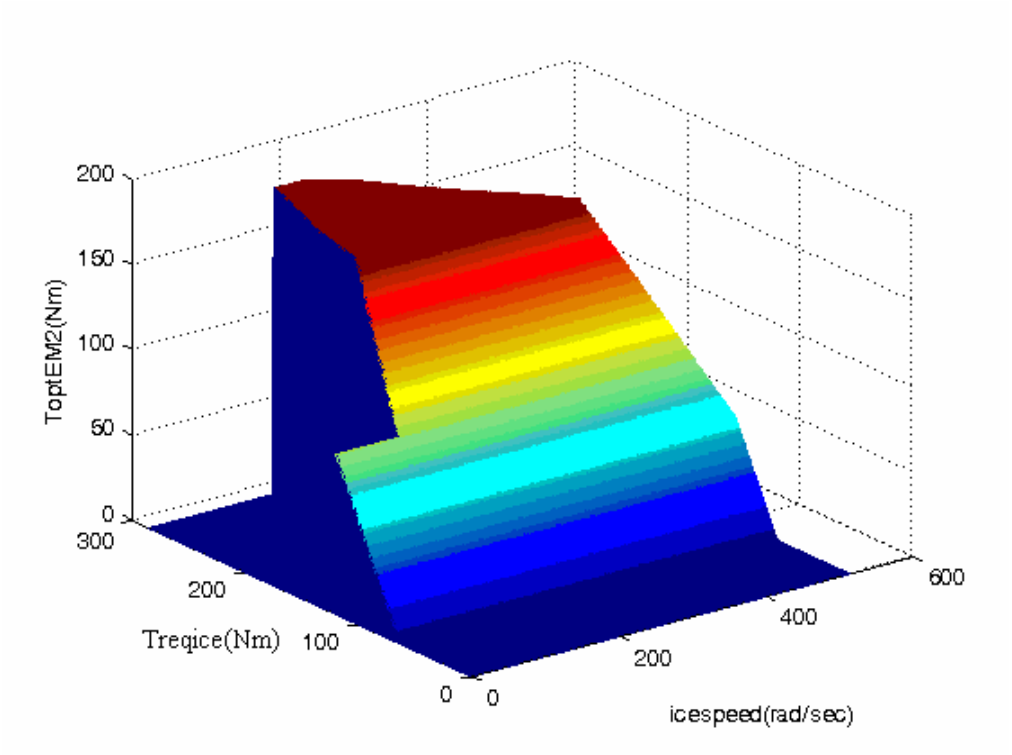

Figure A.2 : Optimum Torque of EM2 for MOES Disharge for 2. Gear Number

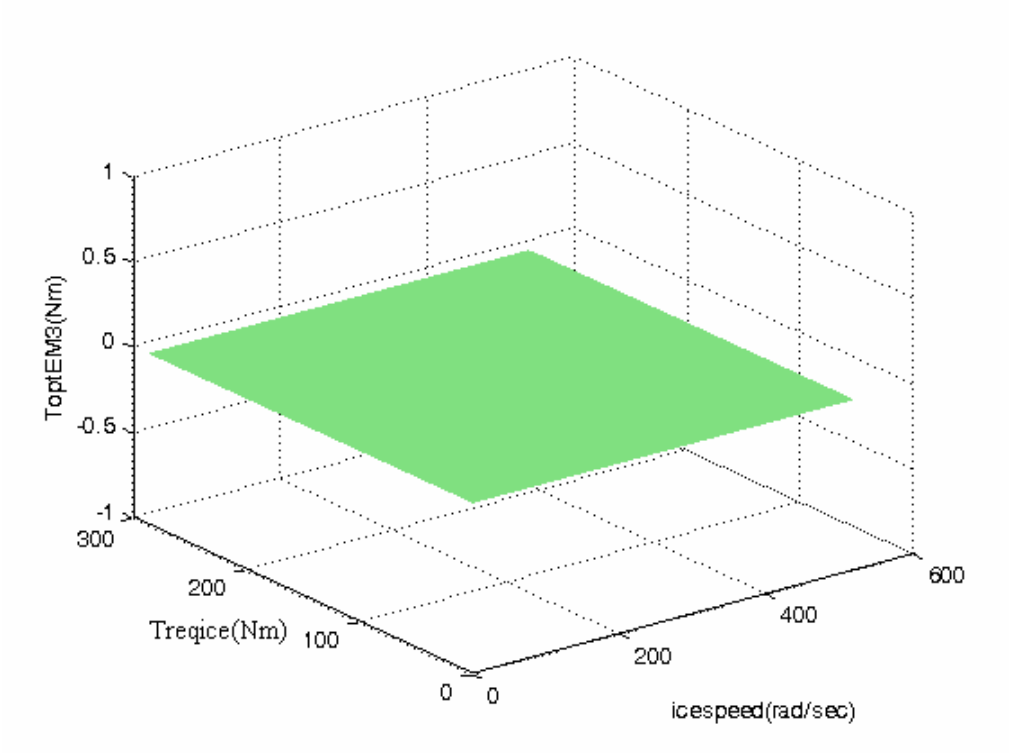

Figure A.3 : Optimum Torque of EM3 for MOES Discharge for 2. Gear Number

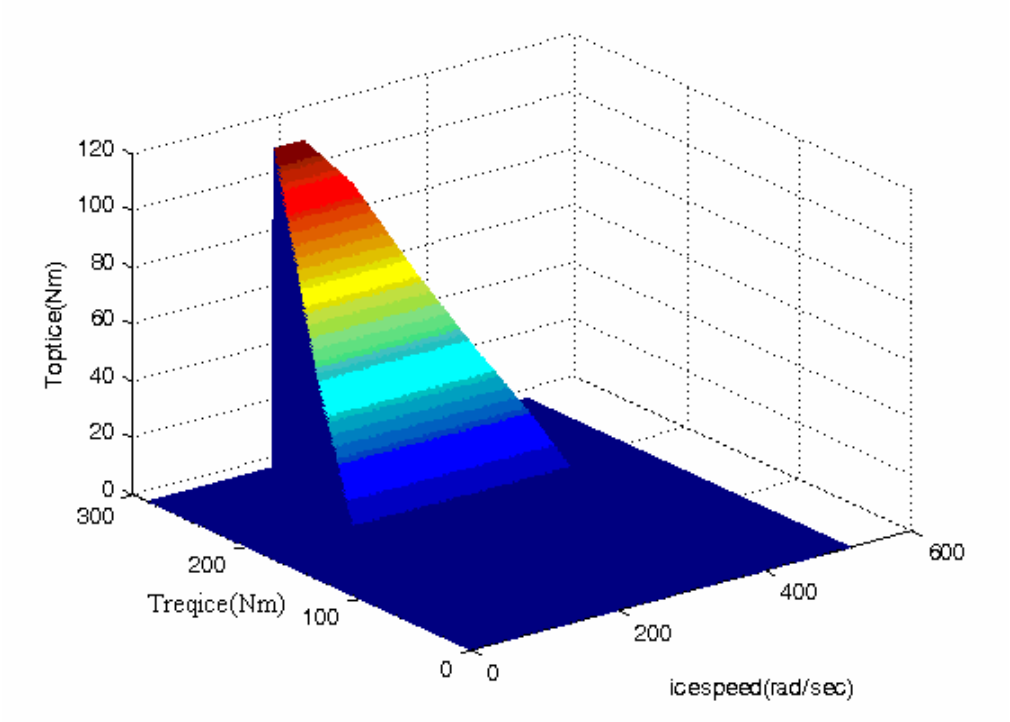

Figure A.4 : Optimum Torque of ICE for MOES Discharge for 2. Gear Number

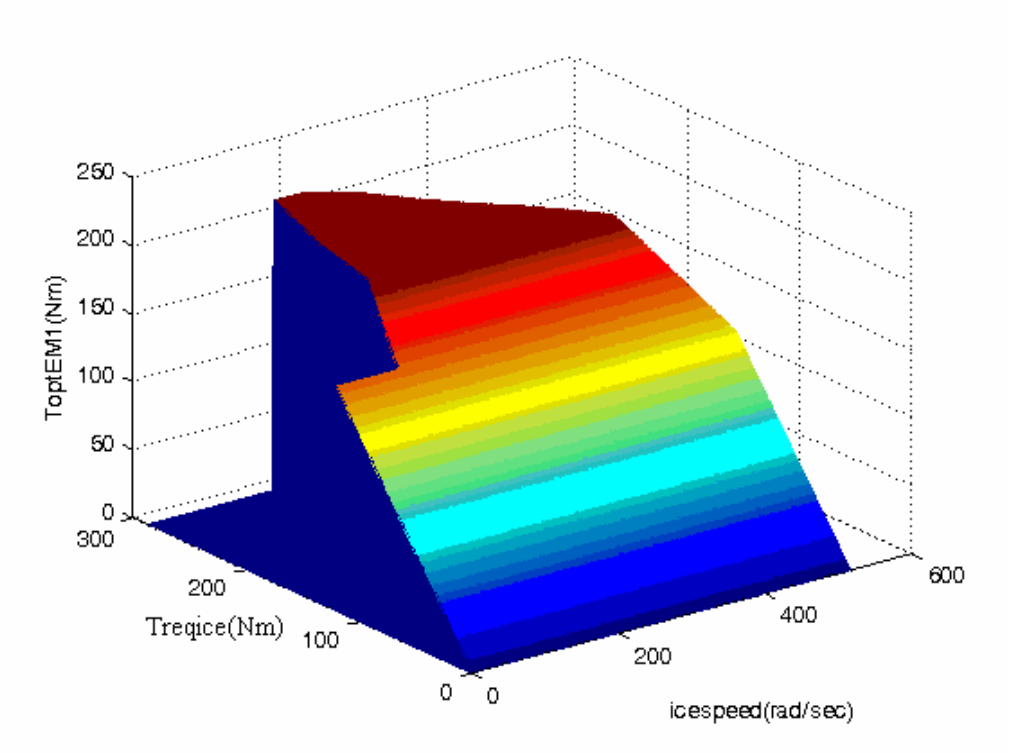

Figure A.5 : Optimum Torque of ICE for MOES Discharge for 3. Gear Number

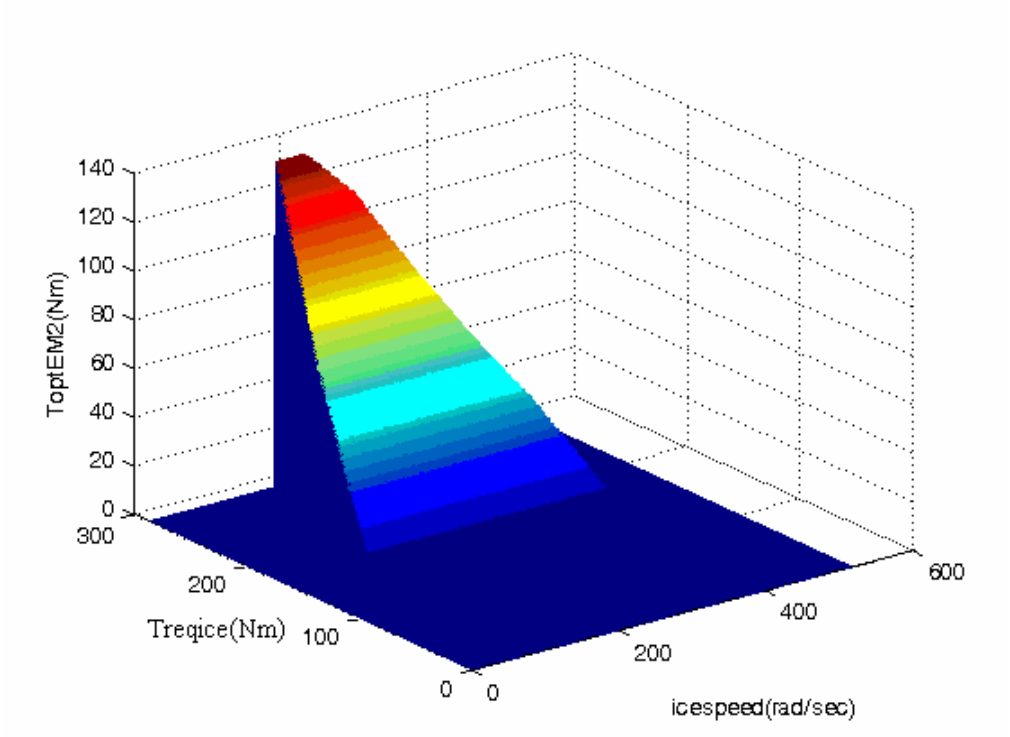

Figure A.6 : Optimum Torque of EM2 for MOES Discharge for 3. Gear Number

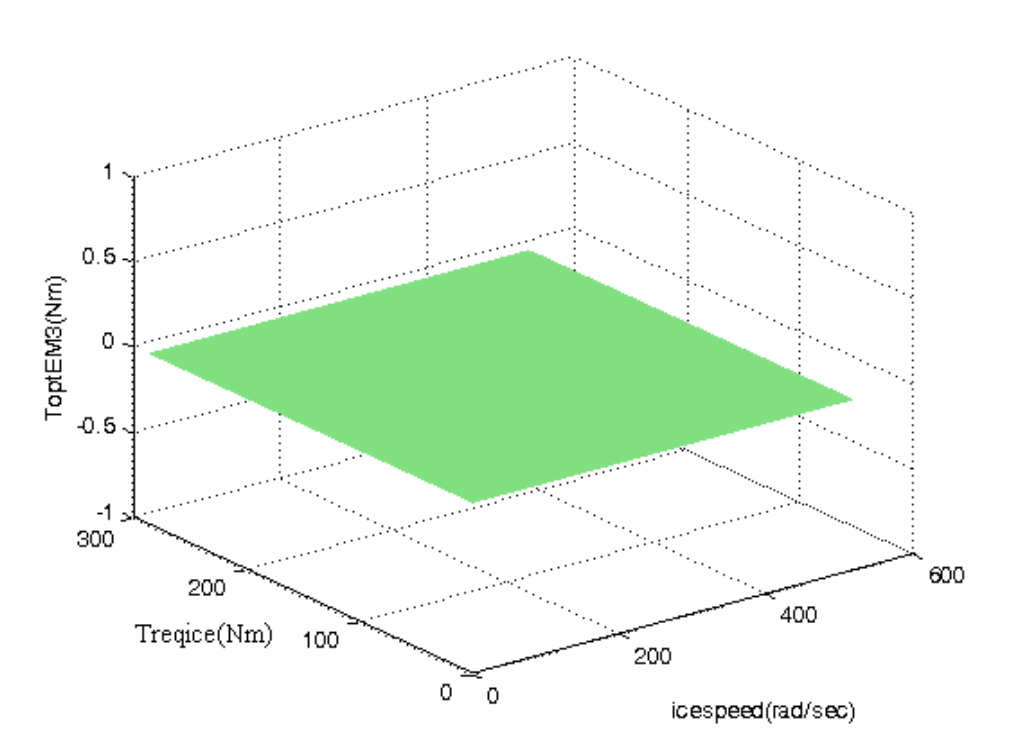

Figure A.7 : Optimum Torque of EM3 for MOES Discharge for 3. Gear Number

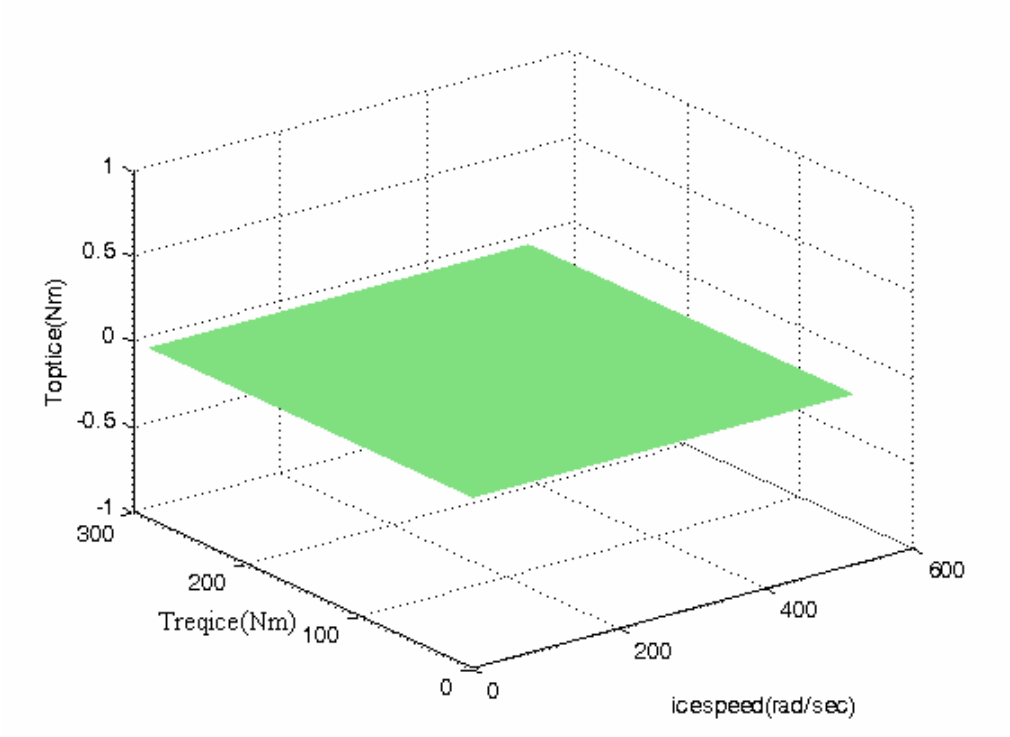

Figure A.8 : Optimum Torque of ICE for MOES Discharge for 3. Gear Number

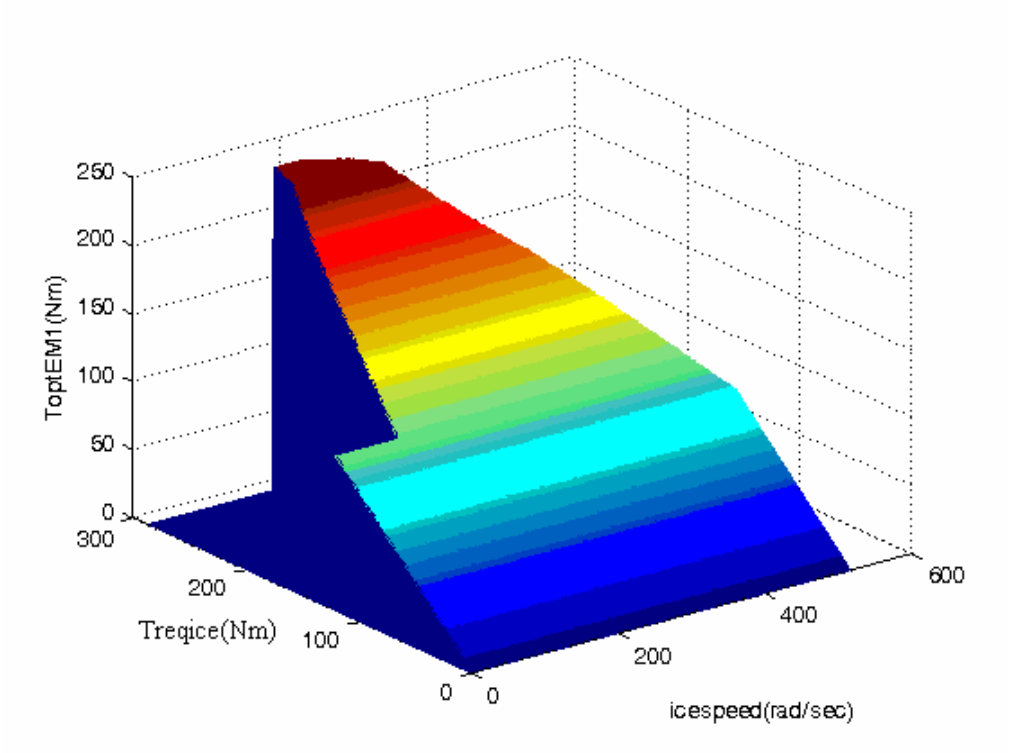

Figure A.9 : Optimum Torque of EM1 for MOES Discharge for 4. Gear Number

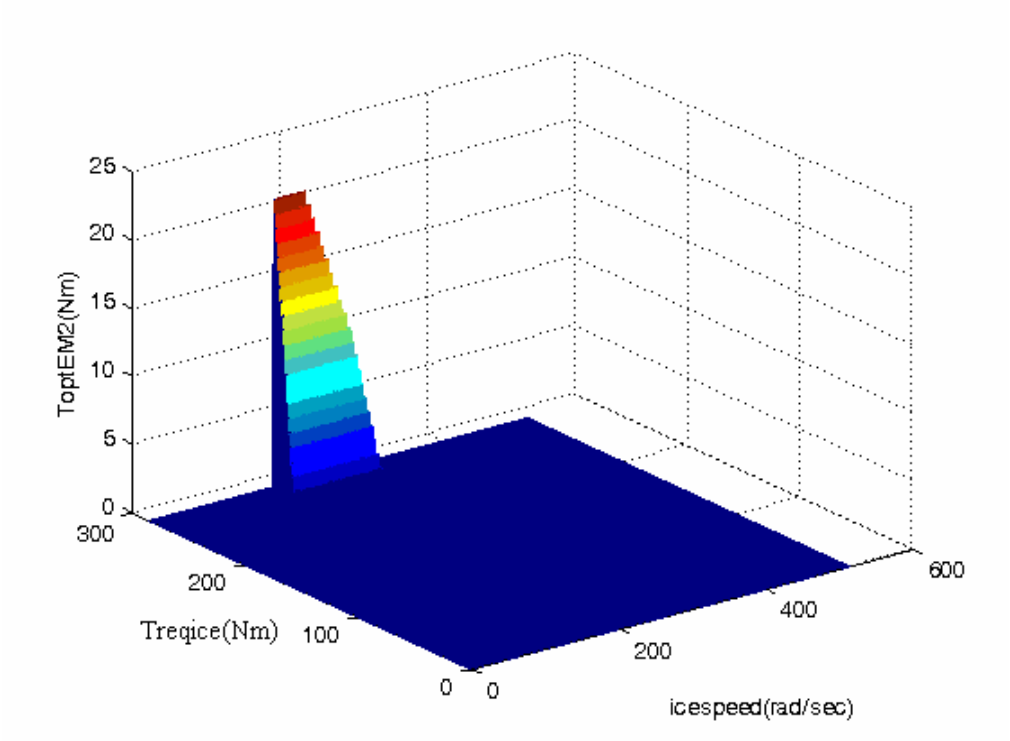

Figure A.10 : Optimum Torque of EM2 for MOES Discharge for 4. Gear Number

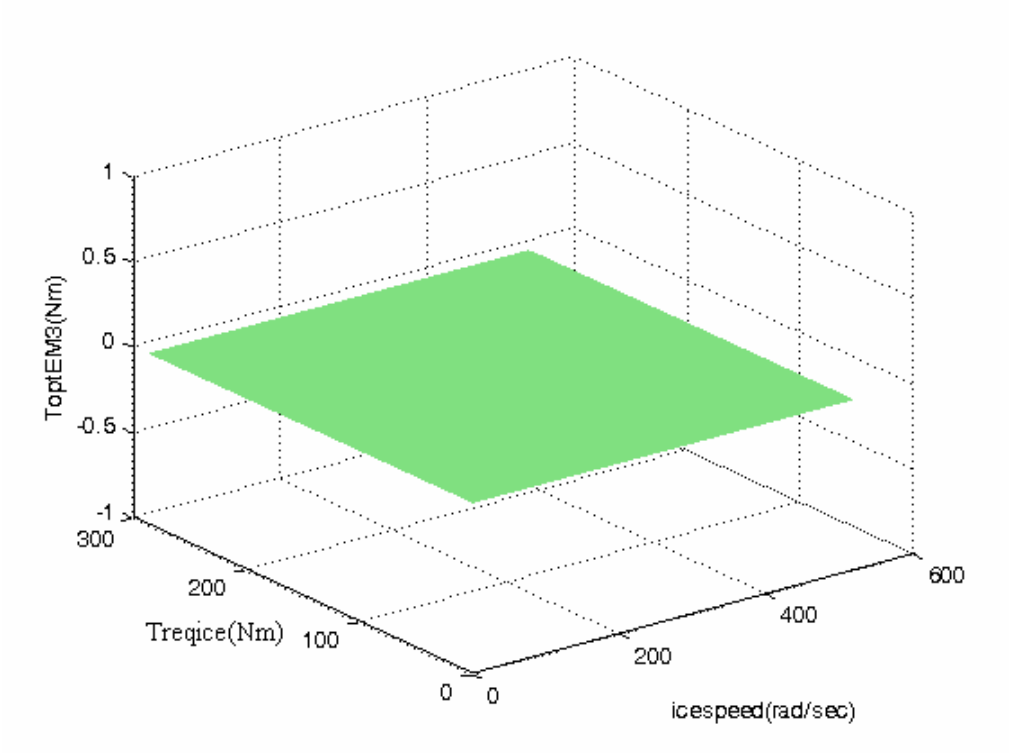

Figure A.11 : Optimum Torque of EM3 for MOES Discharge for 4. Gear Number

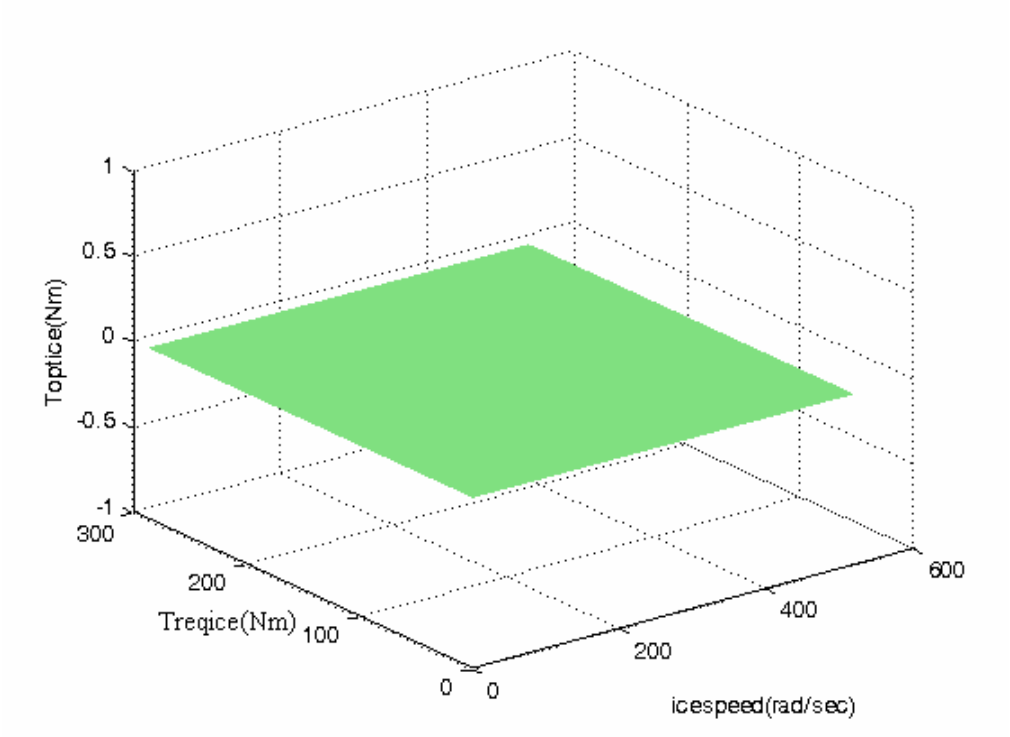

Figure A.12 : Optimum Torque of ICE for MOES Discharge for 4. Gear Number

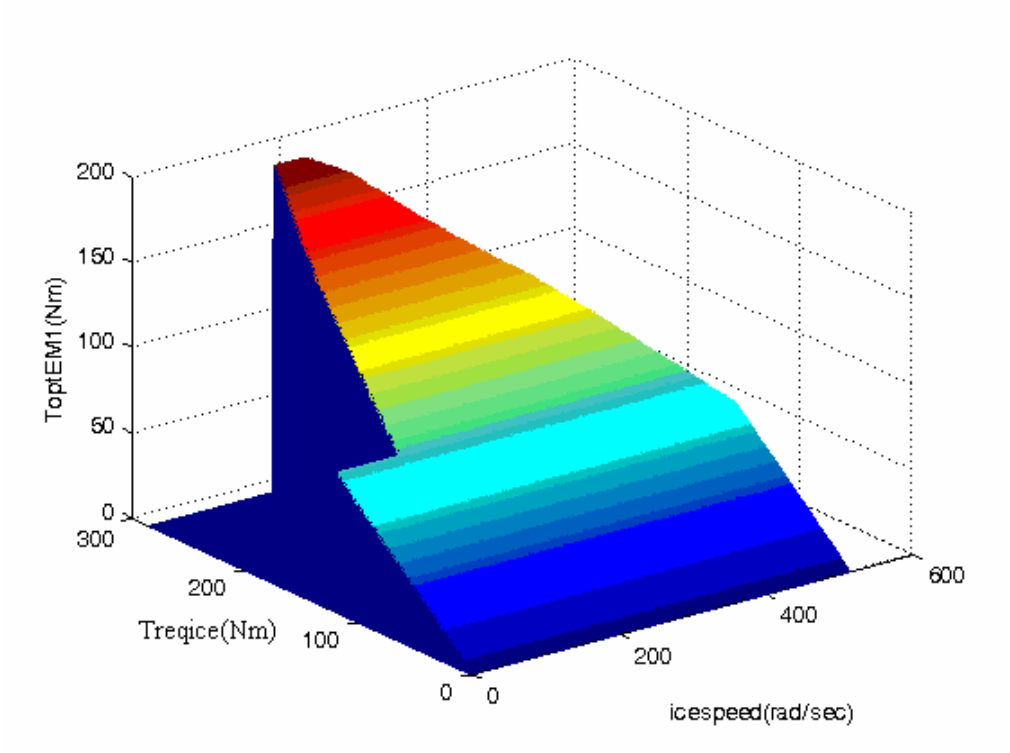

Figure A.13 : Optimum Torque of EM1 for MOES Discharge for 5. Gear Number

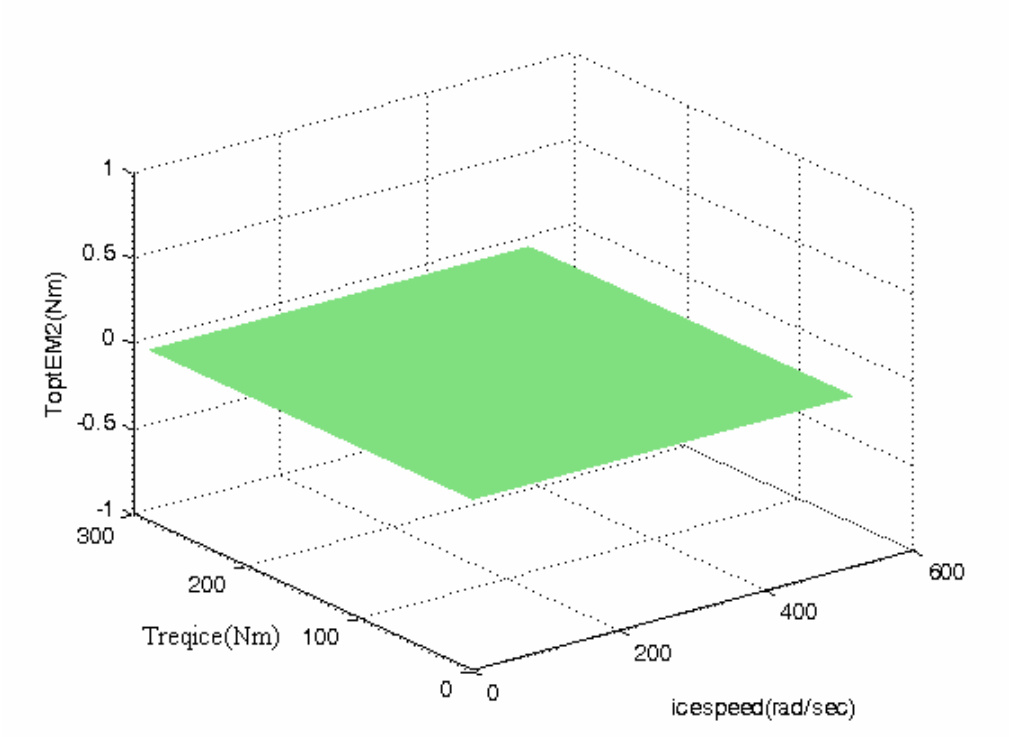

Figure A.14 : Optimum Torque of EM2 for MOES Discharge for 5. Gear Number

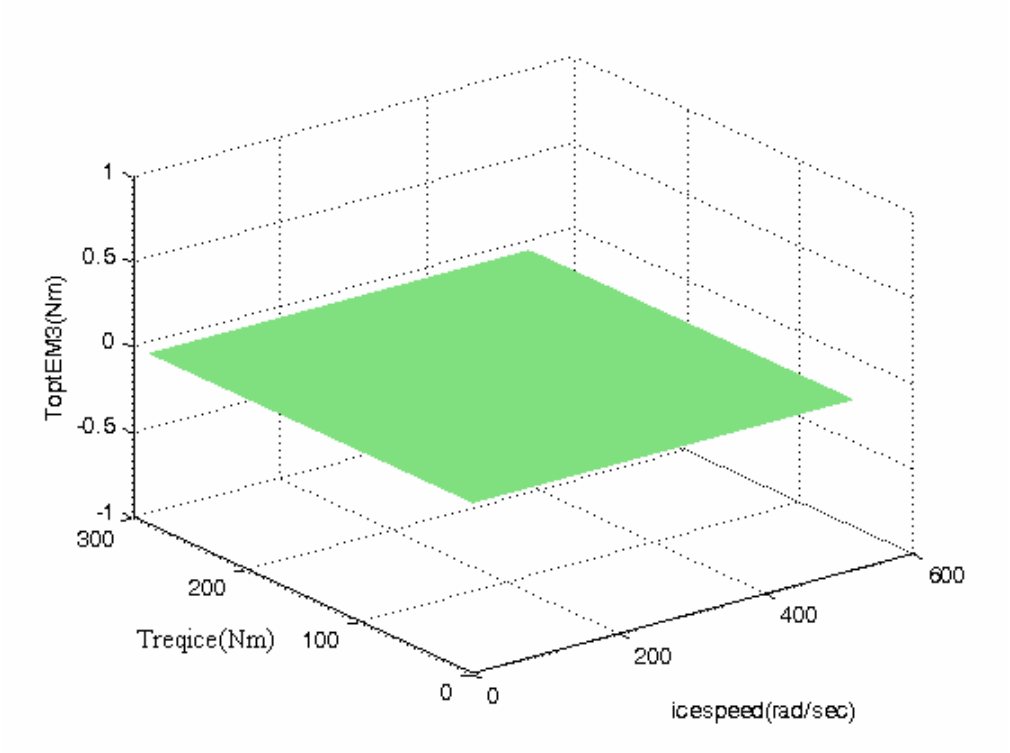

Figure A.15 : Optimum Torque of EM3 for MOES Discharge for 5. Gear Number

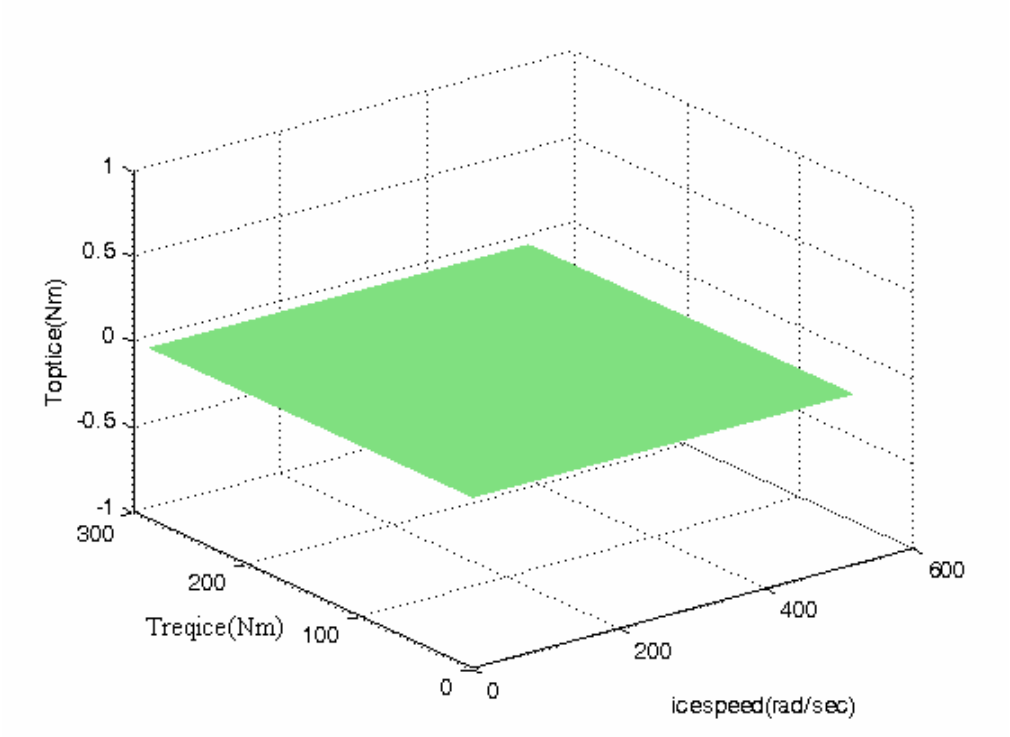

Figure A.16 : Optimum Torque of ICE for MOES Discharge for 5. Gear Number

APPENDIX B : Only ICE Mode Simulation Results

APPENDIX B

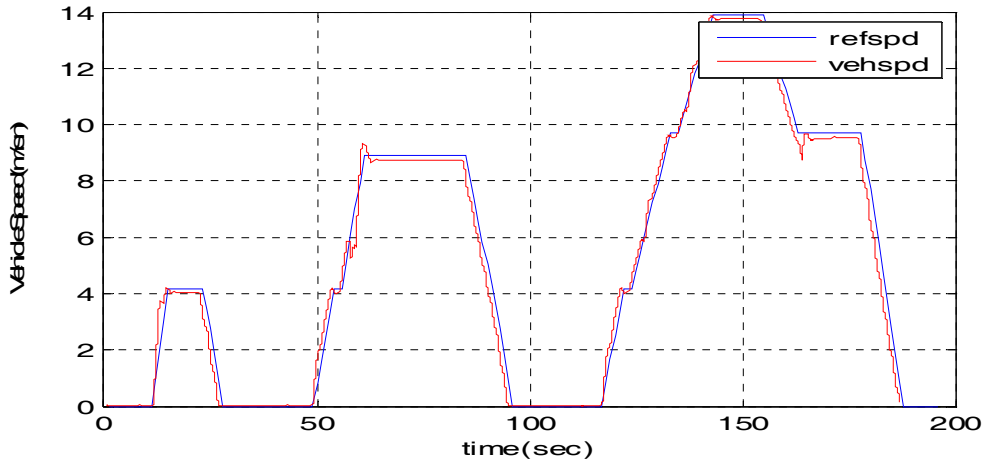

Figure B.1 : Vehicle Speed and Reference Speed in Only ICE Mode

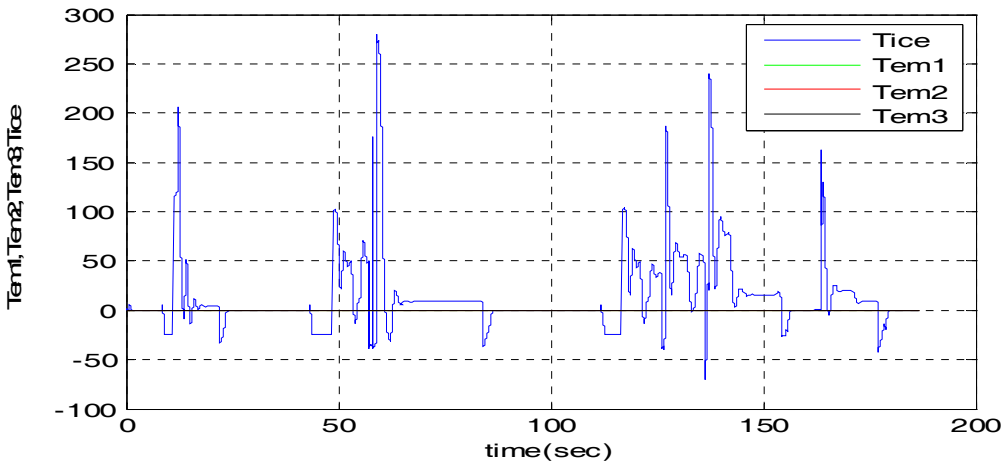

Figure B.2 : Component Torques in Only ICE Mode

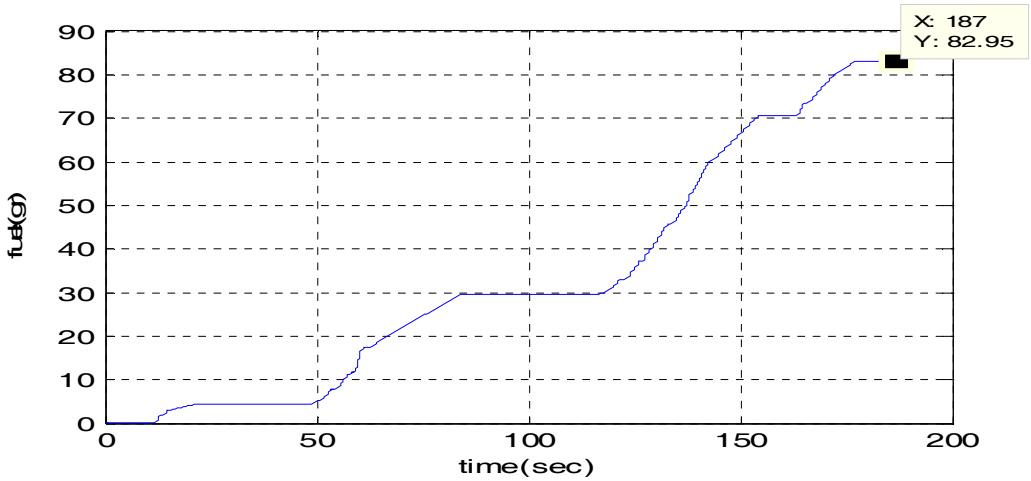

Figure B.3 : Fuel Consumption in Only ICE Mode

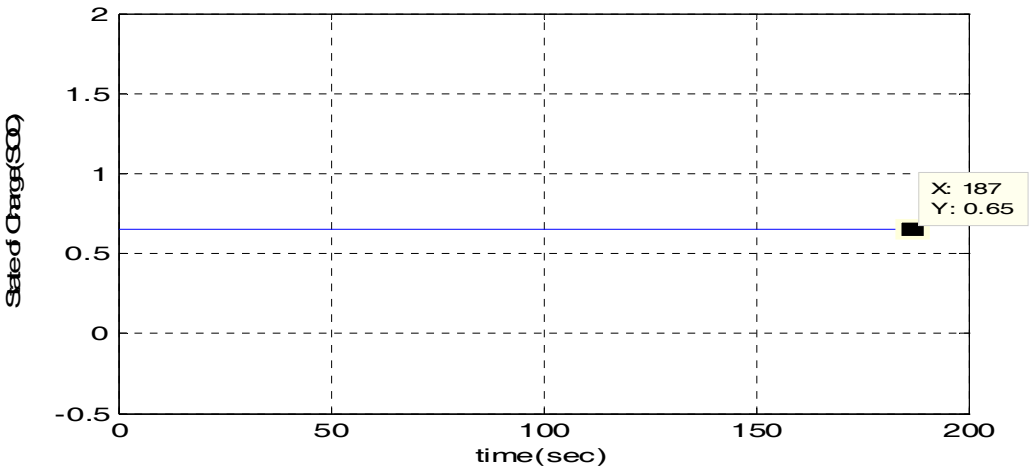

Figure B.4 : SOC in Only ICE Mode

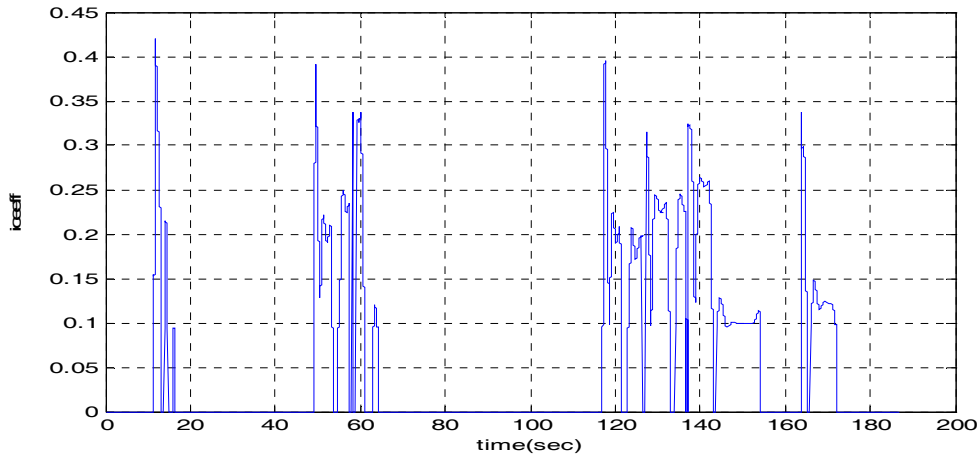

Figure B.5 : ICE Efficiency of Only ICE Mode

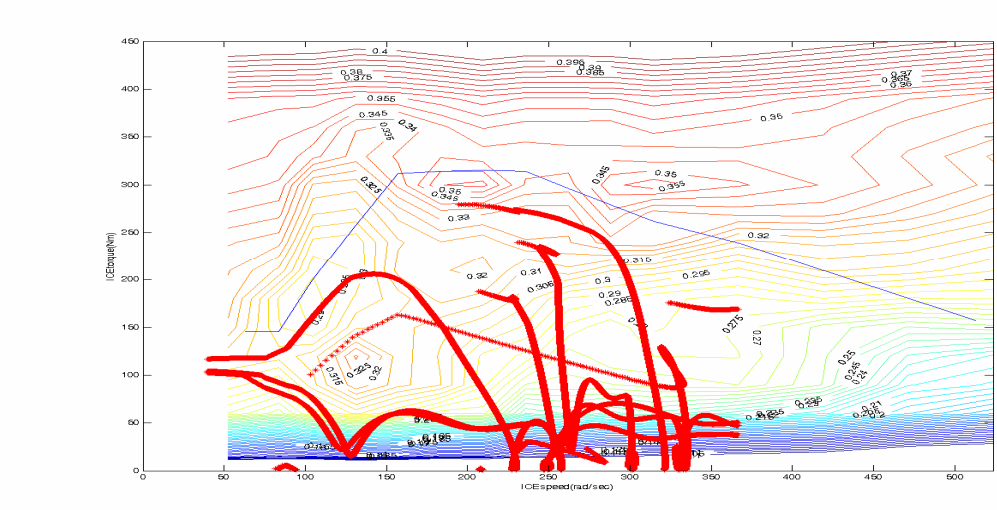

Figure B.6 : ICE Operating Points in Only ICE Mode

APPENDIX C : Only Regenerative Braking Mode Simulation Results

APPENDIX C

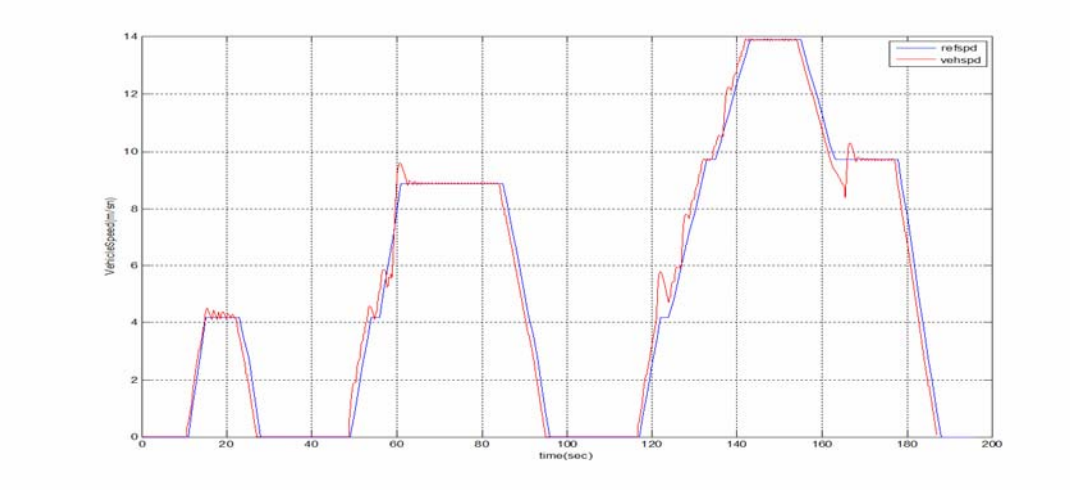

Figure C.1: Vehicle Speed and Reference Speed in Only Regenerative Braking Mode

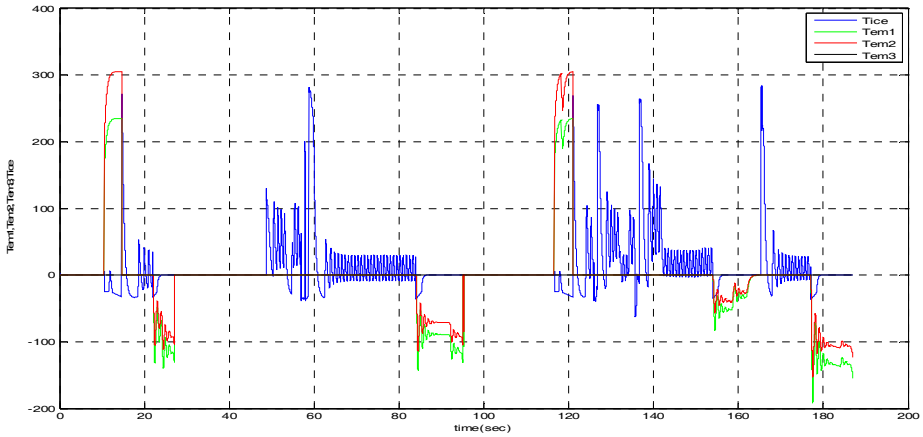

Figure C.2 : Component Torques in Only Regenerative Braking Mode

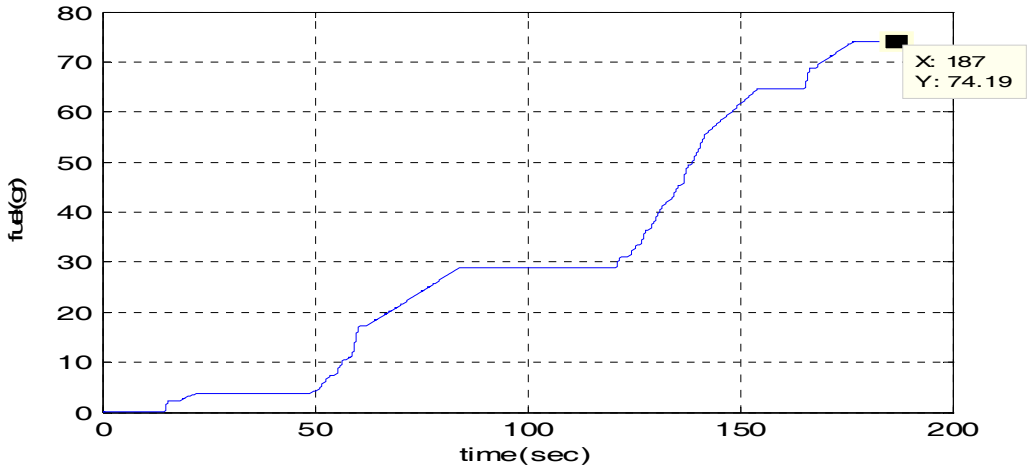

Figure C.3 : Fuel Consumption in Only Regenerative Braking Mode

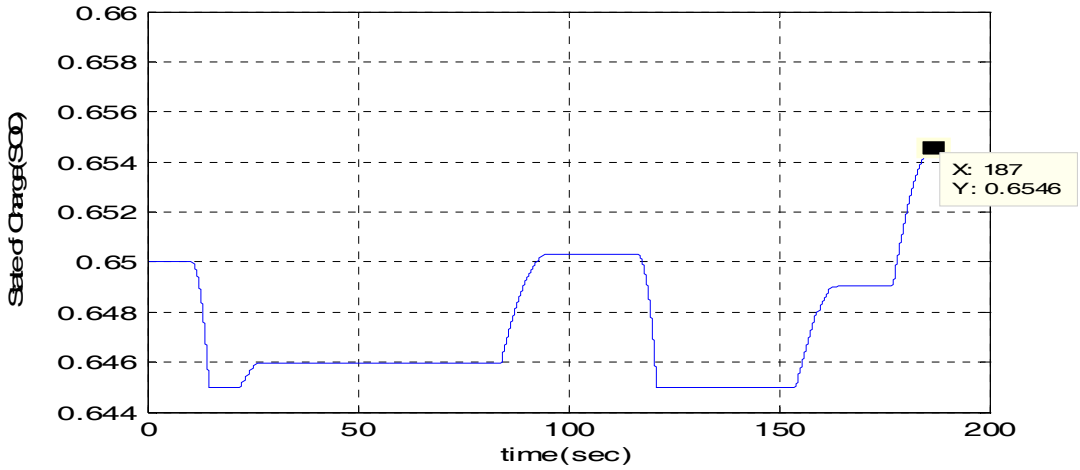

Figure C.4 : SOC in Only Regenerative Braking Mode

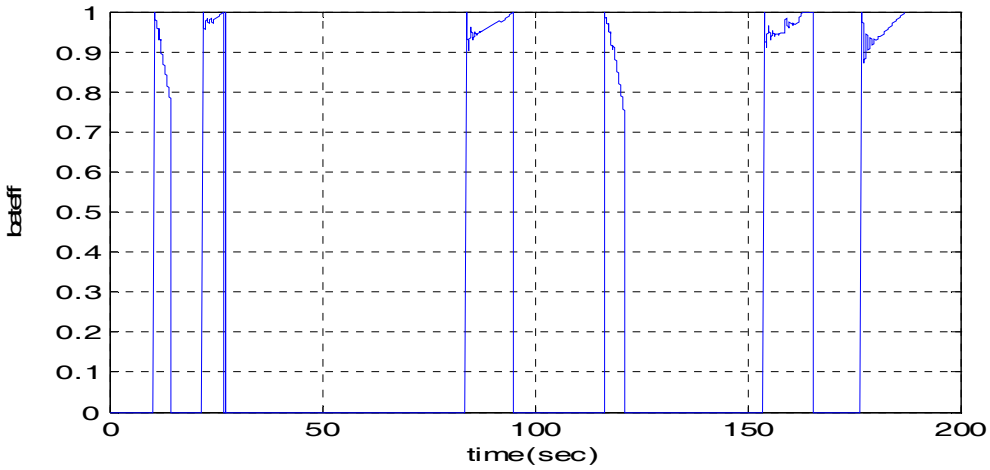

Figure C.5 : Battery Efficiency in Only Regenerative Braking Mode

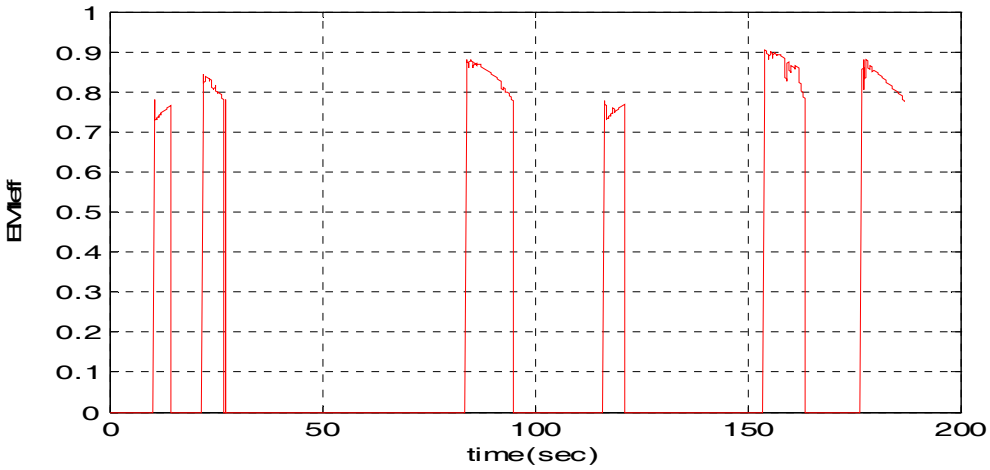

Figure C.6 :EM1 Efficiency in Only Regenerative Braking Mode

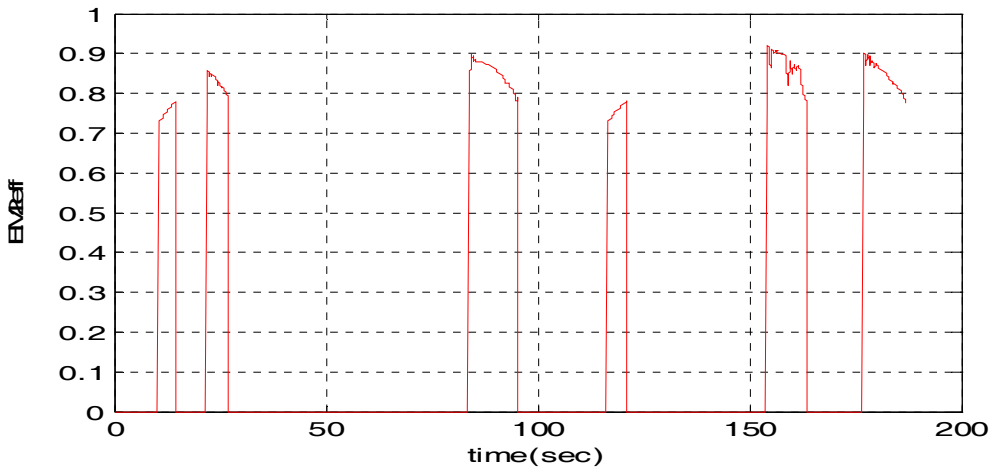

Figure C.7 :EM2 Efficiency in Only Regenerative Braking Mode

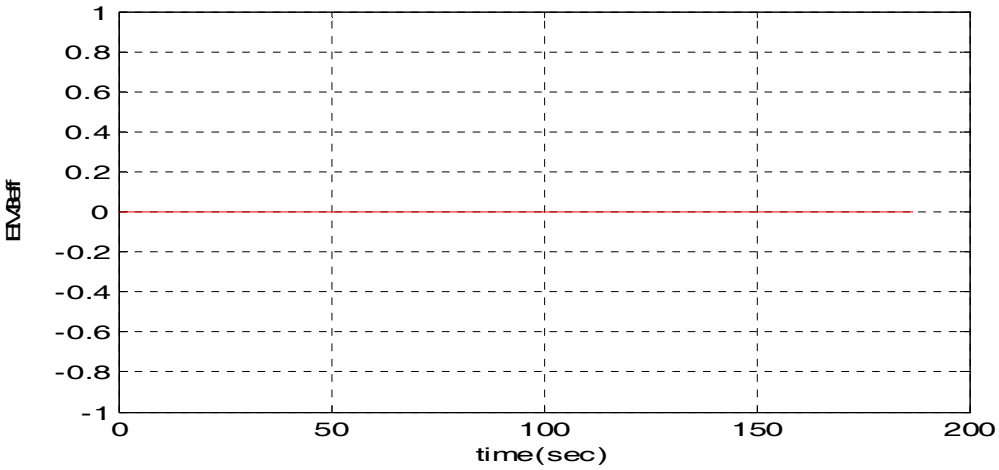

Figure C.8 :EM3 Efficiency in Only Regenerative Braking Mode

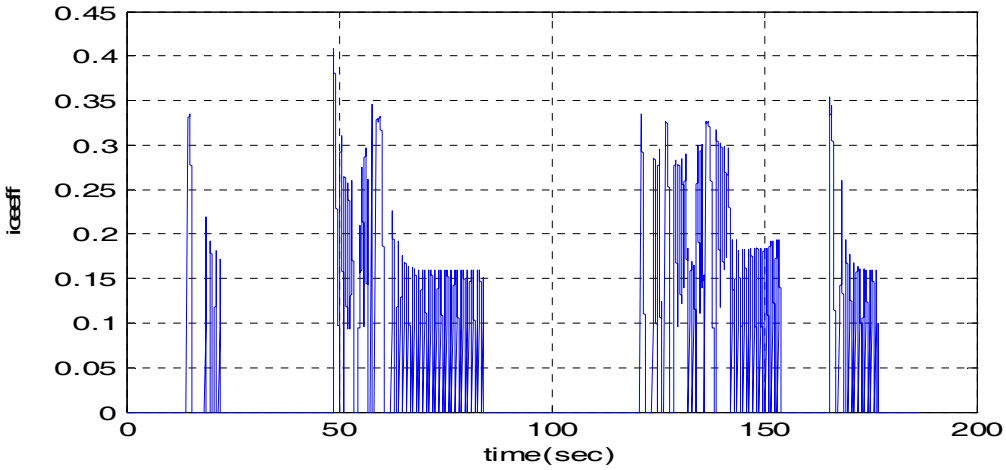

Figure C.9 :ICE Efficiency in Only Regenerative Braking Mode

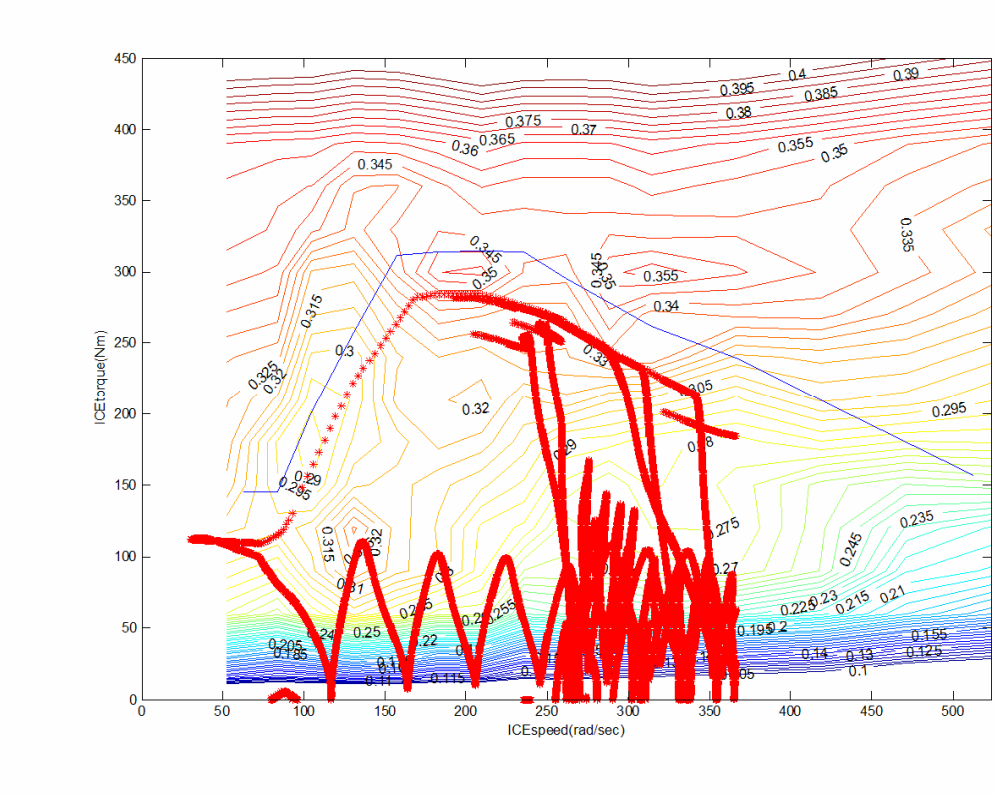

Figure C.10 : ICE Operating Points in Only Regenerative Braking Mode

APPENDIX D: Maximizing Overall Efficiency Strategy(MOES) Simulation Results

APPENDIX D

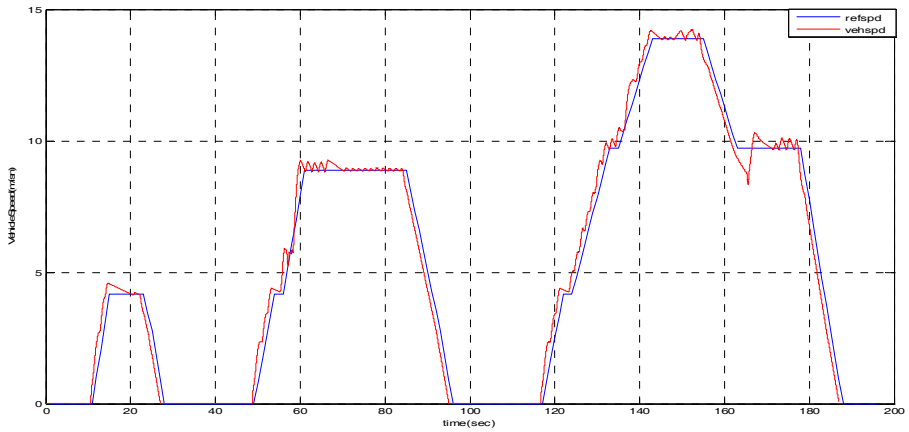

Figure D.1: Vehicle Speed and Reference Speed in MOES Mode

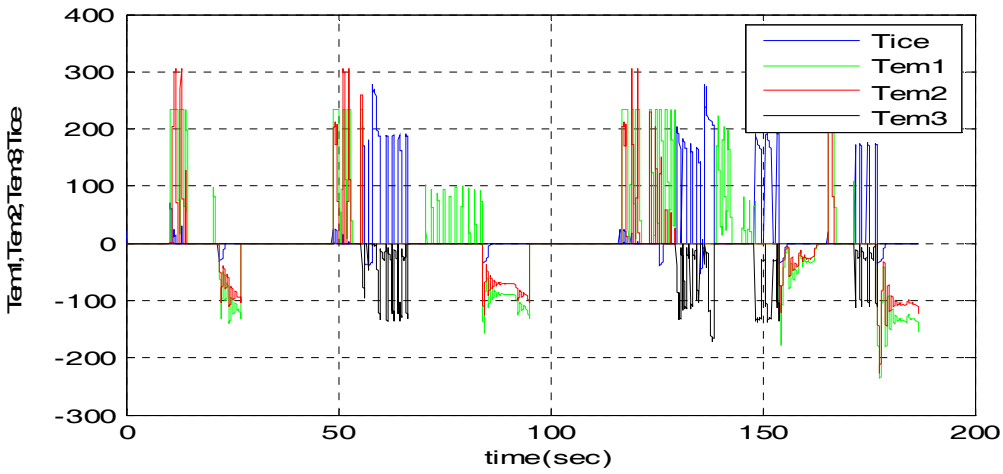

Figure D.2 : Component Torques in MOES Mode

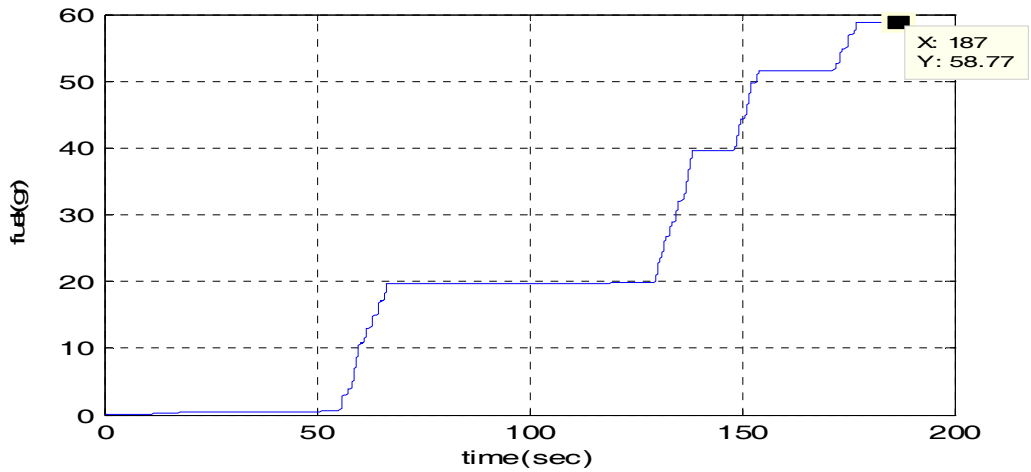

Figure D.3 : Fuel Consumption in MOES Mode

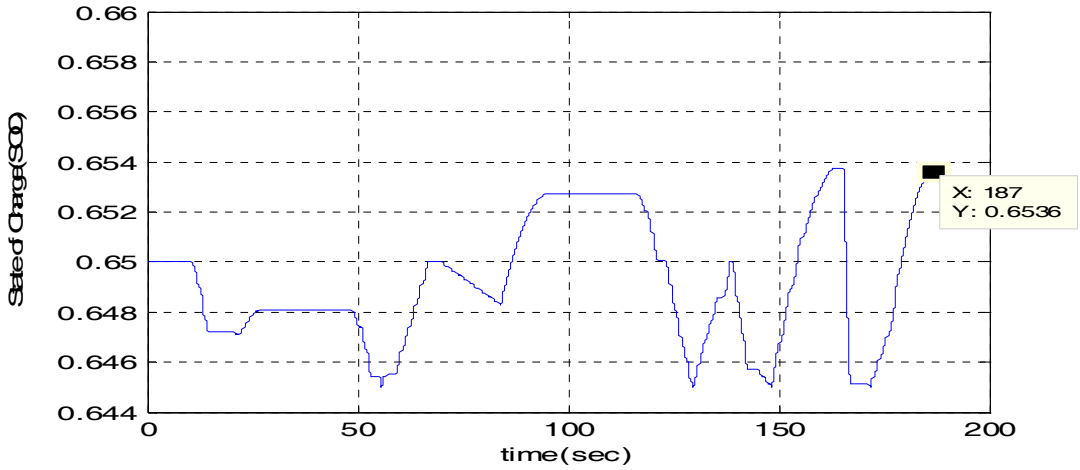

Figure D.4 : SOC in MOES Mode

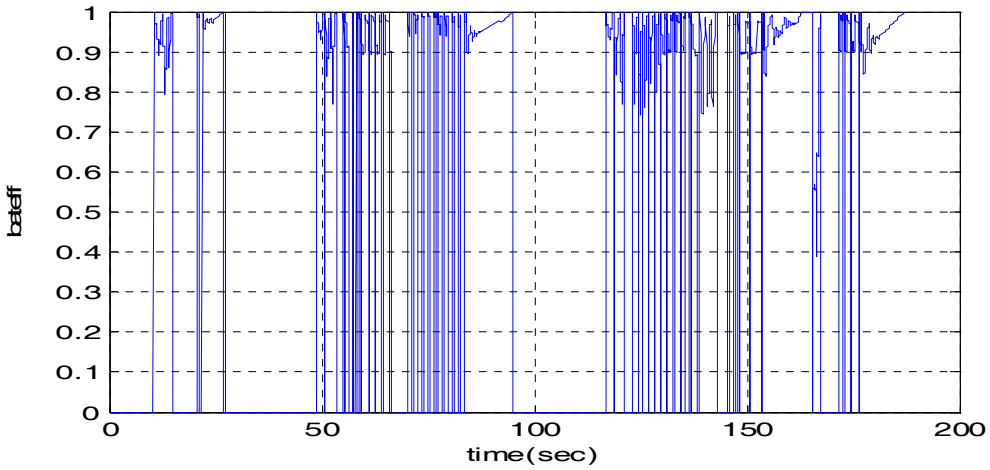

Figure D.5 : Battery Efficiency in MOES Mode

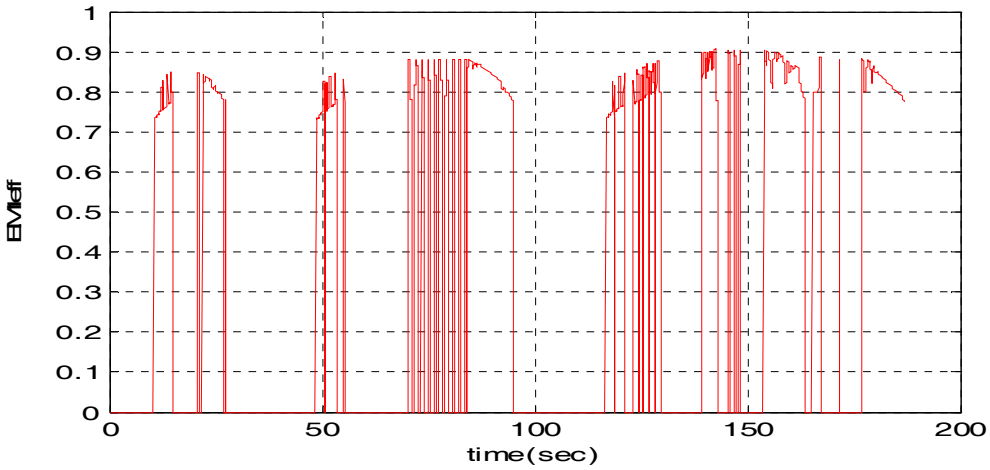

Figure D.6 :EM1 Efficiency in MOES Mode

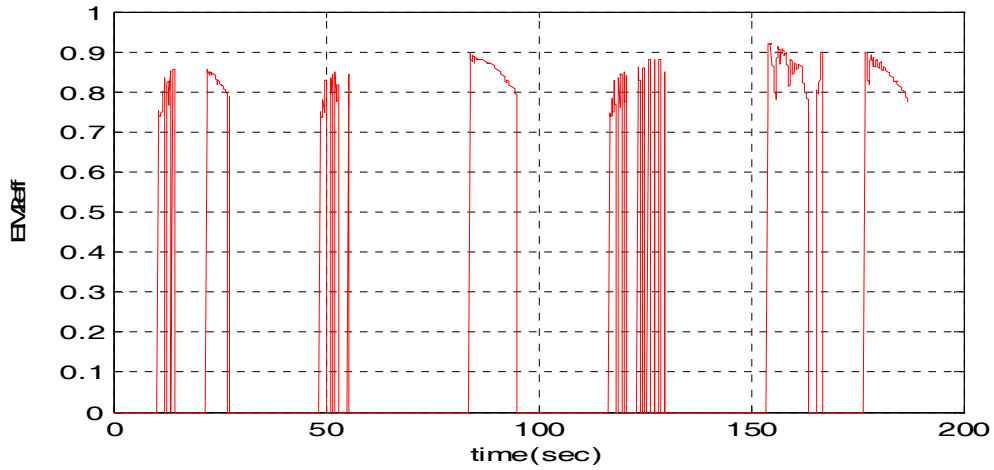

Figure D.7 :EM2 Efficiency in MOES Mode

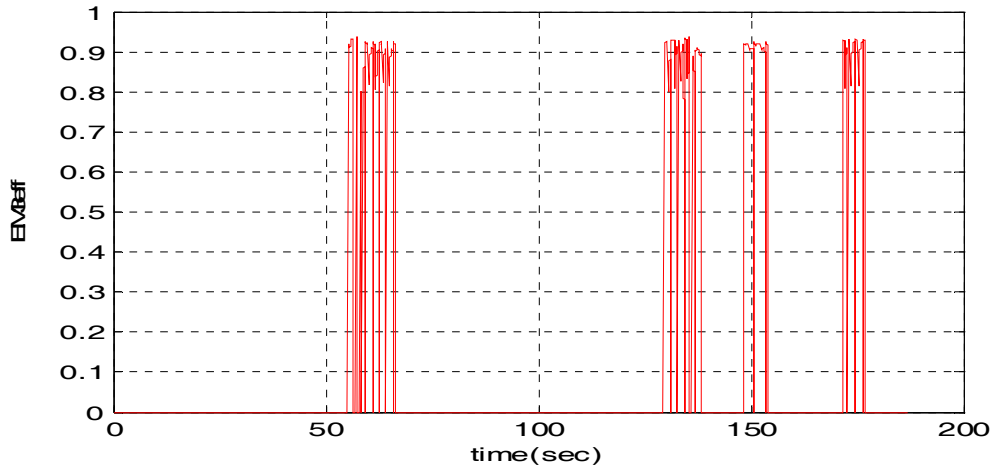

Figure D.8 :EM3 Efficiency in MOES Mode

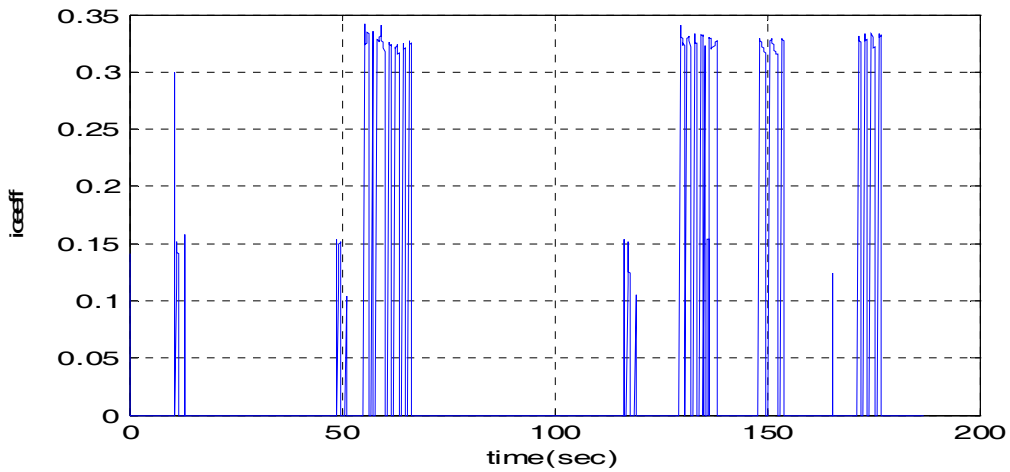

Figure D.9 :ICE Efficiency in MOES Mode

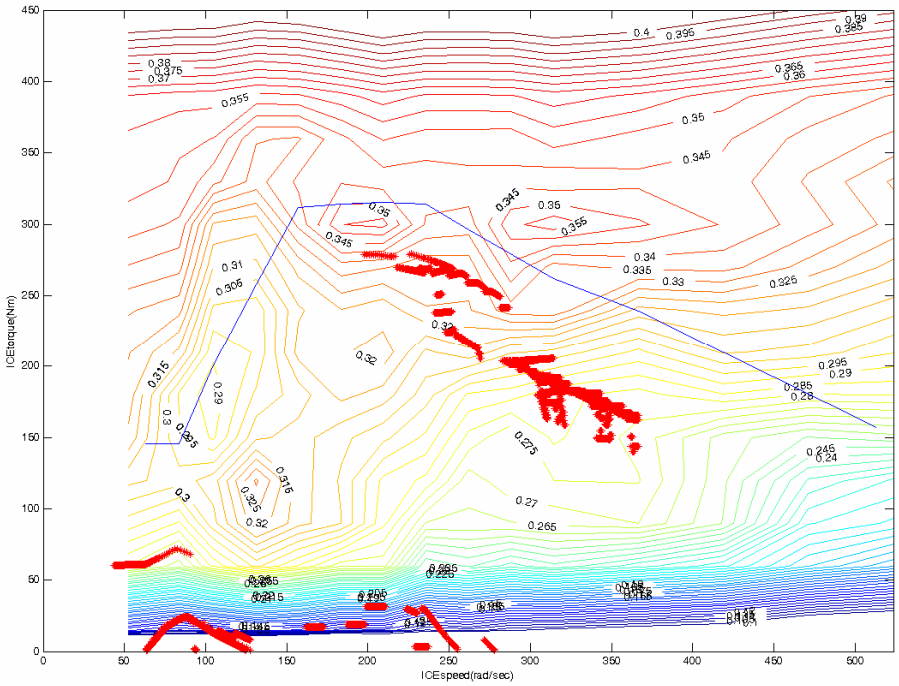

Figure D.10 : ICE Operating Points in MOES Mode

BIOGRAPHY

Volkan Sezer was born in 1983 in Düzce. After finishing his primary education, he went to Düzce Arsal Anatolian high school and graduated in 2001. He received a B.Sc. degree from Yıldız Technical University electronics and telecomunication engineering department in 2005 .

Same year he began his M.Sc. education in mechatronics engineering department at İstanbul Technical University.